

การตัดแปรโดยความร้อนขึ้นของสตาร์ชถั่วมะแฮะ *Cajanus cajan* (L.) Millsp. ในภาวะที่มี
สารประกอบแคลเซียมต่างกันและสมบัติทางเคมีกายภาพของสตาร์ชตัดแปร

นางสาวสุวภัทร ศรีจันททองศิริ



บทคัดย่อและแฟ้มข้อมูลฉบับเต็มของวิทยานิพนธ์ตั้งแต่ปีการศึกษา 2554 ที่ให้บริการในคลังปัญญาจุฬาฯ (CUIR)
เป็นแฟ้มข้อมูลของนิสิตเจ้าของวิทยานิพนธ์ ที่ส่งผ่านทางบัณฑิตวิทยาลัย

The abstract and full text of theses from the academic year 2011 in Chulalongkorn University Intellectual Repository (CUIR)
are the thesis authors' files submitted through the University Graduate School.

วิทยานิพนธ์นี้เป็นส่วนหนึ่งของการศึกษาตามหลักสูตรปริญญาวิทยาศาสตรดุษฎีบัณฑิต
สาขาวิชาเทคโนโลยีทางอาหาร ภาควิชาเทคโนโลยีทางอาหาร
คณะวิทยาศาสตร์ จุฬาลงกรณ์มหาวิทยาลัย
ปีการศึกษา 2559
ลิขสิทธิ์ของจุฬาลงกรณ์มหาวิทยาลัย

HEAT-
MOISTURE MODIFICATION OF PIGEONPEA *Cajanus cajan* (L.) Millsp. STARCH
IN THE PRESENCE OF DIFFERENT CALCIUM COMPOUNDS AND PHYSICO-
CHEMICAL PROPERTIES OF MODIFIED STARCH.

Miss Suwapat Srijunthongsiri



A Dissertation Submitted in Partial Fulfillment of the Requirements
for the Degree of Doctor of Philosophy Program in Food Technology
Department of Food Technology
Faculty of Science
Chulalongkorn University
Academic Year 2016
Copyright of Chulalongkorn University

Thesis Title HEAT-MOISTURE MODIFICATION OF PIGEONPEA
Cajanus cajan (L.) Millsp. STARCH IN THE PRESENCE
OF DIFFERENT CALCIUM COMPOUNDS AND
PHYSICO-CHEMICAL PROPERTIES OF MODIFIED
STARCH.

By Miss Suwapat Srijunthongsiri

Field of Study Food Technology

Thesis Advisor Assistant Professor Pasawadee Pradipasena, Sc.D.

Thesis Co-Advisor Professor Vanna Tulyathan, Ph.D.

Accepted by the Faculty of Science, Chulalongkorn University in Partial Fulfillment of the
Requirements for the Doctoral Degree

..... Dean of the Faculty of Science
(Associate Professor Polkit Sangvanich, Ph.D.)

THESIS COMMITTEE

..... Chairman
(Associate Professor Saiwarun Chaiwanichsiri, Ph.D.)

..... Thesis Advisor
(Assistant Professor Pasawadee Pradipasena, Sc.D.)

..... Thesis Co-Advisor
(Professor Vanna Tulyathan, Ph.D.)

..... Examiner
(Associate Professor Jirarat Anuntagool, Ph.D.)

..... Examiner
(Associate Professor Kanitha Tananuwong, Ph.D.)

..... External Examiner
(Assistant Professor Anadi Nitithamyong, Ph.D.)

สุภัทธร ศรีจันทร์ทองศิริ : การดัดแปรโดยความร้อนขึ้นของสตาร์ชถั่วมะแฮะ *Cajanus cajan* (L.) Millsp. ในภาวะที่มีสารประกอบแคลเซียมต่างกันและสมบัติทางเคมีกายภาพของสตาร์ชดัดแปร (HEAT-MOISTURE MODIFICATION OF PIGEONPEA *Cajanus cajan* (L.) Millsp. STARCH IN THE PRESENCE OF DIFFERENT CALCIUM COMPOUNDS AND PHYSICO-CHEMICAL PROPERTIES OF MODIFIED STARCH.) อ.ที่ปรีกษาวิทยานิพนธ์
 หลัก: ศศ. ดร. พาสวดี ประทีปะเสน, อ.ที่ปรีกษาวิทยานิพนธ์ร่วม: ศ. ดร. วรณา ตูลยชัย, 147 หน้า.

งานวิจัยนี้ศึกษาผลของชนิดและปริมาณของสารประกอบแคลเซียมที่ใช้ร่วมการดัดแปรด้วยวิธีความร้อนขึ้นต่อโครงสร้างและสมบัติทางเคมีกายภาพของสตาร์ชถั่วมะแฮะ [*Cajanus cajan* (L.) Millsp.] ที่ภาวะปริมาณความชื้นร้อยละ 30 โดยน้ำหนักของสตาร์ชแห้ง ให้ความร้อนที่อุณหภูมิ 110 องศาเซลเซียส นาน 1 ชั่วโมง โดยศึกษาชนิดของแคลเซียม 3 ชนิด ได้แก่ แคลเซียมไฮดรอกไซด์ (Ca(OH)_2) แคลเซียมคลอไรด์ (CaCl_2) และแคลเซียมแลกเตด ($\text{C}_6\text{H}_{10}\text{CaO}_6$) ที่สัดส่วนแคลเซียมไอออนต่อสตาร์ช 4 ระดับ ได้แก่ 0:1 0.0001:1 0.0004:1 และ 0.0007:1 นอกจากนี้ยังได้ศึกษาผลของอุณหภูมิ (100-120 องศาเซลเซียส) และเวลา (1-2 ชั่วโมง) ที่ใช้ในการดัดแปรสตาร์ชถั่วมะแฮะด้วยความร้อนขึ้นในภาวะที่ไม่มี/มีสารประกอบแคลเซียมที่สัดส่วนแคลเซียมไอออนต่อสตาร์ช 2 ระดับ ได้แก่ 0:1 และ 0.0007:1 แล้ววิเคราะห์สตาร์ชด้วยกล้องจุลทรรศน์ (light, polarized light และ scanning electron) X-ray diffraction (XRD) ศึกษาการพองตัว ปริมาณการละลาย ปริมาณแอมิโลสที่ละลายออกมา สมบัติแป็งเปือก ความคงทนต่อการแช่แข็งและละลาย สมบัติทางการไหล (steady shear และ dynamic) ที่ 25 องศาเซลเซียส และสมบัติทางความร้อน ผลการทดลองพบว่าเม็ดสตาร์ชทุกชนิดมีรูปร่างทั้งกลมและรี เมื่อดัดแปรสตาร์ชลักษณะ birefringence ตรงกลางของเม็ดสตาร์ชบางส่วนหายไป birefringence ของสตาร์ชดัดแปรในภาวะที่มีสารประกอบแคลเซียม (HMT-Ca starch) หายไปมากกว่าสตาร์ชดัดแปรในภาวะที่ไม่มีสารประกอบแคลเซียม (HMT-starch) นอกจากนี้ยังพบว่าสตาร์ชดิบมีโครงสร้างผลึกแบบ C และมีปริมาณผลึกสัมพัทธ์ร้อยละ 38.02 แต่เมื่อผ่านการดัดแปรโครงสร้างผลึกเปลี่ยนเป็นแบบ A และปริมาณผลึกสัมพัทธ์ของ HMT-starch และ HMT-Ca starch ดัดแปรน้อยลงอย่างน้อยร้อยละ 18 และ 11 ตามลำดับ ค่ากำลังการพองตัว การละลาย และปริมาณแอมิโลสที่ละลายออกมาของสตาร์ชดัดแปรด้วยความร้อนขึ้นในภาวะที่มี Ca(OH)_2 หรือ $\text{C}_6\text{H}_{10}\text{CaO}_6$ มีค่าลดลง pasting profile ของ HMT-starch และ HMT-Ca starch แตกต่างจากสตาร์ชดิบ คือไม่พบ peak trough breakdown และ setback โดยค่าความหนืดที่อุณหภูมิ 95 องศาเซลเซียส (η_b) และค่าความหนืดที่อุณหภูมิ 50 องศาเซลเซียส (η_c) ของ HMT-Ca starch มีค่าลดลงเมื่อสัดส่วนแคลเซียมไอออนต่อสตาร์ชเพิ่มขึ้น เมื่อดัดแปรสตาร์ชด้วยความร้อนขึ้นในภาวะที่มี Ca(OH)_2 หรือ $\text{C}_6\text{H}_{10}\text{CaO}_6$ มีผลต่อค่ากำลังการพองตัว การละลาย ปริมาณแอมิโลสที่ละลายออกมา η_b และ η_c มากกว่าสตาร์ชดัดแปรด้วยความร้อนขึ้นในภาวะที่มี CaCl_2 สตาร์ชดัดแปรด้วยความร้อนขึ้นในภาวะที่มี Ca(OH)_2 มีค่าความคงตัวต่อการแช่แข็งและละลายดีที่สุด เจล (ร้อยละ 5 โดยน้ำหนัก) ของสตาร์ชทั้งหมดมีลักษณะการไหลแบบ pseudo-plastic with yield stress ตามแบบจำลองของ Herschel-Bulkley เมื่อใช้ Ca(OH)_2 หรือ $\text{C}_6\text{H}_{10}\text{CaO}_6$ การเพิ่มสัดส่วนแคลเซียมไอออนต่อสตาร์ชทำให้ค่า consistency coefficient (K) ลดลง ส่วนค่า flow behavior index (n) เพิ่มขึ้น แต่ไม่มีผลต่อ yield stress (τ_0) ที่ linear viscoelastic region (ความถี่ 0.1-10 Hz และความถี่ร้อยละ 1) เจลสตาร์ชทุกตัวมีลักษณะเป็นของแข็งแบบยืดหยุ่น (elastic-like solid) HMT-Ca starch มีค่า storage modulus (G') ต่ำกว่าสตาร์ชดิบและ HMT-starch การดัดแปรสตาร์ชด้วยความร้อนขึ้น พบว่าอุณหภูมิในการเกิดเจลในในเซชันสูงขึ้นแต่ก่อนทาลปลดลง โดยสตาร์ชดิบมีอุณหภูมิในการเกิดเจลในในเซชันต่ำที่สุด ในขณะที่ HMT-Ca starch มีอุณหภูมิในการเกิดเจลในในเซชันสูงที่สุด เมื่อเก็บเจลในในเซชันที่อุณหภูมิ 5 องศาเซลเซียส นาน 14 วัน พบว่า สตาร์ชดิบมีค่าการคืนตัวร้อยละ 61.98 ในขณะที่ HMT-starch และ HMT-Ca starch มีค่าการคืนตัวน้อยกว่าอย่างน้อยร้อยละ 14.18 และ 49.64 ตามลำดับ นอกจากนี้ เมื่ออุณหภูมิและเวลาที่ใช้ในการดัดแปรเพิ่มมากขึ้น เป็นผลให้กำลังการพองตัว การละลาย ปริมาณแอมิโลสที่ละลายออกมา ค่าการคืนตัว และ ปริมาณผลึกสัมพัทธ์มีค่าลดลง ในขณะที่อุณหภูมิในการเกิดเจลในในเซชันสูงขึ้น สตาร์ชดัดแปรด้วยความร้อนขึ้นในภาวะที่มี Ca(OH)_2 ที่สัดส่วนแคลเซียมไอออนต่อสตาร์ช เท่ากับ 0.0007:1 ที่อุณหภูมิ 120 องศาเซลเซียส เวลา 2 ชั่วโมง มีค่าความคงตัวต่อการแช่แข็งและละลายดีที่สุด

ภาควิชา เทคโนโลยีทางอาหาร

ลายมือชื่อนิสิต

สาขาวิชา เทคโนโลยีทางอาหาร

ลายมือชื่อ อ.ที่ปรีกษาหลัก

ปีการศึกษา 2559

ลายมือชื่อ อ.ที่ปรีกษาร่วม

5373937823 : MAJOR FOOD TECHNOLOGY

KEYWORDS: HEAT-MOISTURE TREATMENT / CALCIUM COMPOUND / PHYSICO-CHEMICAL PROPERTIES / PIGEONPEA STARCH

SUWAPAT SRIJUNTHONGSIRI: HEAT-MOISTURE MODIFICATION OF PIGEONPEA *Cajanus cajan* (L.) Millsp. STARCH IN THE PRESENCE OF DIFFERENT CALCIUM COMPOUNDS AND PHYSICO-CHEMICAL PROPERTIES OF MODIFIED STARCH.. ADVISOR: ASST. PROF. PASAWADEE PRADIPASENA, Sc.D., CO-ADVISOR: PROF. VANNA TULYATHAN, Ph.D., 147 pp.

The effects of the presence of calcium ions (Ca^{2+}) during heat-moisture treatment (HMT) at a 30% moisture content and 110°C for 1 h on the structures and properties of pigeonpea [*Cajanus cajan* (L.) Millsp.] starch were examined. Calcium hydroxide ($\text{Ca}(\text{OH})_2$), calcium chloride (CaCl_2) and calcium lactate ($\text{C}_6\text{H}_{10}\text{CaO}_6$) were used at Ca^{2+} -starch ratios (g/g) of 0:1, 0.0001:1, 0.0004:1 and 0.0007:1. The effects of HMT temperature (100-120°C) and time (1-2 h) were also studied using $\text{Ca}(\text{OH})_2$ at Ca^{2+} -starch ratios of 0:1 and 0.0007:1. The starches were analysed with microscopy (light, polarized light and scanning electron) and X-ray diffraction, as well as for swelling power, % solubility, amylose leaching, pasting properties, freeze-thaw stability, rheological properties (steady shear and dynamic) at 25°C and thermal properties. Granules of native starch, HMT starch in the absence of calcium compound (HMT-starch) and HMT starch in the presence of calcium compound (HMT-Ca starch) were of round and oval shape. The HMT-starch and HMT-Ca starches showed loss of birefringence at the granule center. The presence of calcium compounds led to a greater loss of birefringence. The native starch exhibited a C-type crystalline pattern with 38.02% relative crystallinity (RC). Upon HMT, a crystalline pattern changed to A- type and % RC was at least 18% and 11% lower for HMT-starch and HMT-Ca starches, respectively. An increase in Ca^{2+} -starch ratio increased % RC. Using $\text{Ca}(\text{OH})_2$ or $\text{C}_6\text{H}_{10}\text{CaO}_6$ led to a decrease in swelling power, % solubility and amylose leaching. For pasting properties, the peak, trough, breakdown and setback, which were prominent in the native starch, were absent in the HMT-starch and HMT-Ca starches. For all the calcium compounds used, an increasing Ca^{2+} -starch ratio decreased the viscosities at the end of the heating period at 95°C (η_h) and the cooling period at 50°C (η_c). Using $\text{Ca}(\text{OH})_2$ or $\text{C}_6\text{H}_{10}\text{CaO}_6$ had a stronger effect of the Ca^{2+} -starch ratio on η_h and η_c than using CaCl_2 . The $\text{Ca}(\text{OH})_2$ gave the best freeze-thaw stability starch. All starch suspensions (5% w/w) showed pseudo-plastic with a yield stress following the Herschel-Bulkley model. As regards the use of $\text{Ca}(\text{OH})_2$ and $\text{C}_6\text{H}_{10}\text{CaO}_6$, an increase in Ca^{2+} -starch ratio decreased the consistency coefficient (K) along with increased the *flow* behavior index (n), but did not affect yield stress (τ_0). At their linear viscoelastic region (0.1–10 Hz and 1% strain), all starch gels also exhibited an elastic-like solid. The HMT-Ca starches had lower storage modulus (G') than the native starch and the HMT-starch. The native starch gave the lowest gelatinization temperatures, while the HMT-Ca starches gave the highest gelatinization temperatures. An increase in the Ca^{2+} -starch ratio increased gelatinization temperatures but decreased the gelatinization enthalpy. After storage at 5°C for 7 and 14 days, the regelatinization peak had a lower temperature than the gelatinization peak. After 14 days storage, the % retrogradation of native starch was 61.98, and that of HMT and HMT-Ca starches was at least 14.18% and 49.64% lower, respectively. Using $\text{Ca}(\text{OH})_2$ and $\text{C}_6\text{H}_{10}\text{CaO}_6$ retarded starch retrogradation better than using CaCl_2 . Increases in HMT temperature and time caused greater loss of birefringence at the granule center and the gelatinization temperatures of HMT-starch and HMT-Ca starches. They also decreased η_h , η_c , swelling power, % solubility, amylose leaching, % retrogradation and % RC of these starches. Using $\text{Ca}(\text{OH})_2$ starch at the Ca^{2+} -starch ratio of 0.0007:1, HMT at 120°C for 2 h gave the best freeze-thaw stability starch.

Department: Food Technology
Field of Study: Food Technology
Academic Year: 2016

Student's Signature

Advisor's Signature

Co-Advisor's Signature

ACKNOWLEDGEMENTS

I would like to express my sincere appreciation to my thesis advisor, Asst. Prof. Pasawadee Pradipasena. I have gained the most valuable experience from her expansive vision and knowledge. Her support, understanding, and encouragement have brought me many grateful opportunities in my life. I would like to express my appreciation to my co-advisor, Prof. Dr. Vanna Tulyathan for her valuable advices, constructive comments, and her time spent throughout this work. I would sincerely like to thank my committee members, Assoc. Prof. Saiwarun Chaiwanichsiri, Assoc. Prof. Kanitha Tananuwong, Assoc. Prof. Jirarat Anuntagool and Asst. Prof. Anadi Nitithamyong who all contributed creative suggestions and shared their opinions about the thesis content to help complete it.

I would like to thank the laboratory technicians and all my friends in the Department of Food Technology, Chulalongkorn University for their help and encouragement. I would like to thank Chulalongkorn University for providing a scholarship for my study and funding this research with financial support coming from the 90th Anniversary of Chulalongkorn University Fund (Ratchadaphiseksomphot Endowment Fund). I am grateful to all staff for all their help and technical support for the DSC experiment from Perkin Elmer (Thailand) Co. Ltd.

Finally, I am especially grateful to my father, mother, brother, aunt (Mrs. Thansiri Huajaikaew), uncle (Mr. Awut Huajaikaew) and cousin who have always encouraged and assisted me financially and psychologically in accomplishing this work.

CONTENTS

	Page
THAI ABSTRACT	iv
ENGLISH ABSTRACT.....	v
ACKNOWLEDGEMENTS.....	vi
CONTENTS.....	vii
LIST OF TABLES	x
LIST OF FIGURES	xiii
CHAPTER I INTRODUCTION.....	1
CHAPTER II LITERATURE REVIEWS	5
2.1 Pigeonpea grains.....	5
2.2 Starch.....	6
2.2.1 Physical properties of the starch.....	13
2.2.1.1 Gelatinization and retrogradation	13
2.3 Modified starch.....	19
2.3.1 Physical modification	20
2.3.2 Effects of HMT modification on the properties of starch	23
2.4 Nixtamalization	27
CHAPTER III MATERIALS AND METHODS	29
3.1 Materials	29
3.2 Heat-moisture treatment	29
3.2.1 Effect of calcium compound and Ca ²⁺ -starch ratios (calcium concentration) on the structure and physicochemical properties of starch	29
3.2.2 Effect of temperature and time of heat-moisture treatment on the structure and physicochemical properties of starch	31
3.3 Structure characterization	33
3.3.1 Light microscopy.....	33
3.3.2 Scanning electron microscopy.....	33
3.3.3 X-ray diffraction pattern (XRD).....	33
3.4 Determination of chemical and physical properties	34

	Page
3.4.1 pH of starch suspension.....	34
3.4.2 Calcium content.....	34
3.4.3 Swelling power, % solubility and amylose leaching.....	34
3.4.4 Pasting properties	36
3.4.5 Rheological properties.....	36
3.4.6 Differential scanning calorimetry (DSC)	38
3.4.7 Freeze-thaw stability measurement	39
3.5 Statistical analysis	40
CHAPTER IV RESULTS AND DISCUSSION.....	41
4.1 Chemical compositions	41
4.2 Effect of calcium compound on the physicochemical properties of starch.....	43
4.2.1 Structural characteristics	43
4.2.1.1 Light microscopy.....	43
4.2.1.2 Scanning electron microscopy (SEM).....	45
4.2.1.3 X-ray diffraction and relative crystallinity	47
4.2.2 Swelling power, % solubility and amylose leaching.....	51
4.2.3 Pasting properties of starches	56
4.2.4 Rheological properties.....	59
4.2.5 Thermal properties and retrogradation	64
4.2.6 Freeze-thaw stability	74
4.3 Effect of temperature and time of heat-moisture treatment on the physicochemical properties of starch	77
4.3.1 Structural characteristics	77
4.3.1.1 Light microscopy.....	77
4.3.1.2 Scanning electron microscopy (SEM).....	80
4.3.1.3 X-ray diffraction and relative crystallinity	82
4.3.2 Swelling power, % solubility and amylose leaching.....	85
4.3.3 Pasting properties of starches	88
4.3.4 Rheological properties.....	90

	Page
4.3.5 Thermal properties and retrogradation	95
4.3.6 Freeze-thaw stability	102
4.4 The links between XRD study and physical properties (swelling power, amylose leaching, % retrogradation, K, G' and % syneresis).....	104
4.5 Suggested concentration of starch used for applications.....	104
CHAPTER V CONCLUSIONS	107
REFERENCES	110
APPENDIX.....	119
APPENDIX A Figure of results.....	120
APPENDIX B Procedure for amylose standard curve for amylose leaching	137
APPENDIX C AOAC Official Method 943.02.....	139
APPENDIX D AOAC Official Method 975.03.....	140
APPENDIX E AOAC Official Method 984.27	142
VITA	147

LIST OF TABLES

		Page
Table 2.1	X-ray diffraction peak characteristics for crystalline type A, B, and C.....	12
Table 2.2	Different starch modification types and preparation techniques	21
Table 2.3	HMT conditions for starches and references.	25
Table 3.1	Type and amount of Ca ²⁺ -starch ratio that were used for HMT at 110°C and 50 kPa for 1 h.....	31
Table 3.2	Ca ²⁺ -starch ratio, temperature and time used for the heat-moisture treatment in the presence of Ca(OH) ₂	32
Table 4.1	pH and calcium contents of native starch and HMT-starch that treated at 110°C for 1 h.....	42
Table 4.2	Peak intensities from X-ray diffractograms and relative crystallinity of native starch and HMT-starch that treated at 110°C for 1h.....	50
Table 4.3	Swelling power, % solubility and amylose leaching at 95°C of native starch and HMT-starch that treated at 110°C for 1 h.....	55
Table 4.4	Viscosity at the end of the heating period (η_h) and viscosity at the end of the cooling period (η_c) of 10% w/w native starch and HMT-starch that treated at 110°C for 1 h	58
Table 4.5	Herschel-bulkley constants [yield stress (τ_0), consistency coefficient (K) and flow behavior index (n)] of 5 % w/w native starch and HMT-starch that treated at 110°C for 1 h at 25°C and shear rate between 0.1-1000 s ⁻¹	61
Table 4.6	Rheological properties of gels. The power law model was fitted to experimental measurements.....	63
Table 4.7	Thermal properties of native starch and HMT-starch that treated at 110°C for 1 h.....	70
Table 4.8	Thermal properties of retrograded native starch and HMT-starch that treated at 110°C for 1 h stored at 5°C for 7 days.....	71
Table 4.9	Thermal properties of retrograded native starch and HMT-starch that treated at 110°C for 1 stored at 5°C for 14 days.....	72

Table 4.10	Gelatinization and melting of retrograded starch enthalpy of native starch and HMT-starch that treated at 110°C for 1 h.....	73
Table 4.11	The % syneresis of 5% w/w native starch and HMT-starch that treated at 110°C for 1 h.....	76
Table 4.12	Peak intensities from X-ray diffractograms and relative crystallinity of HMT-starch and HMT-Ca(OH) ₂ starch at the Ca ²⁺ -starch ratio of 0:1 and 0.0007:1	84
Table 4.13	Swelling power, % solubility and amylose leaching at 95°C of HMT starch and HMT-Ca(OH) ₂ starch at the Ca ²⁺ -starch ratio of 0:1 and 0.0007:1.....	87
Table 4.14	Viscosity at the end of the heating period (η_h) and viscosity at the end of the cooling period (η_c) of 10% w/w HMT-starch and HMT-Ca(OH) ₂ starch at the Ca ²⁺ -starch ratio of 0:1 and 0.0007:1	89
Table 4.15	Herschel-bulkley constants [yield stress (τ_0), consistency coefficient (K) and flow behavior index (n)] of 5 % w/w HMT-starch and HMT-Ca(OH) ₂ starch at the Ca ²⁺ -starch ratio of 0:1 and 0.0007:1 at 25°C and shear rate between 0.1-1000 s ⁻¹	92
Table 4.16	Rheological properties of gels. The power law model was fitted to experimental measurements.....	94
Table 4.17	Thermal properties of HMT-starch and HMT-Ca(OH) ₂ starch at the Ca ²⁺ -starch ratio of 0:1 and 0.0007:1.....	98
Table 4.18	Thermal properties of retrograded HMT-starch and HMT-Ca(OH) ₂ starch at the Ca ²⁺ -starch ratio of 0:1 and 0.0007:1 stored at 5°C for 7 days	99
Table 4.19	Thermal properties of retrograded HMT-starch and HMT-Ca(OH) ₂ starch at the Ca ²⁺ -starch ratio of 0:1 and 0.0007:1 stored at 5°C for 14 days	100
Table 4.20	Gelatinization and melting of retrograded starch enthalpy of HMT-starch and HMT-Ca(OH) ₂ starch at the Ca ²⁺ -starch ratio of 0:1 and 0.0007:1	101
Table 4.21	The % syneresis of 5% w/w HMT-starch and HMT-Ca(OH) ₂ starch at the Ca ²⁺ -starch ratio of 0:1 and 0.0007:1	103
Table 4.22	The close packing concentration of starches studied in this research	105

Table 4.23	The close packing concentration of starches studied in this research	106
Table E.1	Suggested operating parameters for ICP emission spectroscopy	145



LIST OF FIGURES

		Page
Figure 2.1	Pigeonpea grains	5
Figure 2.2	Scanning electron microscope images of pigeonpea starch granules.	5
Figure 2.3	Structures of amylose molecule.	7
Figure 2.4	Structures of amylopectin molecule.....	8
Figure 2.5	Cluster model of amylopectin. C = C-chain (reducing end). Solid lines indicate α -(1 \rightarrow 4)-D-glucan chain; arrows indicated α -(1 \rightarrow 6) linkage.....	10
Figure 2.6	Three dimensional crystalline structures for crystalline type A and B.....	11
Figure 2.7	X-ray diffraction pattern for crystalline type A, B, and C.	12
Figure 2.8	Idealized diagram of the gelatinization of a starch granule	14
Figure 2.9	Schematic representation for phase transitions of starch during heating and cooling and aging.	17
Figure 4.1	Microscope and polarized light microscope images of starch granules.	44
Figure 4.2	Scanning electron micrographs of starch granules.	46
Figure 4.3	The X-ray pattern of native starch and HMT-starch that treated at 110°C for 1 h.....	49
Figure 4.4	Viscoelastic properties of 5% w/w native starch and HMT-starch that treated at 110°C for 1 h at 25°C, 1% strain and frequency ranging 0.1 to 10 Hz.....	62
Figure 4.5	Storage modulus (G') of 5% w/w native starch and HMT-starch that treated at 110°C for 1 h at 25°C, 1% strain and frequency ranging 0.1 to 10 Hz.....	62
Figure 4.6	Thermogram of native starch and HMT-starch that treated at 110°C for 1 h.....	69
Figure 4.7	Microscope and polarized light microscope images of starch granules.	79
Figure 4.8	Scanning electron micrographs of starch granules.	81

Figure 4.9	The X-ray pattern Effect of HMT-starch and HMT-Ca(OH) ₂ starch at the Ca ²⁺ -starch ratio of 0:1 and 0.0007:1.....	83
Figure 4.10	Viscoelastic properties of 5% w/w HMT-starch (a) and HMT-Ca(OH) ₂ starch (b) at the Ca ²⁺ -starch ratio of 0:1 and 0.0007:1 at 25°C, 1% strain and frequency ranging 0.1 to 10 Hz.	93
Figure 4.11	Thermogram of HMT-starch and HMT-Ca(OH) ₂ starch at the Ca ²⁺ -starch ratio of 0:1 and 0.0007:1.	97
Figure A.1	Light microscope images of starch granules.....	120
Figure A.2	Polarized light microscope images of starch granules.	121
Figure A.3	Scanning electron micrographs of native starch and HMT-starch granules.	122
Figure A.4	Scanning electron micrographs of HMT-Ca(OH) ₂ starch granules...	123
Figure A.5	Scanning electron micrographs of HMT-CaCl ₂ starch granules.....	124
Figure A.6	Scanning electron micrographs of HMT-C ₆ H ₁₀ CaO ₆ starch granules.	125
Figure A.7	Pasting profile and viscosity of 10% w/w native starch and HMT-starches that treated at 110°C for 1 h.	126
Figure A.8	Thermogram of retrograded native starch and HMT-starches that treated at 110°C for 1 h stored at 5°C for 7 days.	127
Figure A.9	Thermogram of retrograded native starch and HMT-starches that treated at 110°C for 1 h stored at 5°C for 14 days.	128
Figure A.10	Light microscope images of starch granules.....	129
Figure A.11	Polarized light microscope images of starch granules.	130
Figure A.12	Scanning electron micrographs of HMT-starch granules that treated at 100°C.	131
Figure A.13	Scanning electron micrographs of HMT-starch granules that treated at 110°C.	132
Figure A.14	Scanning electron micrographs of HMT-starch granules that treated at 120°C.	133
Figure A.15	Pasting profile of 10% w/w HMT-starch and HMT-Ca(OH) ₂ starch at the Ca ²⁺ -starch ratio of 0:1 and 0.0007:1	134

- Figure A.16** Thermogram of retrograded HMT-starch and HMT-Ca(OH)₂ starch at the Ca²⁺-starch ratio of 0:1 and 0.0007:1 stored at 5°C for 7 days. 135
- Figure A.17** Thermogram of retrograded HMT-starch and HMT-Ca(OH)₂ starch at the Ca²⁺-starch ratio of 0:1 and 0.0007:1 stored at 5°C for 14 days. 136
- Figure A.18** Amylose standard curve for determination of amylose concentration in the supernatant obtained in section 3.4.3 138



CHAPTER I

INTRODUCTION

Starch, a renewable resource, possesses diverse functional properties. It thus has been widely used for numerous applications in various industries, including food and non-food (Adebowale *et al.*, 2005). However, use of native starches sometimes does not provide optimal properties for the design of quality products. Furthermore, native starches still have some drawbacks, which can impair product quality. Such suboptimal properties include retrogradation, syneresis, and instability to heat, shear and pH (Nayouf *et al.*, 2003; Watcharatewinkul *et al.*, 2009; Yadav *et al.*, 2013). The modified starch method is a promising approach to increase the utilizations of starch and make it practical in many applications. Moreover, the functionality of starch depends upon starch type and modifications. The combination between modification methods could produce starch for different products since chemical and physical modifications cause changes in starch structures and result in property changes. Physical modification is a simple, low cost process and is considered environmentally friendly (Sun *et al.*, 2014). The physically modified starch is regarded as natural and safe. Thus, it is a product that fits well current consumer trends (Jacobs and Delcour, 1998; Lawal, 2005; Li *et al.*, 2011; Watcharatewinkul *et al.*, 2009). Heat-moisture modification/treatment (HMT) is a physical modification technique in which starch is modified by heating at limited moisture content (< 35% w/w) and high temperatures ($\approx 84\text{-}120^\circ\text{C}$ for 15 min-16 h) (da Rosa Zavareze and Dias, 2011; Li *et al.*, 2011; Olayinka *et al.*, 2008; Varatharajan *et al.*, 2010). The effect of HMT on starch

depends on the treatment condition, particularly moisture content, temperatures and processing time.

Even though the granule structure was not destroyed during the treatment, changes in X-ray diffraction patterns were found. It has been suggested that the original double helices in the amorphous region and crystalline structure of the native granule are disrupted and recrystallization occurs resulting in the formation of new crystallites (Lawal, 2005; Osundahunsi *et al.*, 2011; Pukkahuta *et al.*, 2008). Due to the reorganization of amylose and amylopectin inside the starch granule, its physicochemical properties changed (Jiranuntakul *et al.*, 2011). Compared to native starch, heat-moisture treated starch (HMT-starch) has a higher gelatinization temperature but less granule swelling and amylose leaching (da Rosa Zavareze and Dias, 2011; Hoover *et al.*, 1993; Sun *et al.*, 2014). This indicates that HMT increases the stability of starch against heat. It has been reported that this treatment leads to a reduction of starch retrogradation and promotes freeze-thaw stability (da Rosa Zavareze and Dias, 2011).

In thermal-alkaline treatment, whole grains are boiled in a calcium hydroxide ($\text{Ca}(\text{OH})_2$) solution for 30-60 min, and then soaked in the alkaline solution for 12-16 h (Bryant and Hamaker, 1997; Mondragón *et al.*, 2004b; Sefa-Dedeh *et al.*, 2004). Partial melting of starch granules, solubilization and denaturation of protein, saponification of lipids, and leaching of amylose occur during this treatment (Mendez-Montevalvo *et al.*, 2006; Mondragón *et al.*, 2004a). When using $\text{Ca}(\text{OH})_2$, it was reported that calcium ion complexes with amylose, amylose-lipid and protein were formed (Ruiz-Guiérrez *et al.*, 2012). It was determined by thermal analysis with a differential scanning calorimeter that the onset, peak and conclusion temperatures

increased by replacing $\text{Ca}(\text{OH})_2$ solution with a solution of either calcium chloride (CaCl_2) or calcium lactate ($\text{C}_6\text{H}_{10}\text{CaO}_6$) in the soaking step. Soaking in a $\text{C}_6\text{H}_{10}\text{CaO}_6$ solution gave the highest values of these transition temperatures (Ruiz-Guiérrez *et al.*, 2012). This modification process gives flour for making Mesoamerican breads and snacks.

In Thailand pigeonpea is an under-utilized crop, therefore, studies of its utilization will give high priority to the social and economic constraints to farmers. Pigeon pea grain is not commonly used for local food and is used for animal feed (Wallis *et al.*, 1988). Land Developing Department of Thailand has been promoting pigeon pea planting to improve soil quality. The seed yield is about 880 to 1,220 kg/rai (Phaikaew *et al.*, 1996). The seed had high in starch content but low in fat content. Starch from this crops should be fully utilized either to make value added products. The knowledge on structures and properties of its starch will facilitate its utilization for industrial applications, which will benefit farmers and industries in Thailand. Through modification, more applications can be derived from this starch.

This research aimed to combine physical modification (HMT) with mild chemical modification using calcium compounds by HMT in the presence of a calcium compound. The calcium compounds used in this study were food additives permitted by The Food and Drugs Administrations (FDAs) of many countries. For this modification, the calcium solutions were used instead of distilled water. The starch-Ca interactions, which might occur during modification, could stabilize starch granules. Therefore HMT in the presence of a calcium compound might give different structures and physicochemical properties of starch from HMT in the absence of any calcium compounds. Hence, this modification will broaden the properties of starch for

various applications. Interestingly, the starch in this research is pigeonpea starch, as it is low in fat content.

Hypothesis and Objectives: This research is based upon the hypothesis that the presence of calcium compounds as well as temperature and time used during HMT are responsible for the structures and physicochemical properties of starch. Therefore, this research aimed:

1. To determine the impact of the presence of different calcium compounds, namely Ca(OH)_2 , CaCl_2 and $\text{C}_6\text{H}_{10}\text{CaO}_6$, during heat-moisture treatment and the weight ratio of calcium ions to starch (Ca^{2+} -starch ratio) on the structures and physicochemical properties of starch.
2. To investigate the influence of temperature and time of heat-moisture treatment on the structures and physicochemical properties of HMT-starch and HMT-Ca starch.

CHAPTER II

LITERATURE REVIEWS

2.1 Pigeonpea grains

Pigeonpea grains (Figure 2.1) is high in starch content (33-45%). The protein and fat contents in pigeonpea grains are 19% and 3%, respectively (Nwokolo, 1987; Roskhrua *et al.*, 2014). Its starch granules are kidney-like in shape (Figure 2.2) with sizes ranging from 4.88 to 60.87 μm in diameter (Roskhrua *et al.*, 2014).



Figure 2.1 Pigeonpea grains

Source: [http://www.tropicalforages.info/key/Forages/Media/Html/Tropical Forages](http://www.tropicalforages.info/key/Forages/Media/Html/Tropical%20Forages) (2016)

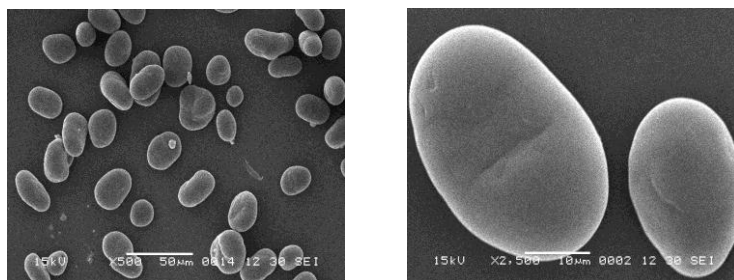


Figure 2.2 Scanning electron microscope images of pigeonpea starch granules
Source: Roskhrua *et al.* (2014)

Pigeonpeas (*Cajanus cajan* L) can grow under poor soil conditions and tolerate dry weather in Australia, Thailand, Indonesia and India (Duke, 1981; Odeny, 2007). It gives high yields of dry seed. These have led to increase interest in the crop. In Thailand, pigeonpea is grown in the north, northeast and in some parts of the south (สังเวียง โพธิ์ศรี ดุสิต มานะจติ และ วีรพล ธรรมคุณ, 2521). Pigeonpeas are both a food crop (dried peas, flour or green vegetable) and a cover crop (Kaushal *et al.*, 2012). It is used in both human consumption and animal feed (Hoover *et al.*, 1993).

2.2 Starch

Starch consists of two polymers—amylose and amylopectin. Starch naturally occurs in the form of a biopolymer granule giving with a unique physical and chemical characteristics (Jacobs and Delcour, 1998). Starch is generally stored in plant cells, including in the leaf, seed, roots, tubers and cereal grains. Starch granule has various sizes and shapes depending on the plant species and locations (Jacobs and Delcour, 1998; Klein *et al.*, 2013). The ratio between amylose and amylopectin varies with plant species (Zobel and Stephen, 1995). The chemical compositions and granular structure of starch affect its functional properties (Jayakody and Hoover, 2008; Klein *et al.*, 2013).

Amylose is a linear chain containing 99% α -(1, 4) and 0.5% α -(1, 6) glucosidic linkages (Figure 2.3a). The sizes of amylose have been shown to vary among botanical sources (Buléon *et al.*, 1998; Jayakody and Hoover, 2008). The degree of polymerization (DP) of amylose ranges from 324 to 4920 glucose units with 9 to 20 branch points (Smith, 1982). The amylose chain has a helical structure with six anhydroglucose units per turn. Hydroxyl group of glucosyl residues are located on the outer surface of the helix, while the internal cavity is a hydrophobic tube.

Therefore, hydrophobic complexing agents can lie within the inner amylose helices and be stabilized by van der Waals' forces between adjacent C-hydrogen of amylose (Figure 2.3b). Its structure allows amylose to form a complex with fat or iodine (Bao and Bergman, 2004; Whistler and BeMiller, 1999). Amylose chains can form inter-hydrogen bonds and create a three-dimensional structure starch gel.

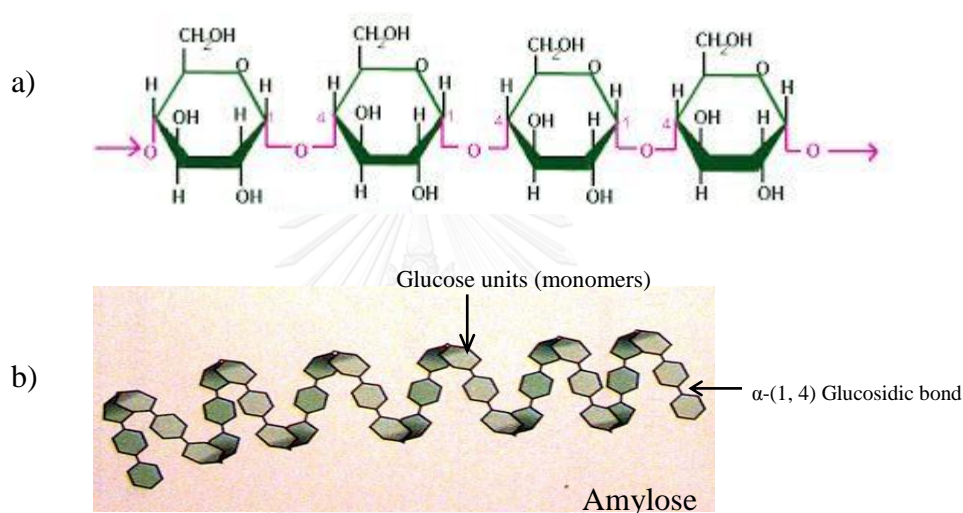


Figure 2.3 Structures of amylose molecule
Source: Smith (1982)

Amylopectin (Figure 2.4) is a highly branched polymer formed by 95% α -(1, 4) glucosidic linkage as a backbone and 5% α -(1, 6) glucosidic linkage branches (Hizukuri, 1985). The DP of amylopectin has been shown to range from 9600 to 15,900 (Buléon *et al.*, 1998; Jayakody and Hoover, 2008; Morrison and Karkalas, 1990).

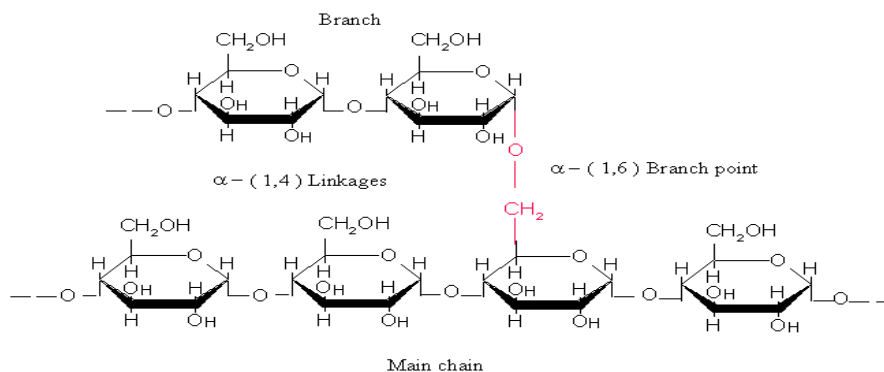


Figure 2.4 Structures of amylopectin molecule
Source: Smith (1982)

In amylopectin, short unit chains are clustered together, and the units of clusters are interconnected by longer chains. The model for the fine structure of amylopectin is polymodal distribution proposed by Hizukuri (1986) as shown in Figure 2.5. In this model, the amylopectin molecule consist of a main chain (C-chain), support chains (B-chain), and outer chains (A-chain). The definitions of the different types of chains and segments of chains, included in this structure are outlined in Figure 2.5 as follows (Hizukuri, 1985):

- The C-chain carries the one reducing end group of the amylopectin molecule and carries other chains. There is only one C-chain per amylopectin molecule and it can be identified by a reducing end located only in the C-chain.
- The B-chain is the chain that connects to the C-chain and/or other B-chains, which can be further divided into B1, B2, and B3 depending on their respective length and the number of clusters their span describe as following:

- B1-chains extend within a single cluster; B1-chains generally have a DP of 15-25,
 - B2-chains extend between two clusters, and so on. By extending clusters, these longer chains provide structural integrity for the whole molecule, and also the long ranging correlations within the granule. B2-chains typically have a DP of 40-50, and
 - B3-chains extend between three clusters and are longer than B1 and B2. B3-chains with a DP of >37.
- A-chains are of α -(1, 6) glucosidic linkage with the B-chains which in turn can be linked to other B-chains or the backbone of the amylopectin molecule (C-chain). The A-chains are shortest (DP= 6-15) and are linked to the amylopectin molecule by a single α -(1, 6) glucosidic linkage. Being linked by a single α -(1, 6) glucosidic bond, A-chains are identified as outer chains.

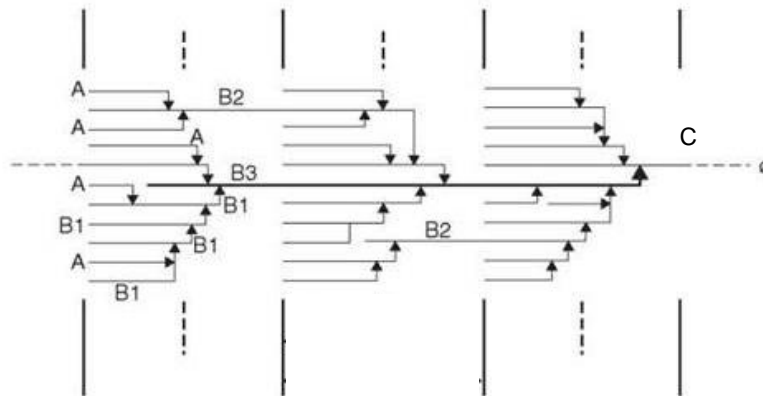
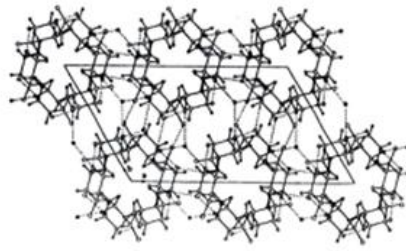


Figure 2.5 Cluster model of amylopectin. C = C-chain (reducing end). Solid lines indicate α -(1 \rightarrow 4)-D-glucan chain; arrows indicated α -(1 \rightarrow 6) linkage
Source: Hizukuri (1985)

The crystalline structures of starch are identified and classified into A, B, or C type through X-ray diffraction patterns (Zobel and Stephen, 1995). The differences between A and B crystalline structures are packing of the helices water content as shown in Figure 2.6 and the quantity of water molecules stabilizing them (Zobel and Stephen, 1995). Double helices of A-type crystalline forms in a monoclinic lattice with unit cell parameters of 2.124 nm wide, 1.172 nm thick and 1.069 nm high with λ equaling 123.5° . The crystalline has maltotriose as a repeating unit and 4 water molecules per 12 glucose residues, 3.6%, per unit cell. B-type crystalline forms in a hexagonal lattice with unit cell parameters of 1.85 nm wide as well as 1.85 nm thick and 1.04 nm. B-crystalline has a greater “opening” between the packing of double helices and a maltose moiety as a repeating unit as well as 36 water molecules, comprising 25%, per cell unit (Hizukuri, 1996; Imberty *et al.*, 1991).

A type



B type

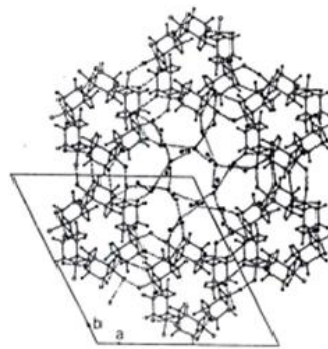


Figure 2.6 Three dimensional crystalline structures for crystalline type A and B
Source: Zobel and Stephen (1995)

The A-pattern is found in cereal starch while the B-pattern is found in root and tuber starches. The C-pattern is a mixture of the A- and B-patterns and found in beans and peas (Huang *et al.*, 2007; Singh *et al.*, 2006; Zobel *et al.*, 1988). Figure 2.7 shows the X-ray diffraction pattern of starch. Pigeonpea starch was reported to have the typical crystallinity pattern of pea starch, the C-type (Kaur and Sandhu, 2010; Ratnayake *et al.*, 2001). Table 2.1 shows the X-ray diffraction characteristics for these three crystalline types (Hizukuri, 1996). According to Bogracheva *et al.* (1999), pea starches have a weak intensity peak at $5.6^\circ 2\theta$, which is characteristically the B-type polymorph, a strong peak at $17.9^\circ 2\theta$, characteristically the A-type

polymorphs, and another peak at $17^\circ 2\theta$ a combination of A and B type polymorphs. The position of small peaks in pea starches can be anywhere between a 5 and 6 degree goniometer angle and various 2θ angle locations as reported by Ratnayake *et al.* (2002).

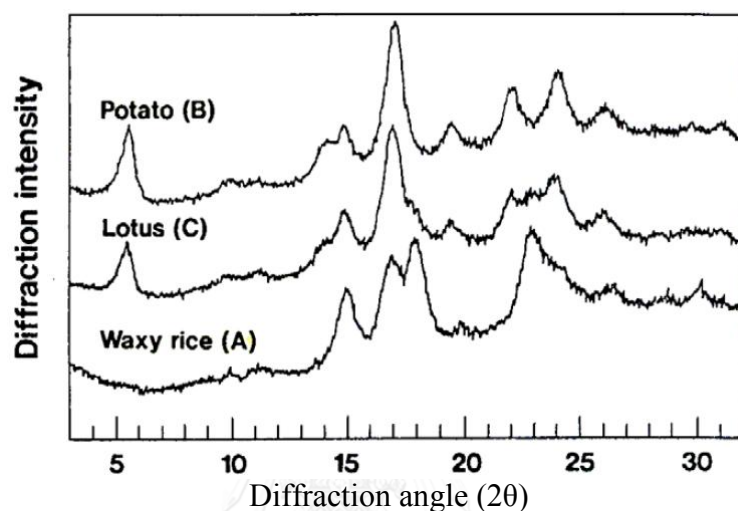


Figure 2.7 X-ray diffraction pattern for crystalline type A, B, and C
Source: Hizukuri (1996)

Table 2.1 X-ray diffraction peak characteristics for crystalline type A, B, and C

Crystalline type	Peak characteristics	
	Strong peak	Weaker peak
A	$15.18^\circ, 17.13^\circ, 18.03^\circ, 22.86^\circ 2\theta$ (5.83, 5.17, 4.91, 3.89 Å)	$11.49^\circ, 20.06^\circ, 26.69^\circ, 30.36^\circ 2\theta$ (7.70, 4.42, 3.34, 2.94 Å)
B	$6^\circ, 17.16^\circ 2\theta$ (14.71, 5.16 Å)	$15^\circ, 21.82^\circ, 24^\circ, 34^\circ, 58.29^\circ 2\theta$ (5.90, 4.07, 3.7, 2.63, 1.58 Å)
C	$17.2^\circ, 18.1^\circ, 23.1^\circ 2\theta$ (5.15, 4.98, 3.85 Å)	$15.18^\circ, 5.54^\circ 2\theta$ (5.8, 15.7 Å)

(Hoover and Sosulski, 1985; Horng, 2007; Ratnayake *et al.*, 2001).

2.2.1 Physical properties of the starch

The properties of starch suspension are similar to those of the synthetic polymer solution which forms crystalline at low temperature (Walstra, 2003). It melts at above a given temperature and forms microcrystallites on cooling.

2.2.1.1 Gelatinization and retrogradation

Gelatinization occurs when starch suspension in excess water is heated. By soaking starch in water, the starch granules take up water and swell slightly. Upon heating, the swelling of granules increase as water uptake and temperature increase. Gelatinization occurs when starch granules are heated up to their gelatinization temperature. The gelatinization temperature is the temperature at which birefringence is first lost, and for starch depends on the botanical source (Varavinit *et al.*, 2003). Loss of birefringence can be observed under polarized light. Non-gelatinized starch granules show birefringence which results in what is referred to as a 'maltese cross' pattern (Fitt and Snyder, 1984). When starch is heated with water the insoluble granules are disrupted by the thermal energy supplied, resulting in a loss of the molecular organization responsible for the crystallinity and penetration of water. When the heating is continued, the hydrogen bonds of the starch chain are weak and the crystallites/double helices are broken and melted (BeMiller and Whistler, 1996). Swelling of the granules results in an increase in viscosity and complete loss of crystallinity, as adjudged by the loss of birefringence. Some of the amylose leaches from the granules while the amylopectin is inside and holds the integrity of the swollen granules as illustrated in Figure 2.8 (Lu *et al.*, 2009).

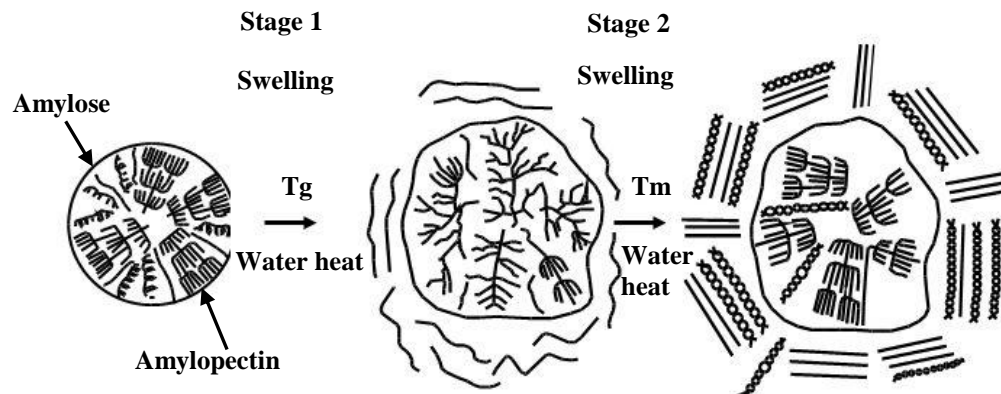


Figure 2.8 Idealized diagram of the gelatinization of a starch granule
Source: Swinkels (1985)

During gelatinization, the thermal properties of starch are determined by differential scanning calorimeter (DSC) as changing in endothermic heat flow with increasing temperature. The thermal properties are gelatinization temperatures [the onset (T_o), peak (T_p), conclusion (T_c)] and enthalpy of gelatinization (ΔH_g). For pigeonpea starch, T_o , T_p , T_c and ΔH_g were found to be in the range of 72-74°C, 77-81°C, 82-87°C and 11-17 J/g, respectively (Hoover et al., 1993; Roskhrua *et al.*, 2014). The thermal properties are influenced by the molecular architecture of the crystalline region, which corresponds to the distribution of amylopectin short chains, DP 6–11 (Li *et al.*, 2011; Noda *et al.*, 1996). Gelatinization involves the melting and uncoiling of the external chains of amylopectin that are packed together as double helices in clusters. A higher gelatinization temperature is an indication of more perfect crystals or a higher co-operative unit, longer chains in the crystal or a larger crystal size (Miao *et al.*, 2009). The ΔH_g reflects the overall crystallinity of amylopectin. The amount of double helical order in native starches

should be strongly correlated to the amylopectin content and granule crystallinity should increase with it and causes an increase in ΔH_g (Tester and Morrison, 1990). The ΔH_g value is calculated from the area of the peak reflecting the loss of double helical order of amylopectin as enthalpy used for gelatinization (Cooke and Gidley, 1992; Tester and Morrison, 1990).

The pasting properties/viscosities during swelling and gelatinization can be recorded using a Rapid Visco Analyzer (RVA). Such highly swollen granules are easily broken and disintegrated by stirring, resulting in a decrease in viscosity. As starch granules swell, hydrated amylose molecules diffuse through the mass to the water, a phenomenon responsible for aspects of paste behavior. At the initial step, the viscosity increases rapidly with an increase in temperature as the granules swell. The peak viscosity is reached when the granules swelling have balanced with the granules broken by stirring. With continued stirring, more granules rupture and fragment causing a further decrease in viscosity (Bao and Bergman, 2004; Whistler and BeMiller, 1999).

On cooling gelatinized starch paste, the reassociation of some starch molecules happens to form precipitate or gel (Whistler and BeMiller, 1999). Retrogradation of the gelatinized starch solution occurs when a heated starch paste cools to below the melting temperature of starch crystallites, and the amylose and amylopectin re-associate and starch molecules partially reassociate to form a precipitate or gel (Vandeputte *et al.*, 2003). The retrogradation of starch proceeds in two crystallization stages. In the first stage, the rigidity and crystallinity of starch gels develop quickly by amylose gelation. In the second, the crystallinity develops slowly by amylopectin (Miles *et al.*, 1985; Yoshimura *et al.*, 1996). Leached amylose can

form and aggregate into double helices and then form microcrystallites. The rapid initial rate of retrogradation relates to the development of amylose-amylose aggregation, with amylose undergoing retrogradation within one day after gelatinization (Bao and Bergman, 2004; Lai *et al.*, 2000; Mita, 1992). Amylopectin forms shorter double helices which can be attributed to the restrictions imposed by the branching structure of the amylopectin molecules. Amylopectin retrogradation proceeds slowly over several weeks of storage and contributes to the long term structural changes of the starch system (Bao and Bergman, 2004; Lai *et al.*, 2000; Mita, 1992). Because the amount of amylopectin in starch is greater than amylose, most of the crystallites formed during long-term starch retrogradation are related to the association of amylopectin chains (Jane and Robyt, 1984; Ring *et al.*, 1987; Sandhu and Singh, 2007; Vandeputte *et al.*, 2003). Figure 2.9 describes the melting and retrogradation of amylopectin as follows: a) new crystalline structure of amylopectin is destroyed during heating in water, and b) its short-branched chain forms a gel-ball, then c) single helix crystals form upon cooling, and finally d) new crystalline forms during aging.

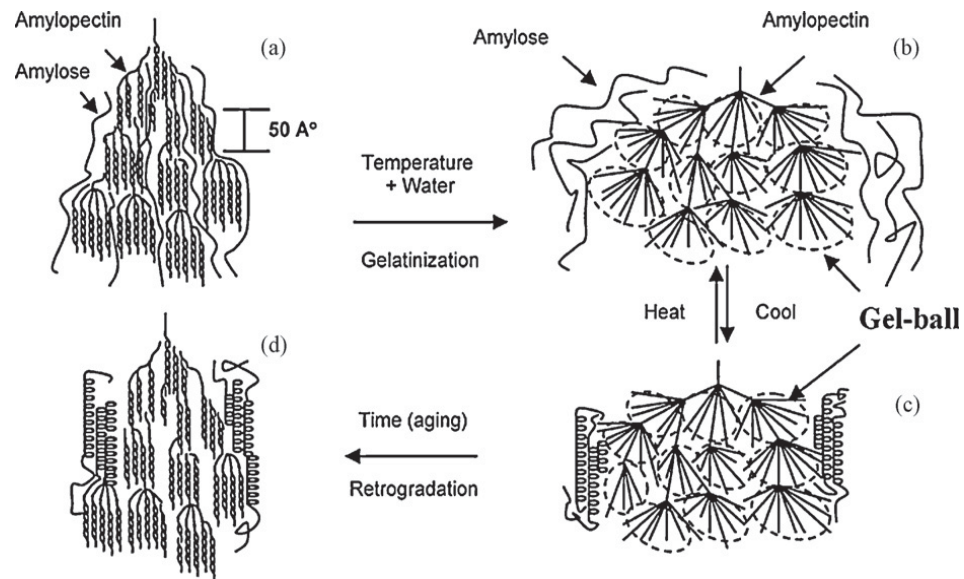


Figure 2.9 Schematic representation for phase transitions of starch during heating and cooling and aging
Source: Yu and Christie (2005)

The retrogradation of gelatinized starch can be measured using DSC by reheating the stored gelatinized starch (Chang and Liu, 1991). The rate of retrogradation strongly depends on the temperature, volume fraction of starch and starch type (Walstra, 2003). Starch retrogradation is governed by a consecutive three step mechanism, which involves nucleation, propagation and maturation or recrystallization. Nucleation, or the formation of nuclei as a sequence of bimolecular processes whereby atoms in the liquid phase join a growing cluster. Propagation or the growth of crystals involves a series of steps in which crystallizing molecules move to the crystal interface and orient themselves into the crystal lattice. During maturation, it has been suggested that crystal perfection and slow crystal growth via Ostwald ripening occurs (Jouppila, 1996; Sahagian and Goff, 1996). Crystallization/recrystallization virtually inhibits at temperature below the glass

transition temperature (T_g). Exponential nature of the temperature dependence of both nucleation and propagation of crystallization is found within the range between T_g and T_c . Rate of nucleation increases as temperature decreases down to the T_g , while rate of propagation increases with temperature up to the T_c . As nucleation (nucleus formation) is retarded at temperature $> 30^\circ\text{C}$, therefore, crystallization occurs at low temperature but only to a limited degree at elevated temperature ($> 30^\circ\text{C}$). Retrogradation should be maximal at the midway temperature between T_g and T_c for long storage period, as the result of both nucleation and propagation take place at moderate rates (Eliasson and Gudmundsson, 1996). The stage of maturation by retrogradation is a function of storage time (Adebowale and Lawal, 2003; Eliasson, 1985). The extent of this association can be interpreted from the area of the peak (enthalpy) during the re-heating of the gelatinized sample (Yoshimura *et al.*, 1999). Compared to native starch, retrograded starch has wider endotherms, indicating that crystallites formed during cooling and aging are large, non-uniform and imperfect. Enthalpy of retrograded starch provides a quantitative measure for the energy required to melt retrograded starch (Karim *et al.*, 2000). The enthalpy required for melting of the retrograded starch is usually between 60–80% smaller than the enthalpy required for gelatinization of the gelatinized native starch because the crystallites in retrograded starch are less stable and easier to break down (Sandhu and Singh, 2007; Sasaki *et al.*, 2000).

Retrogradation of starch is often enhanced when starch gels are subjected to the freezing and thawing process. The rate of retrogradation depends on several variables, including the ratio of amylose to amylopectin, DP of the amylose and amylopectin, starch concentration and storage temperature. The higher amylose to

amylopectin ratios caused the higher retrogradation of the starch gel (Eliasson and Gudmundsson, 1996). It was also found that amylopectin having chain lengths in the range of 75-100 glucose units gave more rapid retrogradation (Zobel and Stephen, 1995). The rate of retrogradation increases with the increased amount of amylose. High concentration of the starch give gel formation and stiffer or more brittle gels occur on longer storage. Storage at low temperature but above the glass transition temperature ($T_g \sim -5^\circ\text{C}$) gave higher the retrogradation than that at room temperature (Eliasson and Gudmundsson, 1996; Varavinit *et al.*, 2002; Walstra, 2003; Whistler and BeMiller, 1999).

2.3 Modified starch

Native starch has been widely used in food processing. The physicochemical properties of this starch and the colloidal sols produced from them are limited in their food applications due to their instability under various temperature, shear force, and pH conditions. Therefore, modification can increase the utilization of starch in various industries, such as the food, paper, and textile industries. Starch modifications are a means of altering the structure and affecting the hydrogen bonding in a controllable manner to enhance and extend their application. The alterations take place at the molecular level, with little or no change taking place in the superficial appearance of the granule. Therefore, the botanical origin of the starch may still be identified microscopically. Starch modification is generally achieved through derivatization such as the etherification, esterification, cross-linking and grafting of starch; conversion (acid or enzymatic hydrolysis and oxidization of starch) or the physical treatment of starch using heat or moisture as described in Table 2.2 (Singh *et al.*, 2007).

2.3.1 Physical modification

Physical modifications of starch such as moisture, heat, and shear force have been gaining wide acceptance because neither by-products nor chemical reagents are present in the modified starch like that of chemical modifications (Bao and Bergman, 2004). Annealing (ANN) and heat-moisture treatment (HMT) are two common physical modifications. These treatments make starch obtain the modified properties without destroying the granule structure. These two related processes require controlling the moisture ratio, temperature, and heating time. However, these treatments use different amounts of water and temperature levels.

ANN is generally carried out by heating granular starch with an intermediate to large quantity of water (40% w/w - > 60% w/w) at a temperature above the glass transition temperature (T_g) but below the starch gelatinization point (40-75°C) for a set period of time (Jayakody *et al.*, 2009; Maache-Rezzoug *et al.*, 2008; Waduge *et al.*, 2006). ANN leads to the reorganization of starch molecules, and amylopectin double helices acquire a more organized configuration (da Rosa Zavareze and Dias, 2011).

Table 2.2 Different starch modification types and preparation techniques

Modification	Types	Preparation
Physical	Heat/moisture treatment	Heat-moisture treatment- Heating starch at a temperature above its gelatinization point with insufficient, moisture to cause gelatinization Annealing-Heating a slurry of granular starch at a temperature below its gelatinization point for prolonged periods of time
	Pregelatinization	Pregels/ instant/ cold-water swelling starches prepared using drum drying/ spray cooking/ extrusion/ solvent-based processing
Conversion	Partial acid hydrolysis	Treatment with hydrochloric acid or ortho-phosphoric acid or sulphuric acid
	Partial enzymatic hydrolysis	Treatment in an aqueous solution at a temperature below the gelatinization point with one or more food-grade amylolytic enzymes
	Alkali treatment	Treatment with sodium hydroxide or potassium hydroxide
	Oxidation/bleaching	Treatment with peracetic acid and/or hydrogen peroxide, or sodium hypochlorite or sodium chlorite, or sulphur dioxide, or potassium permanganate or ammonium persulphate
	Dextrinization	Pyrodextrins-Prepare by dry roasting acidified starch
Derivatization	Etherification	Hydroxypropyl starch- Esterification with propylene oxide
	Esterification	Starch acetylated-Esterification with acetic anhydride or vinyl acetate
		Acetylated distarch adipate-Esterification with acetic anhydride and adipic anhydride
	Cross-linking	Starch sodium octenylsuccinate- Esterification by octenylsuccinic anhydride
Monostarch phosphate- Esterification with ortho-phosphoric acid, or sodium or potassium orthophosphate, or sodium tripolyphosphate		
Distarch phosphate- Esterification with sodium trimetaphosphate or phosphorus oxychloride		
Dual modification	Phosphated distarch phosphate-Combination of treatments for monostarch phosphate and Distarch phosphate	
	Dual modification	Acetylated distarch phosphate- Esterification by sodium trimetaphosphate or phosphorus oxychloride combined with esterification by acetic anhydride or vinyl acetate Hydroxypropyl distarch phosphate- Esterification by sodium trimetaphosphate or phosphorus oxychloride combined with etherification by propylene oxide

(Singh *et al.*, 2007)

ANN has been shown to cause changes to starch structure (increase in granule stability, perfection of starch crystalline, formation of new double helices, interaction between glucan chains and an increase in contrast between crystalline and amorphous lamella) and properties (elevation of gelatinization temperature, narrowing of the gelatinization temperature range decrease in swelling power and amylose leaching, increase in hot and cold paste viscosities) (da Rosa Zavareze and Dias, 2011; Dias *et al.*, 2010; Jayakody *et al.*, 2009; Lan *et al.*, 2008; Waduge *et al.*, 2006).

Heat-moisture treatment (HMT) is a hydrothermal treatment technique that heats starch granules at low levels of moisture (< 35% slurry in water) and a relatively high temperature (80-140°C) above its glass transition temperature but below the temperature when gelatinization occurs, for a period of time ranging from 15 min to 16 h (Chung *et al.*, 2009; da Rosa Zavareze and Dias, 2011; Jacobs and Delcour, 1998). Jayakody and Hoover (2008) postulated that the effect of heat-moisture treatment may be due either to new crystallization or recrystallization and the perfection of small crystalline regions of the starch granule. However, the heat-moisture modification conditions must not allow the starch to reach gelatinization (Gunaratne and Hoover, 2002; Jacobs and Delcour, 1998). For instance, HMT starch at 100°C for 16 h with 30% moisture content (Hoover *et al.*, 1993) and HMT at 110°C for 1 h, especially with 25% moisture content (da Rosa Zavareze *et al.*, 2010; Horndok and Noomhorm, 2007) have been shown to strongly alter the physicochemical properties of starch including: decreasing the swelling power, increasing the stability of starch pastes to heat and shear, reducing amylose leaching and increasing the gelatinization temperature of starch. HMT was used in this study,

therefore, only the effects of HMT on starch properties are reviewed in the next section.

2.3.2 Effects of HMT modification on the properties of starch

Compared to native starch, HMT-starch has a higher gelatinization temperature and broad gelatinization temperature range, with a reduction in gelatinization enthalpy (Chung *et al.*, 2009; da Rosa Zavareze and Dias, 2011; Gunaratne and Hoover, 2002; Hoover *et al.*, 1993; Sun *et al.*, 2014). Heat-moisture treatment also increases the pasting temperature, but decreases the swelling power and amylose leaching (Chung *et al.*, 2009; da Rosa Zavareze and Dias, 2011; Hoover *et al.*, 1993). It has been reported that this treatment leads to a reduction of starch retrogradation and promotes freeze-thaw stability (da Rosa Zavareze and Dias, 2011; Gunaratne and Hoover, 2002; Hoover and Manuel, 1996; Hoover *et al.*, 1993; Sun *et al.*, 2014). The pasting properties of HMT starch sample exhibit a decrease of peak viscosity, breakdown and final viscosity (Pukkahuta *et al.*, 2008). Compared to their native counterpart starches, the HMT of mung bean, finger millet and rice starch granules have cracks on the surface and are more aggregated (Adebowale *et al.*, 2005; da Rosa Zavareze *et al.*, 2010; Jiranuntakul *et al.*, 2011; Li *et al.*, 2011). Changes in the X-ray diffraction pattern from B- to A-type has been found in HMT potato and yam starch (Gunaratne and Hoover, 2002). For HMT starch, the enthalpy of gelatinization decreases as treatment time increases (Arns *et al.*, 2015; Pukkahuta *et al.*, 2008). However, HMT increases the gelatinization temperatures of HMT-starches as the treatment temperature increases (Chung *et al.*, 2009). From their properties, HMT starch may be a good product for making noodles as well as using in canned and frozen food products (da Rosa Zavareze *et al.*, 2010; Horndok and Noomhorm,

2007). The film of HMT starch has a higher tensile strength and puncture energy, but lower solubility than that of native starch (da Rosa Zavareze and Dias, 2011). Heat-moisture treatment in mildly acidic conditions enhances the starch granular stability to heat and shear (Kim and Huber, 2013). From DSC study, HMT-starch showed biphasic thermogram of the starch melting endotherm, which suggested either formation of new crystal or rearrangement of crystalline of HMT-starch. From XRD study, heat-moisture treatment induced changes in both crystalline and amorphous regions in starch granules. The XRD pattern showed that upon heat-moisture treatment crystallites were stronger than the native starch. For example, the native tuber starches have B-type, while their HMT-starches were found to have A-type. In starch granule, crystalline regions are interconnected by the continuous amorphous regions. Biliaderis *et al.* (1986) suggested that there was a presence of intercrystalline amorphous parts and they inhibited the mobility of amorphous chains caused the T_g of native starch to be higher than T_g of the gelatinized starch. The T_g represents the transition of the inherent amorphous state of the starch. Therefore, starches with different T_g were definitely different in the amorphous chain conformation. In heat-moisture treatment, T_g is fully affected by the residual water. Lim *et al.* (2001) found that T_g of HMT-starch was lower than the native starch. This indicated that the intercrystalline parts were transformed into independent amorphous states during heat-moisture treatment. Thus the amorphous portion in the HMT-starch could be increased. The effect of temperature, time and water content used for heat-moisture treatment on the structures and properties of various starch are summarized in Table 2.3.

Table 2.3 HMT conditions for starches and references

Starch source	Temperature (°C)	Time	Water content (%)	Structure and properties	Reference
Cassava	110	10 h	30	Changes in X-ray diffraction pattern from B- to A-type,	Gunaratne and Hoover (2002)
	100	16 h	18-25	Increase in the x-ray intensity in the diffraction pattern of starch, Reduction in relative crystallinity	Watcharatewinkul <i>et al.</i> (2009)
Pea	120	2 h	30	Reduction in swelling power, Increase in past temperature and decreased peak and final viscosity, Increased gelatinization temperature and decreased ΔH_g	Chung <i>et al.</i> (2009)
Pigeon pea	100	16 h	30	Reduction in swelling power Increased gelatinization temperature and decreased ΔH_g Decreased the % syneresis	Hoover <i>et al.</i> (1993)
Potato	100	16 h	24	Reduction in swelling power, Increase in past temperature and decreased peak and final viscosity Increased gelatinization temperature and decreased ΔH_g	Varatharajan <i>et al.</i> (2010)
Sweet potato	110	4-16 h	25	Reduction in swelling power, Increase in past temperature and decreased peak and final viscosity, Increased gelatinization temperature	Collado and Corke (1999)

Table 2.3 (continue) Heat-moisture treatment conditions for starches

Starch source	Temperature (°C)	Time	Water content (%)	Structure and properties	Reference
Sweet potato	110	4-16 h	25	Reduction in swelling power,	Collado and Corke (1999)
				Increase in past temperature and decreased peak and final viscosity, Increased gelatinization temperature	
White sorghum	110	16 h	18-27	Reduction in swelling power and solubility,	Olayinka <i>et al.</i> (2008)
				Increase in past temperature and decreased peak and final viscosity	
				Increased gelatinization temperature and decreased ΔH_g	
Rice	100-110	0.5-1.5 h	15-25	Reduction in relative crystallinity ,	Horndok and Noomhorn (2007)
	100	16 h	18-27	Reduction in swelling power,	Khunae <i>et al.</i> (2007)
	110	1 h	15, 20, 25	Increase in past temperature and decreased peak and final viscosity, Increased gelatinization temperature and decreased ΔH_g	da Rosa Zavareze <i>et al.</i> (2010)
Sago	100-120	1 h	20	Increase in past temperature and decreased peak and final viscosity,	Pukkahuta and Varavimit (2007)
				Increased gelatinization temperature and decreased ΔH_g	
Finger millet	100	16 h	20-30	Increased gelatinization temperature and decreased ΔH_g	Adebowale <i>et al.</i> (2005)
				Reduction in swelling power,	
				Increase in past temperature and decreased peak and final viscosity, Increased gelatinization temperature and decreased ΔH_g	

2.4 Nixtamalization

Flour modified by thermal-alkaline treatment, nixtamalization, has been consumed for more than 100 years. Currently, products from this modified flour are being consumed worldwide. In this treatment, whole grains are boiled in either calcium hydroxide solution ($\text{Ca}(\text{OH})_2$ solution) or sodium hydroxide solution for 30-60 min, and then soaked in the alkaline solution for 12-16 h (Bryant and Hamaker, 1997; Mondragón *et al.*, 2004b; Sefa-Dedeh *et al.*, 2004). During nixtamalization, these phenomena occur in the following order (Mendez-Montealvo *et al.*, 2006; Mondragón *et al.*, 2004a).

- softening of the hull,
- diffusion of water and $\text{Ca}(\text{OH})_2$, in the forms of OH^- ions and Ca^{2+} ions, (or potassium hydroxide) into the kernel,
- swelling and partial gelatinization of starch granules losing crystallinity, leaching of amylose and reaction between the leached amylose chains and calcium ions
- solubilization and denaturation of protein, as well as reaction among denatured proteins and reaction between denatured protein and other components (such as lipid, starch and calcium ions)
- saponification of lipid (formation of calcium salt of fatty acids)

When using $\text{Ca}(\text{OH})_2$, it was reported that calcium ion complexes with amylose, amylose-lipid and protein were formed (Ruiz-Guiérrez *et al.*, 2012). The calcium-amylose, Ca-amylose, interactions inhibit the transferring of water into

starch granules, and thus limit the granule swelling and gelatinization of the middle part of starch granules (Laria *et al.*, 2007; Mondragón *et al.*, 2006; Robles *et al.*, 1988; Rodríguez *et al.*, 1996).

The starch-Ca interaction was reported to occur during thermal-alkaline treatment of flour. The product of the thermal-alkaline processes is a modified corn flour (Mendez-Montevalvo *et al.*, 2006; Sefa-Dedeh *et al.*, 2004). Most studied on heat-moisture treatment have used starches from different sources (such as rice, potato, wheat, maize and sorghum) and different moisture content during heat-moisture treatment. However, to our knowledge, no study has reported effect of salts on the heat-moisture treatment. The main purpose of this study was to investigate effect of HMT using different calcium compounds including Ca(OH)_2 , CaCl_2 and $\text{C}_6\text{H}_{10}\text{CaO}_6$ on chemical and physical properties of pigeonpea starch and different temperature and time of heat-moisture treatment process to characterize their crystallization patterns, pasting properties, thermal properties and rheological behavior. Their potential applications in frozen food industry will be determine. The Ca(OH)_2 was selected as it was used in the thermal-alkaline process. The CaCl_2 and $\text{C}_6\text{H}_{10}\text{CaO}_6$ were selected because they are common food additives use in many food industries (FDA, 2008).

CHAPTER III

MATERIALS AND METHODS

3.1 Materials

Pigeonpea starch was provided by Assistant Professor Dr. Piyanuch Roskhrua, Rajamangala University of Technology Lanna (Nan Campus). It was isolated from the seed of pigeonpea grown in Nan Province, Thailand as described in Roskhrua *et al.* (2014). The starch was kept at $8\pm 2^{\circ}\text{C}$ (SRM-2DB, Sanyo, Thailand). The percentage of dry basis of chemical contents (crude protein, total lipid, crude fiber, ash, carbohydrate and amylose content) were analyzed according to AOAC (2012) and were 0.43 ± 0.03 , 0.31 ± 0.03 , 0.40 ± 0.03 , 0.45 ± 0.04 , 98.42 ± 0.05 and 31.15 ± 0.12 , respectively.

Analytical grade calcium hydroxide, $\text{Ca}(\text{OH})_2$ (Bio Basic, Canada), calcium chloride, CaCl_2 (Ajax Finechem, NZ), and calcium lactate, $\text{C}_6\text{H}_{10}\text{CaO}_6$ (Biological, USA), were used in these experiments.

3.2 Heat-moisture treatment

3.2.1 Effect of calcium compound and Ca^{2+} -starch ratios (calcium concentration) on the structure and physicochemical properties of starch

Prior to the heat-moisture treatment process (HMT), the moisture content of the kept starch was determined by an infrared auto-moisture analyzer (MJ 33, Mettler Toledo, Switzerland), the moisture content was 11.30% and adjusted to 30% w/w by adding an appropriate amount of distilled water. Heat-moisture treatment in the presence of calcium compound was done by dissolving each calcium compound in distilled water before adding to the starch. The amount of calcium compound added

to the water was calculated to obtain the Ca^{2+} -starch ratios. These experiments comprised 3x3 factorial experiments with a control, and they were prepared by varying three types of calcium compound ($\text{Ca}(\text{OH})_2$, CaCl_2 and $\text{C}_6\text{H}_{10}\text{CaO}_6$), and three levels of Ca^{2+} -starch ratios (0:1, 0.0001:1, 0.0004:1 and 0.0007:1) as shown in Table 3.1. The mixture was stirred with a hand mixer (BUO-153263, Buono, Germany) at speed No. 1 for 2 min followed by speed No. 2 for 10 min and then kept in a sealed aluminium foil bag for 2 h at room temperature ($25\pm 1^\circ\text{C}$). After verifying the moisture content, the sample was kept in the sealed aluminium foil bag at $5\pm 1^\circ\text{C}$ for 24 h. Then, a sample (100 g) was transferred into a pressure-resistant glass bottle (250 ml, Schott Duran, Germany). The bottle was tightly sealed, placed and heated in an autoclave (SS-325, Tomy, USA) at 110°C and 50 kPa gauge for 1 h. After this, the sealed bottle was taken out and let stand to cool to room temperature ($25\pm 1^\circ\text{C}$) for 1 h. The heat-moisture treated starch was dried in hot air oven (EDIFA, Binder, USA) at 40°C for 16 h. The moisture content of the dried HMT starch was determined to be 10% w/w. It was ground, sieved through a 100 mesh sieve, kept in the sealed aluminium foil bag at $8\pm 2^\circ\text{C}$. All treated starches were determined for light/polarize light microscopy, scanning electron microscopy, chemical composition, crystalline pattern, swelling power, % solubility, amylose leaching, pasting properties, freeze-thaw stability, rheological properties and the thermal properties, compared to the native starch.

The heat-moisture treated starches in the presence or absence of calcium compound are referred to as HMT-Ca starch or HMT-starch (control), respectively. The heat-moisture treated starch in the presence of $\text{Ca}(\text{OH})_2$, CaCl_2 or

$C_6H_{10}CaO_6$ are referred to as HMT- $Ca(OH)_2$ starch, HMT- $CaCl_2$ starch or HMT- $C_6H_{10}CaO_6$ starch, respectively.

Table 3.1 Type and amount of Ca^{2+} -starch ratio that were used for HMT at 110°C and 50 kPa for 1 h

Treatment	Ca^{2+} :Starch	Concentration of Calcium Solution (mol/L)
Native	0:0	-
HMT	0:1	-
HMT- $Ca(OH)_2$	0.0001:1	0.014
	0.0004:1	0.034
	0.0007:1	0.063
HMT- $CaCl_2$	0.0001:1	0.014
	0.0004:1	0.034
	0.0007:1	0.063
HMT- $C_6H_{10}CaO_6$	0.0001:1	0.014
	0.0004:1	0.034
	0.0007:1	0.063

3.2.2 Effect of temperature and time of heat-moisture treatment on the structure and physicochemical properties of starch

Calcium compound and Ca^{2+} -starch ratio used in this part were selected from the results of the first part that gave lower swelling power, %solubility, amylose leaching and gelatinization enthalpy (ΔH_g), and higher freeze-thaw stability than the common HMT starch and native starch. The process of the heat-moisture

treatment was the same as describe in section 3.2.1, except the heating temperatures and heating times of heat-moisture treatment. The heating temperature and heating times used in this study were listed in Table 3.2. The experimental design is a 3x2x2 factorial experiment: three levels of temperature (100°C, 110°C and 120°C), two levels of time (1 h and 2 h), and two levels of Ca²⁺-starch ratios (0:1 as control and 0.0007:1). All treated starches were determined for light/polarize light microscopy, scanning electron microscopy, crystalline pattern, swelling power, % solubility, amylose leaching, pasting properties, freeze-thaw stability, rheological properties and the thermal properties.

Table 3.2 Ca²⁺-starch ratio, temperature and time used for the heat-moisture treatment in the presence of Ca(OH)₂

Treatment	Ca ²⁺ :Starch	Temperature (°C) /Corresponding Pressure (kPa)	Time (h)
HMT	0:1	100/0	1
			2
		110/50	1
			2
		120/110	1
			2
HMT-Ca(OH) ₂	0.0007:1	100/0	1
			2
		110/50	1
			2
		120/110	1
			2

3.3 Structure characterization

3.3.1 Light microscopy

The shape of starch granules was also observed by light microscopy. Starch was dispersed in distilled water containing glycerin (1:1 v/v). The starch suspension was dropped on a glass slide and placed under an optical microscope (BX 51TF, Olympus, Japan) equipped with Pinnacle Media Center (PCTV USB2, Pinnacle System GmbH, Germany), and the image of starch granules was taken and recorded at a magnification of 100X. The granule birefringence image of the same starch granules was also taken and recorded by placing a polarized film (U-POT, Olympus, Japan) over the light source.

3.3.2 Scanning electron microscopy

The starch powder was spread on a carbon sheet. Then, the carbon sheet containing starch samples was placed on an aluminium stub and dried in an oven at 40°C for 16 h. Subsequently, all of the samples were coated with gold-palladium using an ion sputter (Balzers Union SCD 040, Balzers Union Ltd., Liechtenstein). The shapes and surfaces of the starch granules were determined using a scanning electron microscope (JSM-5410 LV, JEOL Ltd., Japan) at an acceleration potential of 15 kV and magnification of 500X, 1,000X and 2,000X.

3.3.3 X-ray diffraction pattern (XRD)

Prior to crystallinity determination, a sample was kept over a saturated NaCl solution (relative humidity about 75%) in a desiccator under a vacuum for 2 weeks to obtain a sample with moisture content of about 15% w/w (wet basis, wb). Crystallinity of the starch granule was analyzed using a wide angle X-ray diffractometer (D8 Discover, Bruker AXS, Germany) equipped with a copper source

operating at 40 kV and 40 mA, producing X-rays as monochromatic copper K_{α} radiation with a wavelength of 0.154 nm. The diffraction data were collected over an angular range from 5 to 40° (2θ) at increment of 0.02 degree/step and scan speed of 0.5 sec/step. The X-ray pattern was compared with the peak characteristics of the theoretical diffractogram given by Zobel (1964). The relative crystallinity was determined quantitatively from the ratio of the sharp peak area to the total peak area (Nara and Komiya, 1983) using a peak-fitting software (Topas version 3, Bruker AXS, Germany).

3.4 Determination of chemical and physical properties

3.4.1 pH of starch suspension

The pH of the starch was determined following AOAC (2012) No. 943.02.

3.4.2 Calcium content

Prior to determining the calcium content, the starch was washed out with distilled water at a starch-water ratio of 1:10 (3 times). The starch was dried in a hot air oven (EDIFA, Binder, USA) at 40°C for 16 h. The calcium content in the starch was determined following AOAC (2012) No. 975.03 and No.984.27.

3.4.3 Swelling power, % solubility and amylose leaching

The method of Ceballos *et al.* (2007) was used to determine swelling power and % solubility. Starch suspension (1% w/w) was heated from 40 to 95°C at 6°C/min and kept at 95°C for 30 min in a Rapid Visco Analyzer (RVA, Model 4D, Newport Scientific, Australia). The gelatinized starch suspension was immediately centrifuged at 8,000xg for 5 min at 25°C (IEC Muti Rf, Thermo IEC, USA). The supernatant and sediment were separated using a micropipette (Pipet-Lite, Rainin

Instrument, USA), weighed and dried at 100°C (24 h for supernatant and 48 h for sediment), and then weighed again. The swelling power and solubility were calculated using Equations 1 and 2, respectively.

$$SP = (w_{sed}/w_{sed_d}) \quad [1]$$

$$S = (w_{sup_d}/w_{sam_{db}})(100) \quad [2]$$

where SP = swelling power (g wet gel/g dry gel)

S = solubility (%)

w_{sed} = weight of wet sediment (g)

w_{sed_d} = weight of dried sediment (g)

w_{sup_d} = weight of dry solid in supernatant (g)

$w_{sam_{db}}$ = weight of sample on dry basis = 0.4±0.02 g

For amylose leaching determination, the amylose content in the supernatant was determined as described by Chrastil (1987). A supernatant of 1 ml was added to 6 ml of 0.3 M NaOH and heated at 95±1°C for 30 min in a water bath (WNB22, Memmert, Germany). Then, 1 ml of 0.5% trichloroacetic acid (AppliChem Panreac, Germany) and 0.05 ml of 0.1 N I₂-KI solution was added to 0.1 ml of this solution. The solution was kept in a dark room at room temperature (25±1°C) for 30 min. The absorbance was measured at 630 nm using a UV-visible spectroscope (Spectronic GENESYS 20, Thermo scientific, USA). The standard curve was constructed using pure potato amylose (Sigma, UK) as shown in Appendix B. The percentage amylose leaching was calculated and reported as mg of amylose leached per 100 mg of original amylose content in the dry sample using Equation 3.

$$AL = 100[C_A(10^3 D_S)T_S]/(w_{\text{sam}_{\text{db}}} A/100) \quad [3]$$

where

AL = amylose leaching (%)

C_A = amylose concentration in supernatant

D_S = correction for dilution of supernatant (ml of final solution per ml of supernatant)

T_S = total volume of supernatant (ml)

w_{sam_{db}} = weight of sample on dry basis (mg)

A = amylose content in dry sample (%)

3.4.4 Pasting properties

The pasting properties of starch were determined using a Rapid Visco Analyser and Thermocline software (Newport Scientific, Australia). A starch suspension of 10% w/w and 28 g total weight was obtained by adding a pre-calculated amount of starch and mixing to preweighed distilled water in the RVA sample canister. The RVA plastic paddle was manually rotated for 30 s to uniformly disperse the starch suspension before measurement. The temperature-stirring rate-stirring time profile of Standard #1 was used. This profile consisted of stirring at 960 rpm and 50°C for 10 s, and then while stirring at 160 rpm, heating from 50 to 95°C at 10°C/min, holding at 95°C for 3 min, cooling to 50°C at 12°C/min, and then holding at 50°C for 2 min. The total run time was 13 min.

3.4.5 Rheological properties

Starch was weighed and then dispersed into distilled water to obtain the concentration of 5% w/w. The starch suspension was stirred using a magnetic stirrer for 15 min at room temperature (25°C), heated to 95±1°C and kept at 95±1°C

for 30 min in a boiling-water bath (WNB22, Memmert, Germany), while it was kept stirring. The starch paste was centrifuged at 190xg for 2 min to remove air bubbles and kept in 40°C for 15 min in a water bath (ONE7, Memmert, Germany) before measurements to prevent gel formation. Both the steady shear and viscoelastic properties of starch paste were determined using a stress-controlled rheometer (Bohlin Gemini™ 150, Malvern Instruments, UK), equipped with a 40 mm-diameter cone and plate test fixture (CP 1/40, cone angle 1°, gap 500 µm). Starch paste (1.5 ml) was loaded onto the plate and was covered with paraffin liquid (Ajax Finechem, NZ) to prevent water evaporation. The temperature of the paste was allowed to reach equilibrium of 25±0.5°C for 30 s on the plate. The steady shear measurement was carried out by sweeping from the shear rate of 0.1 to 1000 s⁻¹ in 300 s.

The viscoelastic properties were determined at the predetermined linear viscoelastic region of all paste of 1% strain and frequency range from 0.1 to 10 Hz. The average values of storage modulus (G') and loss modulus (G'') were reported.

The power law model, Equation 4 (Herschel-Bulkley) or Equation 5-7, was used for the calculation of the steady shear properties or frequency dependence;

$$\tau = \tau_0 + K\dot{\gamma}^n \quad [4]$$

where τ = shear stress (Pa)

τ_0 = yield stress (Pa)

$\dot{\gamma}$ = shear rate (s⁻¹)

K = consistency coefficient (Pa·sⁿ);

n = flow behavior index.

$$G'(\omega) = G'_1 \omega^a \quad [5]$$

$$G''(\omega) = G''_1 \omega^b \quad [6]$$

$$\begin{aligned} \tan \delta (\omega) &= G''(\omega)/G'(\omega) \\ &= (G''/G')_1 \omega^c \\ &= (\tan \delta)_1 \omega^c \end{aligned} \quad [7]$$

where G' = storage modulus (Pa) at a frequency of 1 Hz

G''_1 = loss modulus (Pa) at a frequency of 1 Hz

ω = angular frequency (Hz)

a, b and c = exponential constant.

3.4.6 Differential scanning calorimetry (DSC)

A sample (4 ± 0.2 mg, db) was placed in pre-weighed stainless-steel DSC pan. Distilled water (12 μ l) was added. The pan was hermetically sealed and the sample was allowed to equilibrate overnight before analysis at room temperature ($29 \pm 1^\circ\text{C}$). The thermal properties, onset temperature (T_o), peak temperature (T_p), conclusion temperature (T_c) and enthalpy (ΔH), of the starch were studied by heating the pan from 20°C to 140°C at the rate of $10^\circ\text{C}/\text{min}$ in a differential scanning calorimeter (DSC8000, Perkin- Elmer, USA) and then cooled down to 20°C at $10^\circ\text{C}/\text{min}$. The resulting paste was kept in the sealed DSC pan at $5 \pm 1^\circ\text{C}$ for 7 and 14 days in refrigerator (MIR-153, Sanyo, Japan). After storing, the paste was reheated again in DSC from 20°C to 140°C at the rate of $10^\circ\text{C}/\text{min}$. An empty pan was used as a reference. The degree of retrogradation was calculated as shown in Equation 8:

$$\% \text{ retrogradation} = (\Delta H_2 / \Delta H_1) 100 \quad [8]$$

where ΔH_1 = Enthalpy of gelatinization (first heating curve)

ΔH_2 = Enthalpy of re-gelatinization (re-heating curve)

3.4.7 Freeze-thaw stability measurement

Starch was weighed and then dispersed into distilled water to obtain the concentration of 5% w/w. Sodium azide (0.04% w/w) was added to prevent microbial spoilage. The starch suspension was stirred using a magnetic stirrer for 15 min at room temperature (25°C), heated to 95±1°C and kept at 95±1°C for 30 min in a boiling-water bath, while it was kept stirring. Twelve ml of starch paste were poured into a 15 ml plastic tube, stored at -25°C for 20 h in the freezer (SF-0991 NG, Sanyo, Thailand), and then thawed at 40°C for 2 h in a water bath (WNB22, Memmert, Germany). A total of five freeze-thaw cycles was studied. To measure the water separation from starch paste, a plastic syringe (5 ml) without the tip and plunger were used. A single piece of filter paper (11 mm diameter Whatman#5) was placed on the bottom of the syringes, and 0.02-0.03 g cotton was placed on top. Distilled water (1 ml) was added to the syringes to moisten the cotton, and then the cotton layer was pressed with a glass rod to ensure a complete seal at the bottom of the syringe (Pongsawatmanit and Srijunthongsiri, 2008). The syringes were centrifuged at 2000xg for 10 min to remove excess water from the cotton, and then weighed (W_0). For each selected freeze-thaw cycle, a thawed paste sample of about 2.5±0.03 g was added into the prepared syringe and weighed (W_1), then centrifuged at 2000xg for 10 min, and then weighed again (W_2). The water was automatically removed from the syringe during centrifugation. The percentage of syneresis was calculated as:

$$\% \text{ syneresis} = 100(W_1 - W_2)/(W_1 - W_0) \quad [9]$$

At least 4 measurements were carried out to ensure the reproducibility of the data.

3.5 Statistical analysis

All analysis was performed at least in triplicate and the average value was reported. Analysis of variance (ANOVA) and Duncan's multiple range tests of the data were analyzed using SPSS software (version 17, SPSS Inc., USA).



CHAPTER IV

RESULTS AND DISCUSSION

4.1 Chemical compositions

Table 4.1 shows the pH and calcium content in starch suspension. The pH of the native starch and HMT-starch (no Ca^{2+} added) were 4.38 and 4.41, respectively. For the HMT- $\text{Ca}(\text{OH})_2$, HMT- CaCl_2 and HMT- $\text{C}_6\text{H}_{10}\text{CaO}_6$ starches pH were in the range of 7.55-8.64, 5.85-6.12 and 4.42-4.65, respectively.

For calcium content, the native starch contained 86.70 ppm. Heat-moisture treatment in the presence of a calcium compound had an increase in calcium content with an increase in Ca^{2+} -starch ratio. However, when using a calcium compound during heat-moisture treatment, the calcium contents in HMT-Ca starches were higher than those in native starch by 50-564 ppm (Table 4.1). This indicated that calcium salts interacted with granules of pigeonpea starches.

Table 4.1 pH and calcium contents of native starch and HMT-starch that treated at 110°C for 1 h

Type of Pigeonpea Starch	Type of Calcium Compound	Ca ²⁺ :Starch	pH of Starch Suspension	Calcium Content (ppm)
Native starch	-	-	4.38 ^h ± 0.02	86.70 ^j ± 0.34
Heat-moisture treated at 110°C, 1 h	-	0:1	4.41 ^h ± 0.04	81.74 ^k ± 0.42
	Ca(OH) ₂	0.0001:1	7.55 ^c ± 0.04	234.65 ^g ± 0.16
		0.0004:1	8.04 ^b ± 0.06	457.13 ^c ± 0.24
		0.0007:1	8.64 ^a ± 0.08	650.92 ^a ± 0.71
	CaCl ₂	0.0001:1	5.85 ^e ± 0.09	137.10 ⁱ ± 0.42
		0.0004:1	5.98 ^e ± 0.04	262.56 ^f ± 0.44
		0.0007:1	6.12 ^d ± 0.08	426.73 ^d ± 1.05
	C ₆ H ₁₀ CaO ₆	0.0001:1	4.42 ^h ± 0.00	168.22 ^h ± 0.65
		0.0004:1	4.57 ^g ± 0.01	394.51 ^e ± 0.37
		0.0007:1	4.65 ^f ± 0.01	584.91 ^b ± 0.94

The reported values are means ± SD.

Means with different letters (a, b, ...) in each column are significantly different ($P \leq 0.05$).

4.2 Effect of calcium compound on the physicochemical properties of starch

4.2.1 Structural characteristics

4.2.1.1 Light microscopy

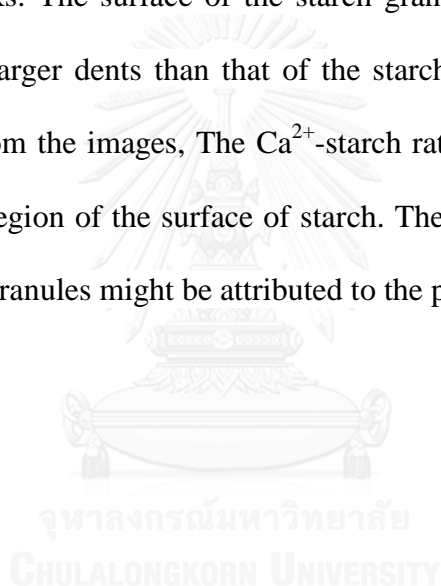
Figure 4.1 shows granular images of the native, HMT and HMT-Ca starches from light/polarized light micrographs. The light microscope images show that the starch granules were round and oval and there were slightly differences between the native and all HMT modified starch (Figure A.1). Both exhibited characteristic birefringence patterns under polarized light. As the granules still exhibited a diffuse polarized cross, suggesting the presence of an ordered complex. However, all HMT starch (with/without calcium salts) displayed a loss of birefringence at the granule center indicating partial melting or disruption of ordered structure occurred during heat-moisture treatment. The images also show that the presence of calcium compounds during treatment caused an increase in the loss of birefringence at the center of the granule. They also show that Ca(OH)_2 and $\text{C}_6\text{H}_{10}\text{CaO}_6$ caused more birefringence lost than CaCl_2 (Figure A.2). From the images, the Ca^{2+} -starch ratio did not apparently affect the extent of birefringence loss at the center of the granule. The decrease in birefringence intensity at the granule center suggested that the thermal energy imparted to the double helices during heat-moisture treatment might have increased their mobility, thereby resulting in a loss of radial orientation (Chung *et al.*, 2009).

Native				
Ca^{2+} :Starch HMT 0:1				
			$\text{Ca}(\text{OH})_2$	CaCl_2
	$\times 100$	$\times 100$	$\times 100$	$\times 100$
			$\times 100$	$\times 100$
0.0001:1				
0.0004:1				
0.0007:1				
			$\text{C}_6\text{H}_{10}\text{CaO}_6$	$\times 100$
			$\times 100$	$\times 100$

Figure 4.1 Microscope and polarized light microscope images of starch granules

4.2.1.2 Scanning electron microscopy (SEM)

Figure 4.2 shows the granular structure of native, HMT-starch and HMT-Ca starches taken from a scanning electron microscope. Pigeon pea starch granules were oval to elliptical to irregular in shape. The surface of the native starch granules appears smooth with no evidence of fissure, but the modified starches had some dents. The HMT-Ca starches appeared to have more dents on the surfaces than the HMT-starch. Moreover, the surface of the starch granules treated with $C_6H_{10}CaO_6$ had cracks. The surface of the starch granules treated with $Ca(OH)_2$ or $C_6H_{10}CaO_6$ showed larger dents than that of the starch granules treated with $CaCl_2$ (Figure A.3-A.5). From the images, The Ca^{2+} -starch ratio did not significantly affect the area of the dent region of the surface of starch. The surface degradation of HMT and HMT-Ca starch granules might be attributed to the partial melting.



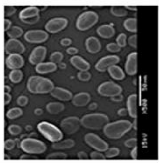
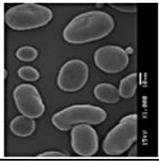
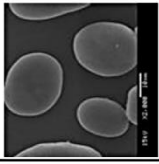
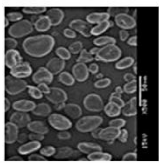
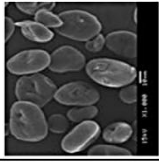
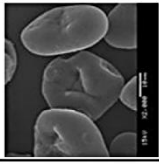
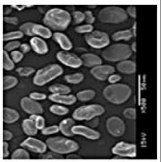
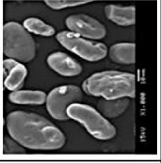
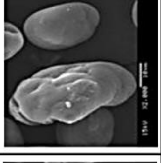
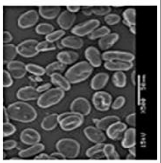
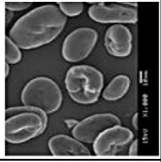
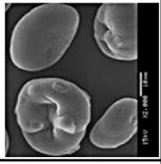
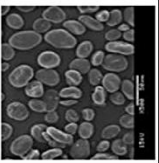
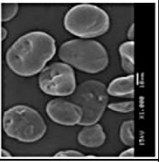
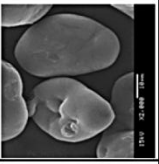
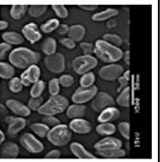
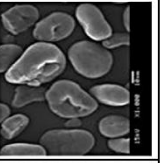
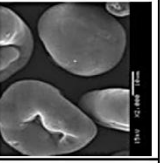
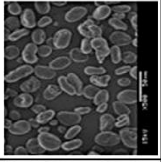
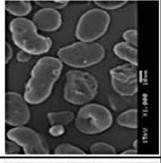
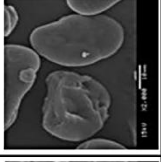
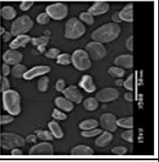
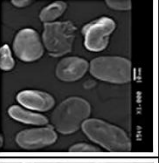
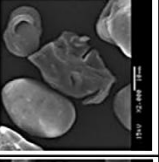
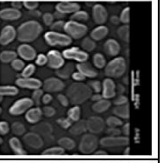
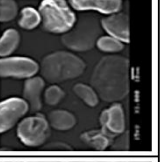
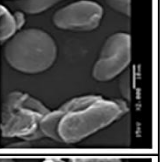
Native				
Ca²⁺:Starch HMT 0:1				
	Ca(OH)₂			
				
0.0001:1				C₆H₁₀CaO₆
0.0004:1				x 500
0.0007:1				x 1000
				x 500
				x 1000
				x 2000

Figure 4.2 Scanning electron micrographs of starch granules

4.2.1.3 X-ray diffraction and relative crystallinity

The crystalline patterns of pigeon pea starch and all HMT starches as determined by X-ray diffraction are shown in Figure 4.3. Native starch showed characteristic C-type diffraction patterns (consisting of a mixture of A- and B-type crystalline structures), with diffraction strong peaks at 17.2° , 18.1° and 23.1° 2θ and weak peaks at 5.5° and 15.2° 2θ (Hoover and Sosulski, 1985; Horng, 2007; Ratnayake *et al.*, 2001). A peak at 5.5° 2θ was not detected for HMT-starch and HMT-Ca starches (Figure 4.3) indicating the disappearance of characteristic B-type diffraction patterns. Thus heat-moisture treatment changed the crystalline pattern of native starch from C- to A-type. The intensity of the diffraction peak and relative crystallinity of native, HMT and HMT-Ca starches are shown in Table 4.2. The heat-moisture treatment caused an increase in peak intensities at 11.5° , 15.2° , 17.2° , 18.1° , 20.0° , 23.1° and 26.5° 2θ . The presence of calcium compound during heat-moisture treatment and an increase in Ca^{2+} -starch ratio resulted in increasing peak intensities at these angles. These peak intensities were higher when $\text{Ca}(\text{OH})_2$ and $\text{C}_6\text{H}_{10}\text{CaO}_6$ were used than when CaCl_2 was used. The increase in these peak intensities of diffraction suggested that there was structural rearrangement within the crystalline domain of the starch granules due to the thermal energy displacing the double helical chains between starch crystals leading to the formation of a better packaged and more ordered crystalline array than that of the native starch (da Rosa Zavareze and Dias, 2011; Klein *et al.*, 2013). The results in Table 4.2 shows that the % relative crystallinity (% RC) of native pigeonpea starch was 38.02%, while those of the HMT-starch and HMT-Ca starches were lower (31.09-34.08%). It was also found that % RC increased with an increase in Ca^{2+} -starch ratio (or increased of Ca^{2+} concentration). The type of

calcium did not affect the % RC of the HMT-Ca starches. Compared to the native starch, the lower % RC of HMT and HMT-Ca starches could be accounted for by the fact that some crystalline order was lost as starch being partially melted during heat-moisture treatment (Khunae *et al.*, 2007; Sun *et al.*, 2014). This finding was agreed with the result of the T_g study by Lim *et al.* (2001). Lim *et al.* (2001) found that T_g of HMT-corn or potato starch was lower than the native starch. This indicated that the intercrystalline amorphous parts were transformed into independent amorphous states during heat-moisture treatment. Thus, the amorphous portion in the HMT-starch could be increased. For HMT-Ca starches, The increase in crystallinity as Ca^{2+} -starch ratio increased could have arisen due to the following reasons: (1) stabilization of starch granules due to effect of water structure maker caused by ions, resulting from Ca^{2+} -starch interaction, (2) formation of additional crystallites (resulting from interactions between amylose-amylose, amylose-amylopectin, amylopectin-amylopectin), and (3) changes in orientation of the starch crystallites, loss of less order weaker crystallites but leading to the formation of a better packaged (more densely packed structure) and ordered crystalline array than those from HMT-starch.

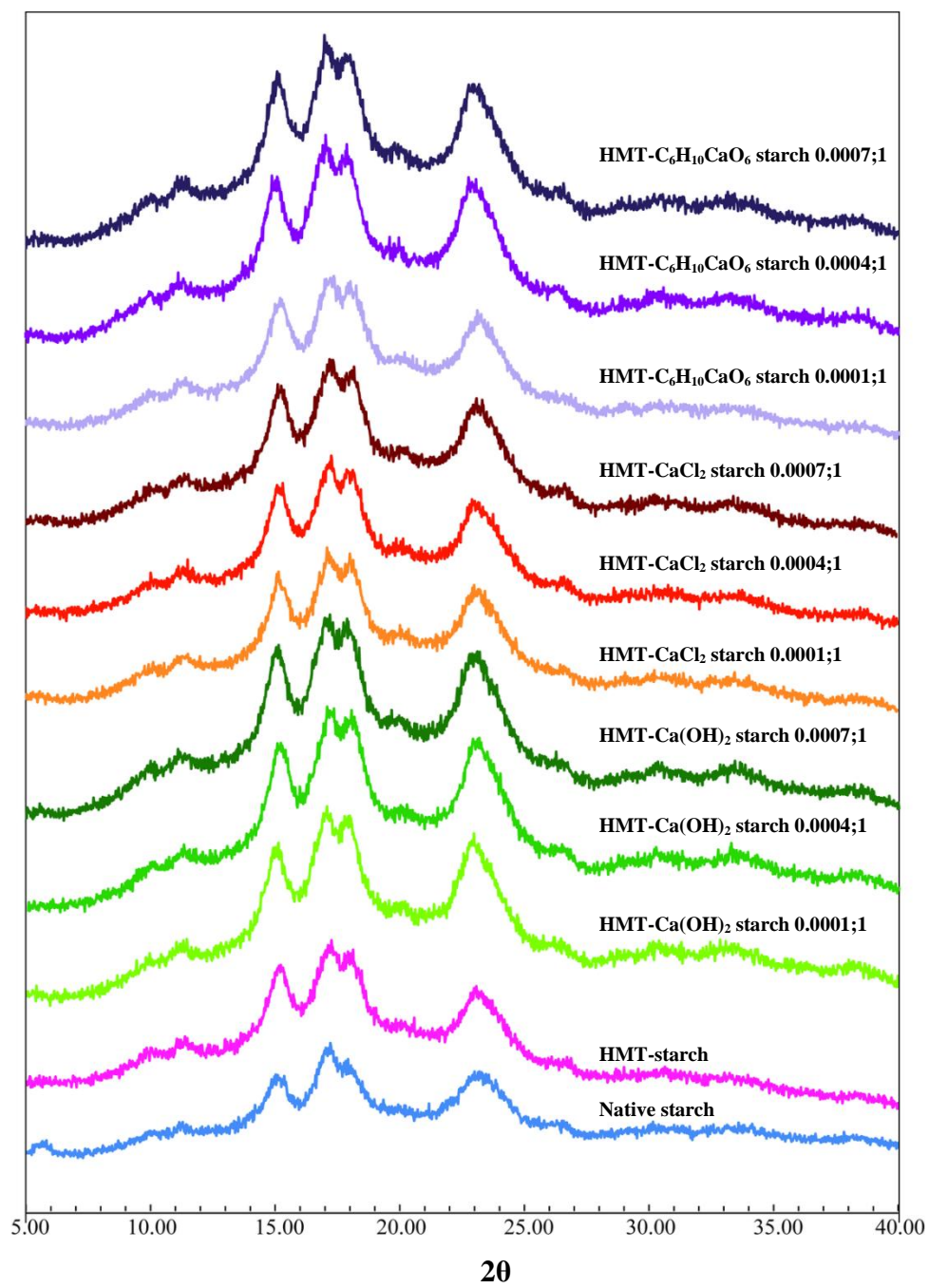


Figure 4.3 The X-ray pattern of native starch and HMT-starch that treated at 110°C for 1 h

Table 4.2 Peak intensities from X-ray diffractograms and relative crystallinity of native starch and HMT-starch that treated at 110°C for 1h

Type of Pigeonpea Starch	Type of Calcium Compound	Ca ²⁺ :Starch	5.54	11.49	15.18	17.20	18.10	20.00	23.10	26.50	RC (%)
Native starch	-	-	503	703 ^f	1184 ^f	1473 ^g	1306 ^g	878 ^f	1197 ^f	717 ^f	38.02 ^a ± 0.39
Heat-moisture treated at 110°C, 1 h	-	0:1	-	1086 ^e	1805 ^e	2014 ^f	1914 ^f	1371 ^e	1600 ^e	905 ^e	31.09 ^e ± 0.10
	Ca(OH) ₂	0.0001:1	-	1169 ^d	2035 ^e	2387 ^e	2316 ^e	1530 ^e	2119 ^b	1175 ^e	31.45 ^d ± 0.12
		0.0004:1	-	1274 ^e	2254 ^b	2600 ^b	2537 ^b	1678 ^b	2311 ^a	1287 ^b	32.79 ^e ± 0.02
		0.0007:1	-	1380 ^a	2379 ^a	2642 ^a	2611 ^a	1719 ^a	2316 ^a	1318 ^a	34.08 ^b ± 0.67
	CaCl ₂	0.0001:1	-	1100 ^e	1985 ^e	2114 ^e	2061 ^e	1338 ^e	1740 ^d	990 ^d	31.73 ^d ± 0.50
		0.0004:1	-	1088 ^e	1863 ^d	2114 ^e	2011 ^e	1321 ^e	1722 ^d	986 ^d	32.28 ^{od} ± 0.13
		0.0007:1	-	1139 ^d	1984 ^e	2239 ^d	2144 ^d	1420 ^d	1856 ^e	1064 ^e	32.89 ^e ± 0.47
	C ₆ H ₁₀ CaO ₆	0.0001:1	-	1044 ^d	2001 ^e	2243 ^d	2163 ^d	1418 ^d	1842 ^e	1001 ^{od}	31.50 ^d ± 0.15
		0.0004:1	-	1225 ^b	2275 ^b	2638 ^{ab}	2550 ^{ab}	1669 ^b	2262 ^a	1275 ^b	32.74 ^e ± 0.42
		0.0007:1	-	1232 ^a	2385 ^a	2669 ^a	2561 ^a	1680 ^b	2277 ^a	1305 ^a	33.75 ^b ± 0.26

CPS: count per second.

RC: relative crystallinity

The reported values are means

Means with different letters (a, b, ...) in each column

are significantly different ($P \leq 0.05$).

4.2.2 Swelling power, % solubility and amylose leaching

The swelling power, % solubility and amylose leaching of starch, determined at 95°C, decreased significantly after heat-moisture treatment (Table 4.3). Compare with the HMT-starch, the HMT-Ca(OH)₂ and HMT-C₆H₁₀CaO₆ starches significantly reduced swelling power, % solubility and amylose leaching ($p \leq 0.05$). For these two HMT-Ca starches, as Ca²⁺-starch ratio was increased these three properties decreased.

Heat-moisture treatment induces rearrange of starch chains in the rubber state. The rearrange of these starch chains occurs within amorphous and/or crystalline of granules. Changing of structure within starch granules results in decreasing swelling power, % solubility and amylose leaching. From Table 4.1, HMT-starch had pH of 4.41, while HMT-CaCl₂ starches and HMT-C₆H₁₀CaO₆ starches had pH of 5.85-6.12, and 4.42-4.65, respectively. Compared to HMT-starch, the extent of distorted birefringence in the middle of the granules by CaCl₂ and C₆H₁₀CaO₆ might due to their acidic pH. This was explain by Kim and Huber (2013) that the heat-moisture treatment in mildly acidic condition did not enhanced long-range crystallinity, but reduced native long-range chain associations within crystalline regions and altered chain arrangement within amorphous regions of starch granules. As a result, these enhanced granules stability to heat and shear, therefore, swelling of granules and amylose leaching from granules decreased. It was also reported that salts (such as NaCl, LiCl and KCl) could interact with starch molecules and restrain the recrystallization of starch. Under the limited water content (25-35%), initial swelling of starch is affected/restricted by the solvation effect of salt (Day *et al.*, 2013). The interaction between starch and salt become dominate as salt concentration increased.

Regardless of water content, in the presence of salt, the interactions of cations (Ca^{2+} in this research) with the OH^- of starch reduced the initial swelling of amorphous regions. These interactions might reduce swelling power of HMT-Ca starches as compared to HMT-starch. In starch film, CaCl_2 (20% w/w) was found to be completely dissolved in starch/poly vinyl alcohol (PVA) matrix (Jiang *et al.*, 2012). This indicated that CaCl_2 could effectively destroy the crystals of starch and PVA and acted as plasticizer in starch-PVA film. Therefore, in the same manner, the calcium compounds, which were presented during heat-moisture treatment, might also act as plasticizer in starch granules and destroy the crystallites in starch, and then caused rearrangement of starch chains to form new stronger crystallites as compared to heat-moisture treatment in the absence of calcium compound. Thus, HMT-Ca starches had lower swelling power, % solubility and amylose leaching than HMT-starch. However, from XRD result (Table 4.2), % relative crystallinity of native starch was higher than that of HMT-starch and HMT-Ca starches. This indicated that the new stronger crystallites in HMT-starch and HMT-Ca starch might be lower in number than the crystallites in native starch.

Cations and anions in the presence of common counter ion can be arranged based on their salting out effects. For the cations of Hofmeister series are as follows: $\text{K}^+ > \text{Rb}^+ > \text{Na}^+ > \text{Li} > \text{Mg}^{2+} > \text{Ca}^{2+}$. For the anions of Hofmeister series are as follows: $\text{SO}_4^{2-} > \text{HPO}_4^- > \text{OH}^- > \text{citrate}^- > \text{tartrate}^{2-} > \text{acetate}^- > \text{Cl}^- > \text{NO}_3^- > \text{I}^- > \text{SCN}^-$ (Belitz *et al.*, 2009). Ions on the left of the series reduce the solubility of protein (water-structure maker effect). For the HMT- $\text{Ca}(\text{OH})_2$ and HMT- $\text{C}_6\text{H}_{10}\text{CaO}_6$ starches, swelling power, % solubility and amylose leaching were consistently reduced as Ca^{2+} -starch ratio (Table 4.3) was increased (salt of $\text{Ca}(\text{OH})_2$ and $\text{C}_6\text{H}_{10}\text{CaO}_6$ increased).

This can be explained by the water-structure maker effect of both anions (OH^- , lactate $^-$) which stabilized starch granules. Ions of high charge density (e.g. SO_4^{2-}) increase the structure of water and stabilize starch granules; ions of low charge density (e.g. SCN^- , I_3^-) not only break water structure but also tend to form helical complex with starch molecules (Jane, 1993).

For the case of heat-moisture treatment with CaCl_2 , the results were difference. Increasing CaCl_2 salts to starch ratio (Table 4.3), swelling power and amylose leaching tend to increase. The results seem to follow the water structure making effect of anions (Hofmeister series). Chloride ion may break water structure and increase more swelling and solubility of starch granules than the other two HMT-Ca starch. Alternative reason might be due to the fact that CaCl_2 has high solvation (hydration) capacity than $\text{Ca}(\text{OH})_2$ and $\text{C}_6\text{H}_{10}\text{CaO}_6$, led to a lower moisture absorption of starch granules during heat-moisture treatment (Ruiz-Guiérrez *et al.*, 2012). This may cause less diffusion of moisture and calcium into the starch granules during the heat-moisture treatment, therefore, HMT- CaCl_2 starch had higher swelling power and amylose leaching as compared to HMT- $\text{Ca}(\text{OH})_2$ and HMT- $\text{C}_6\text{H}_{10}\text{CaO}_6$ starches.

The following statements might be the alternative explanations for the results of this research. The presence of calcium compound during the heat-moisture treatment enhancing these three properties could be the stabilization of the granules presumably by the calcium ions (Ca^{2+}) reacting on the surface of starch granules (Bryant and Hamaker, 1997; Gough and Pybus, 1973). It has been reported that heat-moisture treatment caused a decrease in swelling power, % solubility and amylose leaching and this accounts for the rearrangement of starch molecule chains such as amylose-amylose, amylose-amylopectin and amylopectin-amylopectin chains to form

the ordered double helical (Gunaratne and Hoover, 2002; Lawal, 2005; Li *et al.*, 2011; Olayinka *et al.*, 2008; Sun *et al.*, 2014; Varatharajan *et al.*, 2010). In a salt solution, cations tend to penetrate the starch granules, due to an attraction between the positively charged cations and the negative Donnan-potential, and by the concentration gradient of cations (Oosten, 1990). Ruiz-Guérrez *et al.* (2012) and Matsuki *et al.* (2012) reported that the Ca^{2+} (concentration of $\text{Ca}(\text{OH})_2$ were 0.5-15% w/w of dry starch) could interacted with starch-OH group especially at the surface of the starch granules and also probably inside granules during the thermal-alkaline process. This results in the formation of calcium-starch-OH complexes that stabilized the granules. Lawal (2005) reported that the swelling power and % solubility of HMT cocoyam starch, reduces as the level of moisture in modification increased from 18% to 27%. The observed higher swelling power and % solubility of HMT- CaCl_2 starches suggests that fewer interactions might occur among starch molecules than those of HMT- $\text{Ca}(\text{OH})_2$ and HMT- $\text{C}_6\text{H}_{10}\text{CaO}_6$ starches. Compared to HMT-starch, the presence of CaCl_2 of all Ca^{2+} -starch ratios led to an approximate 10% change in swelling power and 10% decrease in amylose leaching, but did not affect % solubility.

Table 4.3 Swelling power, % solubility and amylose leaching at 95°C of native starch and HMT-starch that treated at 110°C for 1 h

Type of Pigeonpea Starch	Type of Calcium Compound	Ca ²⁺ :Starch	Swelling Power (g/g)	Solubility (%)	Amylose Leaching (%)
Native starch	-	-	20.73 ^a ± 0.70	29.85 ^a ± 0.80	56.02 ^a ± 0.80
Heat-moisture treated at 110°C, 1 h	-	0:1	10.50 ^b ± 0.22	17.45 ^b ± 0.37	37.26 ^b ± 0.56
	Ca(OH) ₂	0.0001:1	8.36 ^c ± 0.36	14.02 ^d ± 0.36	32.25 ^{de} ± 0.32
		0.0004:1	6.71 ^d ± 0.25	13.39 ^d ± 0.22	29.17 ^f ± 0.16
		0.0007:1	5.80 ^e ± 0.40	10.33 ^f ± 0.34	23.99 ^h ± 0.15
	CaCl ₂	0.0001:1	9.02 ^c ± 0.34	17.10 ^b ± 0.60	31.81 ^e ± 0.29
		0.0004:1	9.16 ^c ± 0.13	17.86 ^b ± 0.40	33.12 ^c ± 0.12
		0.0007:1	10.93 ^b ± 0.45	17.68 ^b ± 0.75	32.71 ^{cd} ± 0.29
	C ₆ H ₁₀ CaO ₆	0.0001:1	8.52 ^c ± 0.40	15.87 ^c ± 0.65	32.92 ^c ± 0.20
		0.0004:1	7.31 ^d ± 0.36	13.82 ^d ± 0.57	28.00 ^e ± 0.81
		0.0007:1	5.30 ^e ± 0.24	11.78 ^e ± 0.48	24.57 ^h ± 0.18

The reported values are means ± SD. Means with different letters (a, b, ..) in each column are significantly different ($P \leq 0.05$).

4.2.3 Pasting properties of starches

The pasting properties of native and HMT pigeon pea starches as determined by RVA are presented in Table 4.4. The pasting temperature, peak and final viscosities, trough, breakdown and setback of the native starch were 83.25°C, 4,061 mPa·s, 5,397 mPa·s, 2,754 mPa·s, 1,308 mPa·s and 2,644 mPa·s, respectively. The RVA profile of the HMT starch does not show any peak, trough, breakdown and setback. All HMT starches exhibited significantly lower viscosity at the end of the heating period at 95°C (η_h) and viscosity at the end of the cooling period at 50°C (η_c) than the native starch. Pasting properties provide information on intermolecular bonding between densely packed starch granules and the rigidity of swollen starch granules during the heating process (Sui *et al.*, 2015; Vandeputte *et al.*, 2003). The pasting temperature of the HMT starches ranged from 94.85-95.13°C. The higher pasting temperature after HMT indicated that the starch granules were strengthened by HMT. The strengthening of intragranular bonded forces causes the starch to require more heat before structural disintegration and paste formation occurs (Adebowale *et al.*, 2009; Eliasson, 1980). The RVA profiles for the HMT-Ca starches were similar to those of the HMT-starch (Figure A.7). The presence of calcium compounds did not affect the pasting temperature (Table 4.4). The effects of type and amount of calcium compounds on the η_h and η_c were determined for the HMT-starch and HMT-Ca starches. Compared to the HMT-starch, the presence of Ca(OH)_2 and $\text{C}_6\text{H}_{10}\text{CaO}_6$ at the Ca^{2+} -starch ratio of $> 0.0004:1$ significantly lowered η_h and η_c ($p \leq 0.05$). In the presence of Ca(OH)_2 or $\text{C}_6\text{H}_{10}\text{CaO}_6$ during HMT, the η_h and η_c of the HMT-Ca starches significantly decreased ($p \leq 0.05$) with an increase in the Ca^{2+} -starch ratio. Pasting curve of HMT- CaCl_2 starch showed that increase of these two

viscosities (η_h and η_c) when Ca^{2+} -starch ratio was 0.0007:1, the values were the highest among all HMT and HMT-Ca starch pastes.

Heat-moisture treatment tends to increase the region of crystallinity of starch granules, as a result of reorientation of the starch molecules (da Rosa Zavareze *et al.*, 2010; Watcharatewinkul *et al.*, 2009). RVA profiles of all HMT starches did not show peak, trough, breakdown and setback, as the result of the high rigidity of all heat-moisture treated starch granules. The effects of the different calcium compounds and each compound with different calcium-starch ratios on η_h and η_c were complimented with their low swelling power, % solubility and amylose leaching (Table 4.3). On account of the restricted swelling of starch granules which was limiting the leaching of amylose into the medium leading to decrease viscosity as compared to native starch.

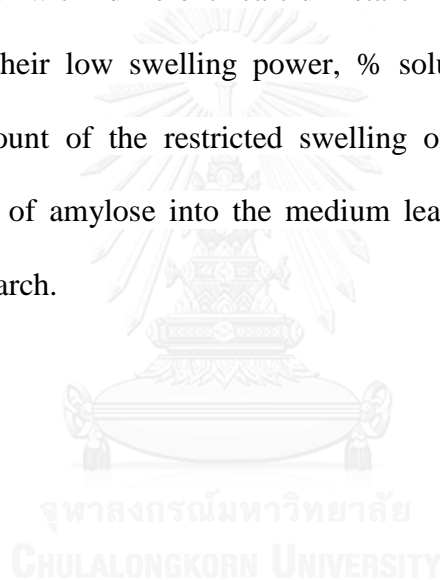


Table 4.4 Viscosity at the end of the heating period (η_h) and viscosity at the end of the cooling period (η_c) of 10% w/w native starch and HMT-starch that treated at 110°C for 1 h

Type of Pigeonpea Starch	Type of Calcium Compound	Ca ²⁺ :Starch	Viscosity at the end of the heating period (95°C) (mPa.s)	Viscosity at the end of the cooling period (50°C) (mPa.s)	Pasting Temperature (°C)
Native starch	-	-	4,067.43 ^a ± 61.61	5,397.00 ^a ± 54.51	83.25 ^e ± 0.51
Heat-moisture treated at 110°C, 1 h	-	0:1	833.32 ^c ± 16.01	1,191.67 ^{cd} ± 25.23	95.13 ^a ± 0.12
	Ca(OH) ₂	0.0001:1	844.00 ^c ± 32.50	1,150.13 ^d ± 40.48	94.85 ^b ± 0.05
		0.0004:1	705.63 ^d ± 24.40	1,093.64 ^d ± 38.15	94.88 ^b ± 0.06
		0.0007:1	564.33 ^e ± 24.47	899.00 ^{ef} ± 28.34	94.93 ^b ± 0.04
	CaCl ₂	0.0001:1	883.73 ^c ± 28.29	1,298.11 ^e ± 28.33	94.90 ^b ± 0.09
		0.0004:1	885.36 ^c ± 24.04	1,274.54 ^e ± 21.02	94.90 ^b ± 0.09
	C ₆ H ₁₀ CaO ₆	0.0007:1	1,029.93 ^b ± 19.86	1,441.17 ^b ± 35.15	94.88 ^b ± 0.08
0.0001:1		855.52 ^c ± 38.13	1,142.87 ^d ± 30.65	94.92 ^b ± 0.03	
	0.0004:1	682.61 ^d ± 30.36	958.68 ^e ± 35.57	94.87 ^b ± 0.03	
	0.0007:1	590.33 ^e ± 30.24	846.68 ^f ± 29.48	94.85 ^b ± 0.05	

The reported values are means ± SD. Means with different letters (a, b, ...) in each column are significantly different ($P \leq 0.05$).

4.2.4 Rheological properties

With non-linear regression, the flow behavior of all starch gels at 25°C and shear rate ranging between 0.1-1000 s⁻¹ showed a pseudo-plastic with yield stress following the Herschel-Bukley model with $R^2 \geq 0.98$. Table 4.5 shows the values of the Herschel-Bukley constants, namely yield stress (τ_0), consistency coefficient (K) and flow behavior index (n), of the native and HMT pigeonpea starch gels. The native starch gel had the highest τ_0 and K along with the lowest n . In the presence of Ca(OH)_2 and $\text{C}_6\text{H}_{10}\text{CaO}_6$ during HMT, an increase in the Ca^{2+} -starch ratio caused a decrease in K and vice versa for n , but did not affect τ_0 . For CaCl_2 , the Ca^{2+} -starch ratio did not affect these three properties.

For native and all HMT starch gels at 25°C, the linear viscoelastic region was found at 1% strain and with frequency ranging from 0.1 to 10 Hz. For all starches (Figure 4.4), the storage modulus (G') was higher than the loss modulus (G''). The G' of the native starch gel was higher than that of the HMT-starch gel. The G' of the HMT-Ca starches was lower than that of the HMT-starch (Figure 4.5). The coefficients [G'_1 , G''_1 and $(\tan \delta)_1$] and the exponents (a , b and c) were obtained from fitting the data using the power law model (Equations 5-7, see page 38) with R^2 ranging between 0.90 and 0.99 as reported in Table 4.6. An increase in the Ca^{2+} -starch ratio decreased the G'_1 for HMT- Ca(OH)_2 and HMT- $\text{C}_6\text{H}_{10}\text{CaO}_6$ starches and vice versa for the HMT- CaCl_2 starch. A higher value of G'_1 or G''_1 indicates a stronger gel structure (Acevedo *et al.*, 2013). The value “ a ” for all gels was < 0.08 (near zero), which indicates that G' is independent of frequency. This is the typical behavior of a weak to stable gel structure (Acevedo *et al.*, 2013; Maache-Rezzoug *et al.*, 2010;

Osundahunsi *et al.*, 2011). The value of $\tan \delta_1$ was < 1 , which also suggests the solid elastic-like behavior of these gels (Acevedo *et al.*, 2013).

The K value of starch gel depends on the effect of swollen granules and amylose leaching which thicken the viscosity of the continuous phase (Osundahunsi *et al.*, 2011). The lower swelling power and amylose leaching resulted in lower viscosity. The results showed that the effects of HMT, different calcium compounds and Ca^{2+} -starch ratio on K , G' and amylose leaching were alike. For polymer solution, K and G' decrease as polymer concentration decreases. In this case, a decrease in K and G' were the results of a decrease in amylose leaching or amylose concentration in the continuous phase (Barrera *et al.*, 2013; Chen *et al.*, 2014).

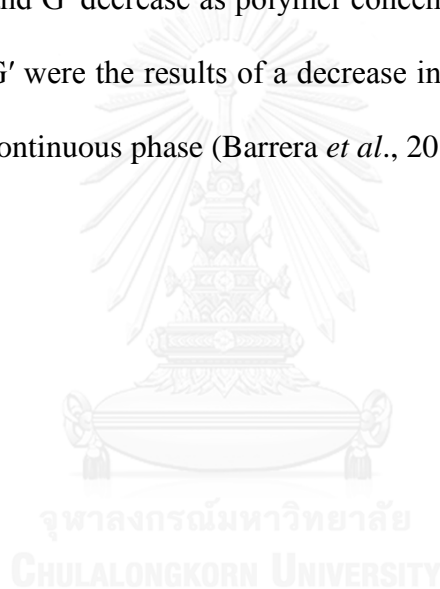


Table 4.5 Herschel-bulkley constants [yield stress (τ_0), consistency coefficient (K) and flow behavior index (n)] of 5 % w/w native starch and HMT-starch that treated at 110°C for 1 h at 25°C and shear rate between 0.1-1000 s^{-1}

Type of Pigeonpea Starch	Type of Calcium Compound	Ca ²⁺ :Starch	τ_0 (Pa)	K (Pa·s ⁿ)	n
Native starch	-	-	7.95 ^a (0.41)	0.83 ^a (0.04)	0.65 ^e (0.01)
Heat-moisture treated at 110°C, 1 h	-	0:1	5.45 ^b (0.11)	0.26 ^c (0.01)	0.69 ^d (0.01)
	Ca(OH) ₂	0.0001:1	2.62 ^{cde} (0.22)	0.20 ^d (0.01)	0.71 ^{cd} (0.02)
		0.0004:1	2.73 ^{cde} (0.19)	0.17 ^{de} (0.00)	0.73 ^c (0.01)
		0.0007:1	2.91 ^{cd} (0.14)	0.11 ^f (0.00)	0.82 ^a (0.01)
	CaCl ₂	0.0001:1	2.96 ^c (0.03)	0.21 ^d (0.02)	0.72 ^c (0.01)
		0.0004:1	2.70 ^{cde} (0.60)	0.17 ^{de} (0.00)	0.74 ^c (0.02)
		0.0007:1	2.30 ^e (0.22)	0.35 ^b (0.09)	0.67 ^e (0.03)
	C ₆ H ₁₀ CaO ₆	0.0001:1	2.37 ^e (0.46)	0.19 ^d (0.01)	0.74 ^c (0.01)
		0.0004:1	2.56 ^{cde} (0.18)	0.14 ^{ef} (0.01)	0.78 ^b (0.02)
		0.0007:1	2.48 ^{de} (0.20)	0.11 ^f (0.00)	0.82 ^a (0.01)

The reported values are means (SD).

Means with different letters (a, b, ..) in each column are significantly different ($P \leq 0.05$).

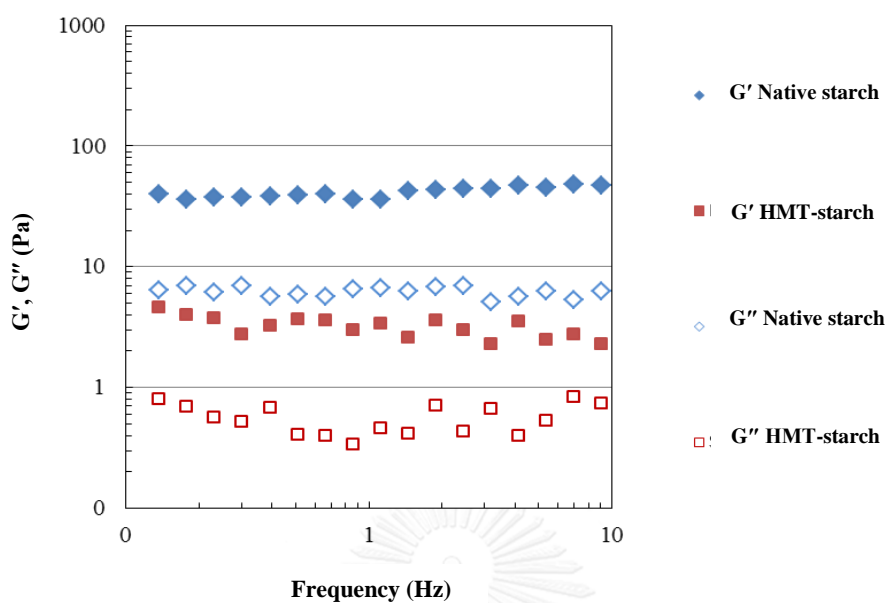


Figure 4.4 Viscoelastic properties of 5% w/w native starch and HMT-starch that treated at 110°C for 1 h at 25°C, 1% strain and frequency ranging 0.1 to 10 Hz

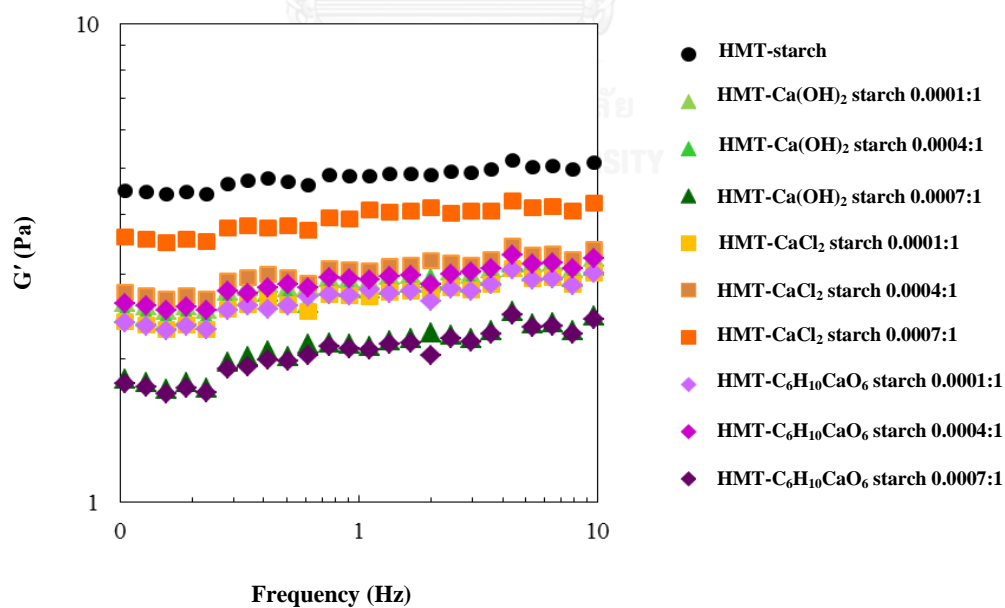


Figure 4.5 Storage modulus (G') of 5% w/w native starch and HMT-starch that treated at 110°C for 1 h at 25°C, 1% strain and frequency ranging 0.1 to 10 Hz

Table 4.6 Rheological properties of gels. The power law model was fitted to experimental measurements

Type of Pigeonpea Starch	Type of Calcium Compound	Ca ²⁺ :Starch	G' ₁ (Pa)	a*	G'' ₁ (Pa)	b*	(tan δ) ₁	c*
Native starch	-	-	39.07 ^a (0.05)	0.08 ^a (0.00)	16.68 ^a (0.01)	0.19 ^a (0.00)	0.43 ^g (0.01)	0.11 ^a (0.00)
Heat-moisture treated at 110°C, 1 h	-	0:1	4.77 ^b (0.02)	0.04 ^e (0.00)	2.94 ^b (0.08)	0.06 ^e (0.00)	0.62 ^b (0.02)	0.02 ^f (0.00)
	Ca(OH) ₂	0.0001:1	2.91 ^{de} (0.02)	0.06 ^c (0.00)	1.63 ^{cd} (0.01)	0.10 ^d (0.00)	0.56 ^d (0.00)	0.04 ^e (0.00)
		0.0004:1	2.77 ^e (0.02)	0.06 ^c (0.00)	1.53 ^d (0.02)	0.11 ^d (0.00)	0.55 ^d (0.01)	0.04 ^e (0.00)
		0.0007:1	2.72 ^e (0.03)	0.07 ^b (0.00)	1.13 ^e (0.02)	0.16 ^b (0.02)	0.53 ^e (0.01)	0.07 ^b (0.00)
	CaCl ₂	0.0001:1	2.16 ^f (0.04)	0.06 ^c (0.00)	1.64 ^{cd} (0.05)	0.11 ^d (0.00)	0.60 ^c (0.03)	0.04 ^e (0.00)
		0.0004:1	3.07 ^d (0.02)	0.05 ^d (0.00)	1.55 ^d (0.04)	0.11 ^d (0.00)	0.50 ^f (0.01)	0.05 ^d (0.00)
		0.0007:1	4.17 ^c (0.08)	0.04 ^e (0.00)	2.86 ^b (0.14)	0.06 ^e (0.00)	0.67 ^a (0.05)	0.01 ^g (0.00)
	C ₆ H ₁₀ CaO ₆	0.0001:1	2.90 ^{de} (0.01)	0.06 ^c (0.00)	1.72 ^c (0.07)	0.10 ^d (0.00)	0.62 ^b (0.02)	0.04 ^e (0.00)
		0.0004:1	2.77 ^e (0.03)	0.06 ^c (0.00)	1.62 ^{cd} (0.00)	0.10 ^d (0.00)	0.56 ^d (0.01)	0.04 ^e (0.00)
		0.0007:1	2.05 ^f (0.02)	0.06 ^c (0.00)	1.19 ^e (0.01)	0.14 ^c (0.00)	0.58 ^c (0.00)	0.06 ^c (0.00)

The reported values are means (SD).

Means with different letters (a, b, ..) in each column are significantly different ($P \leq 0.05$).

*The exponents (*a*, *b* and *c*) were obtained from fitting the data using the power law model (Equations 5 to 7).

4.2.5 Thermal properties and retrogradation

The thermal properties of native, HMT and HMT-Ca starch are shown in Figure 4.6 and Table 4.7. Upon gelatinization, endotherm transition of all heat-moisture treatment starches shifted toward higher temperature than that of the native starch. The native starch exhibited only a single endothermic peak, whereas HMT starch displayed a biphasic endotherm. This endotherm is the gelatinization of amylopectin crystalline structure (Liu *et al.*, 2006). The biphasic endotherm of starch indicated heterogeneity in structural organization caused by heat-moisture treatment (Jiranuntakul *et al.*, 2011; Pancha-arnon and Uttapap, 2013). The first peak biphasic endotherm, granules that have the least stable crystallites melt at a low temperature. The second peak biphasic endotherm might arise from a phase transition of crystalline regions that become more perfect on heat-moisture treatment (Liu, 2005). Heat-moisture treatment has been reported to cause crystallite reorientation and starch molecules interaction, hence restricted swelling and mobility of molecules in amorphous region resulting higher temperature of the endotherms (Donovan *et al.*, 1983; Hoover and Manuel, 1996). Compared to native starch, HMT-starch and HMT-Ca starch showed significantly higher ($p \leq 0.05$) for onset (T_o), peak (T_{p1} and T_{p2}), conclusion (T_c), gelatinization temperature range ($T_c - T_o$) but lower gelatinization enthalpy (ΔH_g). An increase in the Ca^{2+} -starch ratio increased T_o , T_{p1} , T_{p2} , T_c and ($T_c - T_o$), but decreased the ΔH_g .

The higher gelatinization temperatures (T_o , T_p and T_c) suggested the existence of more restricted swollen granules caused by its strong interactions between starch chains induced by heat-moisture treatment. Therefore, a higher temperature is required to disrupt the molecular order (Gunaratne and Hoover, 2002;

Khunae *et al.*, 2007). Adebowale *et al.* (2005) and Perera *et al.* (1997) postulated that an increase in T_o , T_p and T_c is associated with the melting of crystallites which are formed due to starch chain associations through amylose-amylose interactions and/or amylose-amylopectin interactions. This suppresses the swelling and mobility of starch chains of the HMT-starch and HMT-Ca starch granules leading to shift of gelatinization temperature to high T_o , T_p and T_c . However, changes in the thermal properties can be also due to the fact that some of the weak crystallites were destroyed during heat-moisture treatment and the stable crystallites in starch granules remained, therefore, melting of retrograded starch occurred at higher temperature (Altay and Gunasekaran, 2006; Lim *et al.*, 2001; Yadav *et al.*, 2013).

A wider gelatinization temperature range (T_c-T_o) of heat-moisture treated starches in our study could be explained the existing crystallites in the granules of starch in HMT-starch and HMT-Ca starches had more heterogeneity than those in native starch (Khunae *et al.*, 2007; Li *et al.*, 2011; Varatharajan *et al.*, 2010). From the XRD results, the loss of less order/weaker crystallites, formation of better packaged and ordered crystalline array (the A-type) in starch granules, and the lower in % RC upon heat-moisture treatment might account for the lower in ΔH_g of the HMT-starch and HMT-Ca starches, than ΔH_g of native starch. For HMT-starch and HMT-Ca starches, partial melting of amylose and amylopectin occurred during heat-moisture treatment and some of the double helices in the crystalline and non-crystalline regions in granules were disrupted. Therefore, less number of double helices unravelling and melting during gelatinization. This led to the lower ΔH_g in HMT-starch and HMT-Ca starches compared to the native starch. Cooke and Gidley (1992) and Sandhu and Lim (2008) reported gelatinization enthalpy or ΔH_g is mainly

considered requiring for the disruption of the double helices order rather than long-range disruption of crystallinity during gelatinization. This may account for the decreased ΔH_g while crystalline order is increased in heat-moisture treated starch. Heat of gelatinization (ΔH_g) of HMT-Ca starch were lower ($p \leq 0.05$) than HMT-starch as observed in our study (Table 4.7). Lu *et al.* (1996) reported that during heat-moisture treatment degradation of weak structure of amylopectin crystallites occurred and that more stable amylopectin crystallites remained. The decreased ΔH_g as shown for the HMT-Ca starches could be suggested that salt ions penetrate into starch granules and may interfere with some crystallites formation among starch chains during heat-moisture treatment. Besides heat of gelatinization (ΔH_g) decreased as concentration of salts (Ca^{2+} -starch ratio) increased. Except HMT- CaCl_2 starch increasing concentration, ΔH_g were not different ($p > 0.05$)

Similar results have been reported that increase in gelatinization temperatures (T_o , T_p and T_c) and the broadening of the range (T_c-T_o) has been reported to be attributed to Ca^{2+} interaction with hydroxyl groups in the amylose chain in starch (Jane, 1993; Ruiz-Guiérrez *et al.*, 2012). As Ca^{2+} ion has high charge density, has strong electrostatic interactions with water molecules and forms a dipole-metal interaction (complex formation) between starch-OH groups on the surface of the granule, which thus stabilizes the starch granules (Jane, 1993; Ruiz-Guiérrez *et al.*, 2012). Pigeonpea starch has very low fat content (0.31%, db), therefore, an endotherm at about 90-114 °C of an amylose-lipid complex phase transition is not detected.

After storage at $5 \pm 1^\circ\text{C}$ for 7 and 14 days, gelatinized starch molecules reassociate to an ordered structure and this process is referred to as retrogradation. For

all the gelatinized starches in DSC pan stored for 7 and 14 days at 5°C, the results showed that the endotherm to have a low temperature for T_o of 43.20-53.78°C, T_p of 61.29-65.13°C and T_c of 72.52-82.80°C (Tables 4.8 and 4.9). The melting temperatures of retrograded starch shifted more to the lower temperatures than the gelatinization temperatures (Table 4.7). However, the melting temperatures of retrograded starch in the DSC pan stored for 14 days at 5°C were higher than those stored for 7 days. Moreover, the gelatinized starches stored for 14 days had narrower melting temperature range (T_c-T_o) than those stored for 7 days. Compared to the retrograded native starch, the retrograded HMT-starch and HMT-Ca starch had significantly higher ($p \leq 0.05$) T_o , T_p , T_c and wider (T_c-T_o), but lower ΔH_r than the retrograded native starch. An increase in Ca^{2+} -starch ratio increased the T_o , T_p and T_c of the retrograded HMT-Ca starches. According to Miles *et al.* (1985), the retrogradation process of starch consists of two stages. The first stage is the fast development of the gel structure by amylose gelation within 24 h. The endotherm of melt amylose retrograded structure (presumably crystalline structure) can be found at a high temperature of about $> 100^\circ C$ (Boltz and Thompson, 1999; Liu *et al.*, 2007), which was not found in these results. The second stage is the organized structure in the starch gel continues to develop slowly by amylopectin within 2 weeks of storage (Liu *et al.*, 2007; Ward *et al.*, 1994). Therefore, these DSC results for all retrograded starches mainly resulted from amylopectin retrogradation.

The broadening of crystallite melting endotherm reflects melting crystallites of different stability and perfection formed due to starch chain associations (amylose-amylopectin and/or amylopectin-amylopectin) during gel storage (Lawal, 2005). The melting temperature range (T_c-T_o) gives an indication of the quality and

heterogeneity of the re-crystallized amylopectin. From the XRD and amylose leaching results, the order of starch granules rigidity was HMT-Ca(OH)₂ starch ~ HMT-C₆H₁₀CaO₆ starch > HMT-CaCl₂ starch > HMT-starch > native starch and vice versa for amylose leaching. Therefore, the order of the ΔH_r and % retrogradation was HMT-Ca(OH)₂ starch ~ HMT-C₆H₁₀CaO₆ starch < HMT-CaCl₂ starch < HMT-starch < native starch.

The higher values of ΔH_{r14} compared to ΔH_{r7} of all starches indicated the process of aggregation and reformation of crystallinities, and these were established after 14 days of storage compared to 7 days. Consequently, more energy is needed to dissociate the bonding forces after 14 days of storage.

For all starch pastes, the % retrogradation increased with storage time (Table 4.10). The % retrogradation of native starch paste was higher than that of the HMT- starch paste. These results were similar to that reported for the African yam bean starch by Adebowale *et al.* (2009), which the HMT starch had less retrogradation than native starch. The % retrogradation of the HMT-Ca starches was lower than that of the HMT- starch, and an increase in Ca²⁺-starch ratio decreased % retrogradation. The results showed that HMT and HMT in the presence of a calcium compound retard starch retrogradation. The results also showed that HMT of starch in the presence of Ca(OH)₂ and C₆H₁₀CaO₆ could retard starch retrogradation better than HMT in the presence of CaCl₂. The mechanism of retrogradation inhibition could be considered as the Ca²⁺ ions attract with OH groups of starch chain, stabilize the amorphous and entangled matrix of gelatinized starch.

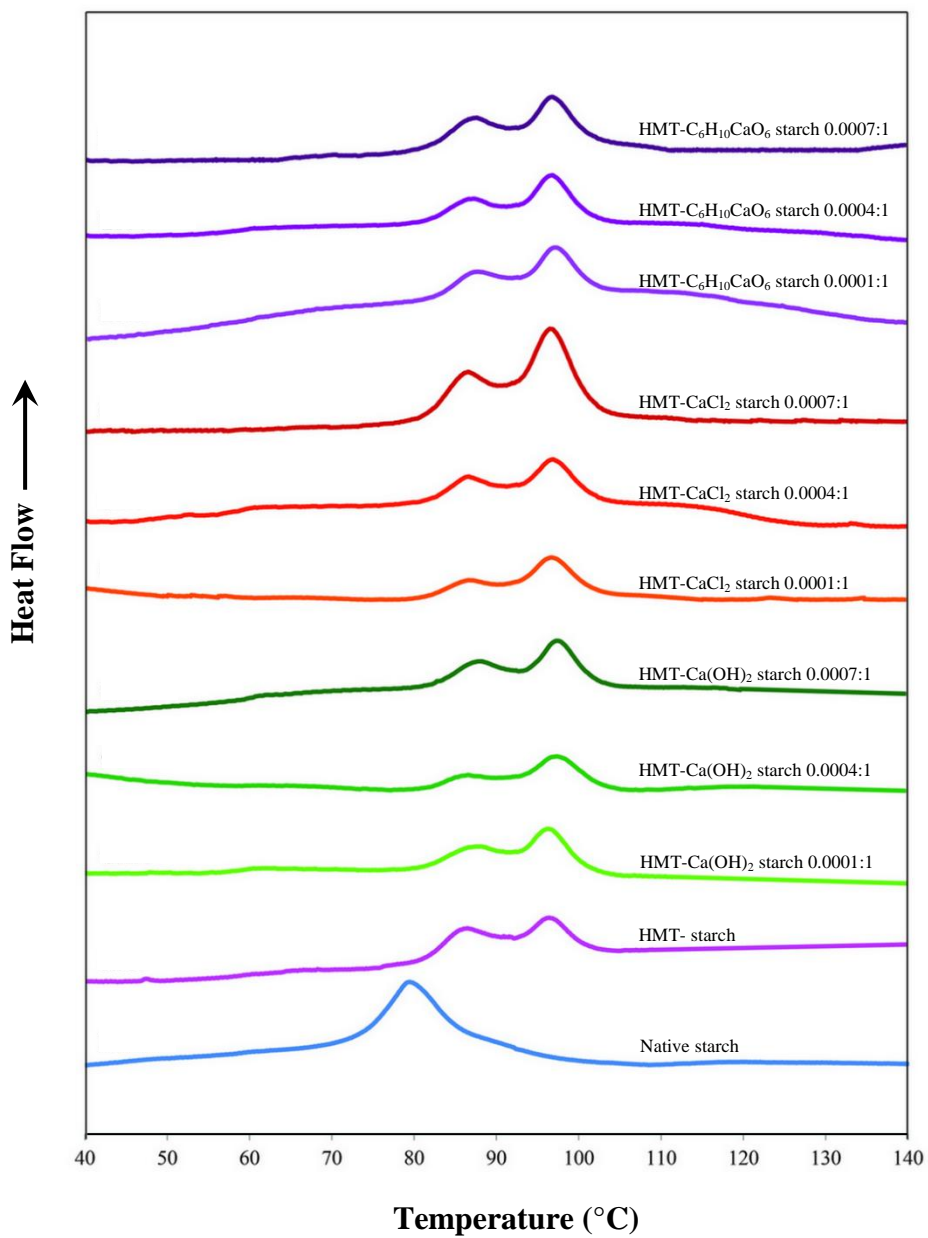


Figure 4.6 Thermogram of native starch and HMT-starch that treated at 110°C for 1 h

Table 4.7 Thermal properties of native starch and HMT-starch that treated at 110°C for 1 h

Type of Pigeonpea Starch	Type of Calcium Compound	Ca ²⁺ :Starch	T _o (°C)	Tp ₁ (°C)	Tp ₂ (°C)	T _c (°C)	T _c -T _o (°C)	ΔH _g (J/g)
Native starch	-	-	73.10 ^h ± 0.44	79.62 ^e ± 0.34	-	87.17 ^h ± 0.17	14.07 ^a ± 0.27	13.50 ^a ± 0.15
Heat-moisture treated at 110°C, 1 h	-	0:1	80.03 ^g ± 0.19	86.41 ^d ± 0.14	94.38 ^c ± 0.31	99.33 ^g ± 0.34	19.30 ^d ± 0.16	10.39 ^b ± 0.24
	Ca(OH) ₂	0.0001:1	80.89 ^f ± 0.40	87.02 ^e ± 0.54	96.44 ^b ± 0.05	101.58 ^f ± 0.21	20.69 ^{bc} ± 0.39	9.98 ^e ± 0.05
		0.0004:1	81.51 ^{de} ± 0.11	87.15 ^e ± 0.15	96.97 ^a ± 0.01	102.42 ^e ± 0.28	20.87 ^{bc} ± 0.30	8.60 ^f ± 0.12
		0.0007:1	82.78 ^a ± 0.22	88.01 ^a ± 0.24	97.10 ^a ± 0.26	104.56 ^a ± 0.40	21.78 ^a ± 0.46	7.78 ^g ± 0.19
C ₆ H ₁₀ CaO ₆	CaCl ₂	0.0001:1	80.84 ^f ± 0.36	86.49 ^d ± 0.14	96.73 ^{ab} ± 0.12	101.60 ^f ± 0.32	20.77 ^{bc} ± 0.65	9.75 ^{cd} ± 0.16
		0.0004:1	81.38 ^{ef} ± 0.23	87.08 ^c ± 0.19	96.50 ^b ± 0.16	102.59 ^{de} ± 0.32	21.21 ^{ab} ± 0.11	9.74 ^{cd} ± 0.06
		0.0007:1	82.07 ^{bcd} ± 0.10	87.54 ^{abc} ± 0.20	95.50 ^b ± 0.35	103.88 ^b ± 0.40	21.81 ^a ± 0.36	9.89 ^e ± 0.13
C ₆ H ₁₀ CaO ₆		0.0001:1	81.81 ^{ed} ± 0.49	86.33 ^d ± 0.07	96.92 ^a ± 0.02	102.20 ^{ef} ± 0.34	20.39 ^e ± 0.16	9.96 ^e ± 0.09
		0.0004:1	82.37 ^{abc} ± 0.49	87.25 ^{bc} ± 0.23	96.91 ^a ± 0.10	103.12 ^{cd} ± 0.36	20.76 ^{bc} ± 0.34	9.57 ^d ± 0.21
		0.0007:1	82.54 ^{ab} ± 0.09	87.75 ^{ab} ± 0.04	96.91 ^a ± 0.07	103.71 ^{bc} ± 0.49	21.17 ^{ab} ± 0.42	8.97 ^a ± 0.08

T_o, T_{p1}, T_{p2}, T_c, T_c-T_o represent the onset, first peak, second peak, conclusion of gelatinization, and the gelatinization temperature range, respectively.

ΔH_g represents the enthalpy of gelatinization.

The reported values are means (SD).

Means with different letters (a, b, ...) in each column are significantly different ($P \leq 0.05$).

Table 4.8 Thermal properties of retrograded native starch and HMT-starch that treated at 110°C for 1 h stored at 5°C for 7 days

Type of Pigeonpea Starch	Type of Calcium Compound	Ca ²⁺ :Starch	T _o (°C)	T _p (°C)	T _c (°C)	T _c -T _o (°C)	ΔH _{r7} (J/g)
Native starch	-	-	43.20 ^g (0.05)	61.86 ^e (0.05)	72.52 ^h (0.00)	29.32 ^f (0.05)	7.17 ^a (0.05)
Heat-moisture treated at 110°C, 1 h	-	0:1	45.63 ^f (0.47)	63.46 ^d (0.26)	76.29 ^g (0.15)	30.40 ^{cd} (0.47)	4.99 ^b (0.04)
	Ca(OH) ₂	0.0001:1	47.16 ^e (0.10)	63.46 ^{bc} (0.42)	77.22 ^f (0.23)	30.06 ^e (0.25)	4.14 ^d (0.06)
		0.0004:1	48.00 ^c (0.02)	64.80 ^a (0.12)	79.62 ^b (0.25)	31.62 ^{ab} (0.27)	3.76 ^e (0.09)
		0.0007:1	48.85 ^a (0.19)	64.64 ^a (0.00)	79.88 ^b (0.15)	31.03 ^c (0.18)	2.72 ^g (0.07)
	CaCl ₂	0.0001:1	47.23 ^e (0.04)	63.28 ^{bc} (0.06)	77.82 ^e (0.12)	30.24 ^{de} (0.23)	4.72 ^c (0.17)
		0.0004:1	47.58 ^d (0.11)	63.28 ^c (0.06)	77.82 ^{de} (0.12)	30.24 ^{de} (0.23)	4.55 ^{cd} (0.05)
		0.0007:1	47.84 ^{cd} (0.10)	63.80 ^b (0.65)	79.74 ^b (0.26)	31.90 ^b (0.36)	4.58 ^{cd} (0.29)
	C ₆ H ₁₀ CaO ₆	0.0001:1	47.14 ^e (0.05)	62.56 ^d (0.15)	78.17 ^d (0.23)	31.03 ^c (0.19)	3.83 ^e (0.07)
		0.0004:1	47.66 ^d (0.04)	63.71 ^{bc} (0.23)	78.76 ^c (0.12)	31.10 ^{bc} (0.11)	3.65 ^e (0.04)
		0.0007:1	48.47 ^b (0.05)	63.90 ^b (0.08)	80.54 ^a (0.28)	32.07 ^a (0.28)	3.32 ^f (0.02)

T_o, T_p, T_c, T_c-T_o represent the onset, peak, conclusion of gelatinization, and the gelatinization temperature range, respectively.

ΔH_{r7} represents enthalpy of retrogradation at 7 days

The reported values are means (SD.)

Means with different letters (a, b, ..) in each column are significantly different ($P \leq 0.05$).

Table 4.9 Thermal properties of retrograded native starch and HMT-starch that treated at 110°C for 1 stored at 5°C for 14 days

Type of Pigeonpea Starch	Type of Calcium Compound	Ca ²⁺ :Starch	T _o (°C)	T _p (°C)	T _c (°C)	T _c -T _o (°C)	ΔH _{r14} (J/g)	
Native starch	-	-	47.73 ^g (0.13)	61.29 ^f (0.20)	75.50 ⁱ (0.06)	27.77 ^e (0.10)	8.37 ^a (0.06)	
Heat-moisture treated at 110°C, 1 h	-	0:1	49.69 ^f (0.35)	63.49 ^d (0.56)	77.50 ^h (0.42)	27.81 ^e (0.76)	5.52 ^b (0.10)	
		Ca(OH) ₂	0.0001:1	51.32 ^e (0.23)	64.10 ^{bc} (0.02)	79.33 ^g (0.25)	28.01 ^e (0.39)	5.08 ^c (0.07)
			0.0004:1	53.19 ^b (0.23)	64.29 ^b (0.12)	80.30 ^f (0.16)	27.11 ^f (0.38)	3.91 ^f (0.04)
	0.0007:1		53.64 ^{ab} (0.17)	65.13 ^a (0.06)	82.55 ^{ab} (0.10)	28.91 ^{cd} (0.08)	3.22 ^g (0.07)	
	CaCl ₂	0.0001:1	52.29 ^c (0.24)	63.68 ^e (0.25)	81.70 ^{de} (0.32)	29.42 ^{abc} (0.29)	5.05 ^c (0.03)	
		0.0004:1	52.29 ^c (0.24)	63.68 ^{cd} (0.40)	82.06 ^{cd} (0.10)	29.77 ^a (0.32)	5.07 ^c (0.07)	
		0.0007:1	53.49 ^{ab} (0.45)	63.42 ^d (0.24)	82.18 ^{bc} (0.25)	28.69 ^d (0.21)	5.23 ^c (0.21)	
	C ₆ H ₁₀ CaO ₆	0.0001:1	51.80 ^d (0.29)	62.64 ^e (0.40)	81.39 ^e (0.23)	29.58 ^{ab} (0.10)	4.60 ^d (0.16)	
		0.0004:1	52.63 ^c (0.20)	63.30 ^d (0.23)	82.35 ^{bc} (0.21)	29.72 ^a (0.17)	4.41 ^e (0.15)	
		0.0007:1	53.78 ^a (0.09)	64.29 ^b (0.22)	82.80 ^a (0.19)	29.01 ^{bcd} (0.25)	3.74 ^f (0.05)	

T_o, T_p, T_c, T_c-T_o represent the onset, peak, conclusion of gelatinization, and the gelatinization temperature range, respectively.

ΔH_{r14} represents enthalpy of retrogradation at 14 days

The reported values are means (SD.)

Means with different letters (a, b, ..) in each column are significantly different ($P \leq 0.05$).

Table 4.10 Gelatinization and melting of retrograded starch enthalpy of native starch and HMT-starch that treated at 110°C for 1 h

Type of Pigeonpea Starch	Type of Calcium Compound	Ca ²⁺ :Starch	ΔH_g (J/g)	ΔH_{r7} (J/g)	ΔH_{r14} (J/g)	%Retrogradation ₇	%Retrogradation ₁₄
Native starch	-	-	13.50 ^a A (0.15)	7.17 ^a C (0.05)	8.37 ^a B (0.06)	53.10 ^a B (0.46)	61.98 ^a A (0.39)
Heat-moisture treated at 110°C, 1 h	-	0:1	10.39 ^b A (0.24)	4.99 ^b C (0.04)	5.52 ^b B (0.10)	48.06 ^b B (0.84)	53.19 ^b A (0.47)
	Ca(OH) ₂	0.0001:1	9.98 ^c A (0.05)	4.14 ^d C (0.06)	5.08 ^c B (0.07)	44.22 ^d B (0.70)	50.90 ^c A (0.54)
		0.0004:1	8.60 ^f A (0.12)	3.76 ^e B (0.09)	3.91 ^f B (0.04)	43.73 ^d B (0.41)	45.45 ^d A (1.09)
		0.0007:1	7.78 ^g A (0.19)	2.72 ^g C (0.07)	3.22 ^g B (0.07)	34.97 ^f B (0.85)	41.42 ^e A (0.19)
	CaCl ₂	0.0001:1	9.75 ^{cd} A (0.16)	4.72 ^c C (0.17)	5.05 ^c B (0.03)	48.42 ^b B (0.82)	51.82 ^{bc} A (0.88)
		0.0004:1	9.74 ^{cd} A (0.06)	4.55 ^{cd} C (0.05)	5.07 ^c B (0.07)	46.72 ^c B (0.77)	52.08 ^{bc} A (0.39)
		0.0007:1	9.89 ^c A (0.13)	4.58 ^{cd} C (0.29)	5.23 ^c B (0.21)	46.35 ^c B (0.90)	52.77 ^{bc} A (2.56)
	C ₆ H ₁₀ CaO ₆	0.0001:1	9.96 ^c A (0.09)	3.83 ^e C (0.07)	4.60 ^d B (0.16)	38.50 ^e B (1.00)	46.23 ^d A (1.74)
		0.0004:1	9.57 ^d A (0.21)	3.65 ^e C (0.04)	4.41 ^e B (0.15)	38.16 ^e B (0.67)	46.09 ^d A (1.33)
0.0007:1		8.97 ^e A (0.08)	3.32 ^f B (0.02)	3.74 ^f B (0.05)	37.06 ^e B (0.17)	41.70 ^e A (0.83)	

The reported values are means (SD.)

Means with different letters (a, b, ..) in each column are significantly different ($P \leq 0.05$).

Means with different letters (A, B, ..) in each row are significantly different ($P \leq 0.05$).

4.2.6 Freeze-thaw stability

The % syneresis increased significantly with increase in the number of freeze-thaw cycles ($p \leq 0.05$). The results showed that for the first two cycles the paste of all heat-moisture treated starches had higher % syneresis than the native starch paste, and vice versa for the last two cycles (Table 4.11). Except for the 1st cycle, all the HMT-Ca starch pastes had lower % syneresis than the HMT starch paste. After five freeze-thaw cycles, the HMT-Ca(OH)₂ starch at the Ca²⁺-starch ratio of 0.0007:1 gave the minimum % syneresis of 42.36, while the native starch gave the maximum % syneresis of 62.36. Freeze-thaw stability is an important factor to be considered when formulating refrigerated and frozen foods (Yadav *et al.*, 2013). A lower syneresis indicates the higher freeze-thaw stability of starch. The order of calcium compounds that gave good freeze-thaw stability for the HMT starch was Ca(OH)₂ > C₆H₁₀CaO₆ > CaCl₂. When using Ca(OH)₂ or C₆H₁₀CaO₆, the higher Ca²⁺-starch ratio resulted in a lower % syneresis. For HMT-CaCl₂ starch, an increase in the Ca²⁺-starch ratio increased % syneresis, however, its increase was lower than that of HMT-starch and native starch. The reduction in % syneresis by heat-moisture treatment was similar to that reported for the water chestnut starch by Yadav *et al.* (2013), which the HMT-starch had lower % syneresis than the native starch.

It has been reported that exudation of water from the starch gel system stored at low temperature could be the result of increasing the intermolecular hydrogen bonding between amylose-amylose, amylose-amylopectin or amylopectin-amylopectin interactions (Hoover *et al.*, 1997; Yadav *et al.*, 2013). As syneresis is resulted to formation of free water exuded from retrograded starch gel with association of amylose molecules progressed. As it is shown from the experiment that

heat-moisture treatment of starch with calcium compounds can stabilize starch granules, less amylose leach out from granules, thus the distance between separate amylose chains is the important factors (Hoover and Manuel, 1996). For the first two cycles, % syneresis of the HMT-starch and HMT-Ca starches were higher than native starch, suggested that the faster retrogradation than the native starch. The reason for this could not be explained. However, in the last three cycles, less % soluble and less amylose leaching out caused lower % retrogradation, and thus lower % syneresis of HMT-Ca starches than HMT-starch (without adding calcium compound) and native starch. The high freeze-thaw stability of HMT-Ca starches suggested that they could be used to improve the freeze-thaw stability of frozen food products. The HMT-Ca(OH)₂ starch displayed the best freeze-thaw stability.

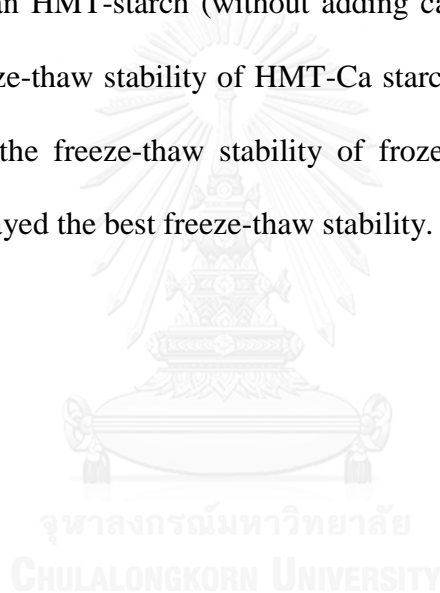


Table 4.11 The % syneresis of 5% w/w native starch and HMT-starch that treated at 110°C for 1 h

Type of Pigeonpea Starch	Type of Calcium Compound	Ca ²⁺ :Starch	Syneresis (%) for Cycle				
			1	2	3	4	5
Native starch	-	-	22.57 ^f ± 1.51	31.64 ^f ± 0.91	42.36 ^a ± 1.48	50.47 ^a ± 0.88	62.36 ^a ± 2.11
Heat-moisture treated at 110°C, 1 h	-	0:1	27.56 ^e ± 1.32	35.87 ^a ± 0.69	41.65 ^a ± 0.94	46.75 ^b ± 0.64	54.71 ^b ± 0.94
	Ca(OH) ₂	0.0001:1	29.09 ^{abcde} ± 1.27	33.89 ^{cde} ± 0.91	38.68 ^b ± 0.44	40.91 ^e ± 0.97	46.25 ^{fe} ± 0.98
		0.0004:1	28.47 ^{cde} ± 1.33	33.29 ^{de} ± 0.62	37.22 ^{cd} ± 0.67	40.64 ^e ± 0.50	44.55 ^b ± 0.57
	0.0007:1	28.07 ^{de} ± 0.46	32.92 ^e ± 0.98	37.81 ^{bcd} ± 0.46	38.54 ^f ± 0.84	42.36 ^h ± 0.72	
	CaCl ₂	0.0001:1	28.98 ^{bcd} ± 0.76	34.48 ^{bc} ± 0.59	38.34 ^{bc} ± 0.53	44.93 ^c ± 0.95	50.73 ^d ± 0.78
		0.0004:1	29.72 ^{abcd} ± 0.59	35.08 ^{ab} ± 0.37	37.70 ^{bcd} ± 0.66	43.64 ^{cd} ± 0.71	52.29 ^c ± 1.18
		0.0007:1	30.72 ^a ± 0.82	34.40 ^{bc} ± 0.61	36.84 ^{cd} ± 0.55	42.59 ^d ± 1.15	52.44 ^c ± 0.93
	C ₆ H ₁₀ CaO ₆	0.0001:1	30.03 ^{abc} ± 1.13	33.67 ^{cde} ± 0.42	39.28 ^b ± 1.11	43.07 ^d ± 0.82	49.97 ^{de} ± 0.35
		0.0004:1	30.32 ^{abcd} ± 0.64	32.86 ^e ± 0.87	36.63 ^d ± 0.77	40.35 ^e ± 1.32	48.38 ^e ± 0.88
		0.0007:1	30.22 ^{ab} ± 1.33	32.74 ^e ± 0.27	36.49 ^d ± 1.28	39.42 ^{ef} ± 1.07	46.44 ^f ± 0.78

The reported values are means ± SD.
Means with different letters (a, b, ...) in each column are significantly different ($P \leq 0.05$).

From these results, the HMT-Ca(OH)₂ starch at the Ca²⁺-starch ratio of 0.0007:1 gave the lowest swelling power, %solubility, amylose leaching and gelatinization enthalpy (ΔH_g). In addition, the HMT-Ca(OH)₂ could be the good freeze-thaw stability as a result of it lowest % syneresis and % retrogradation. Therefore, it was selected to study the effect of temperature and time on the structure and physicochemical properties of starch.

4.3 Effect of temperature and time of heat-moisture treatment on the physicochemical properties of starch

4.3.1 Structural characteristics

4.3.1.1 Light microscopy

Figure 4.7 shows the granular images of the HMT starch in the absence of and the presence of Ca(OH)₂ at different temperatures and times of heat-moisture treatment from light/polarized light microscopy. The light microscope images show that that temperature and time used for heat-moisture treatment did not apparently affect morphology of starch (Figure A.10). As the granules still exhibited a diffuse polarized cross, suggesting the presence of an ordered complex. However, polarized light images show increases in the temperature and time for heat-moisture treatment caused an increase in the loss of birefringence at the granule center (Figure A.11), indicating that more partial melting occurred during heat-moisture treatment. Comparing at constant temperature and time, the presence of Ca(OH)₂ led to a greater loss of birefringence at the granule center than the HMT in the absence of Ca(OH)₂. The higher temperature of HMT resulted in the higher thermal energy that disturbed

the double helices, which form crystallites. This promoted their mobility, and led to a loss of radial orientation (Chung *et al.*, 2009).

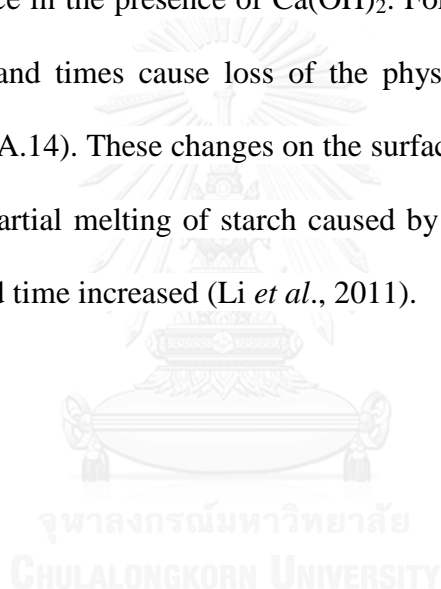


Temperature (°C)/Time (h)	HMT in the absence of Ca(OH)_2		HMT in the presence of Ca(OH)_2	
	$\times 100$	$\times 100$	$\times 100$	$\times 100$
100/1				
100/2				
110/1				
110/2				
120/1				
120/2				

Figure 4.7 Microscope and polarized light microscope images of starch granules

4.3.1.2 Scanning electron microscopy (SEM)

Figure 4.8 shows the granular structure of the HMT starch in the absence of and the presence of Ca(OH)_2 at different temperatures and times of heat-moisture treatment taken from a scanning electron microscope. With heat-moisture treatment, the higher temperature and time level created more dents on the surface of the modified starches. HMT starches in the absence of Ca(OH)_2 , increases in temperature and time caused more cracks and dents in the starch granules than HMT starch took place in the presence of Ca(OH)_2 . For all the modified starches the higher temperatures and times cause loss of the physical integrity of the granular surface (Figure A.12-A.14). These changes on the surface of the starch granules could be attributed to the partial melting of starch caused by increases in thermal force as HMT temperature and time increased (Li *et al.*, 2011).



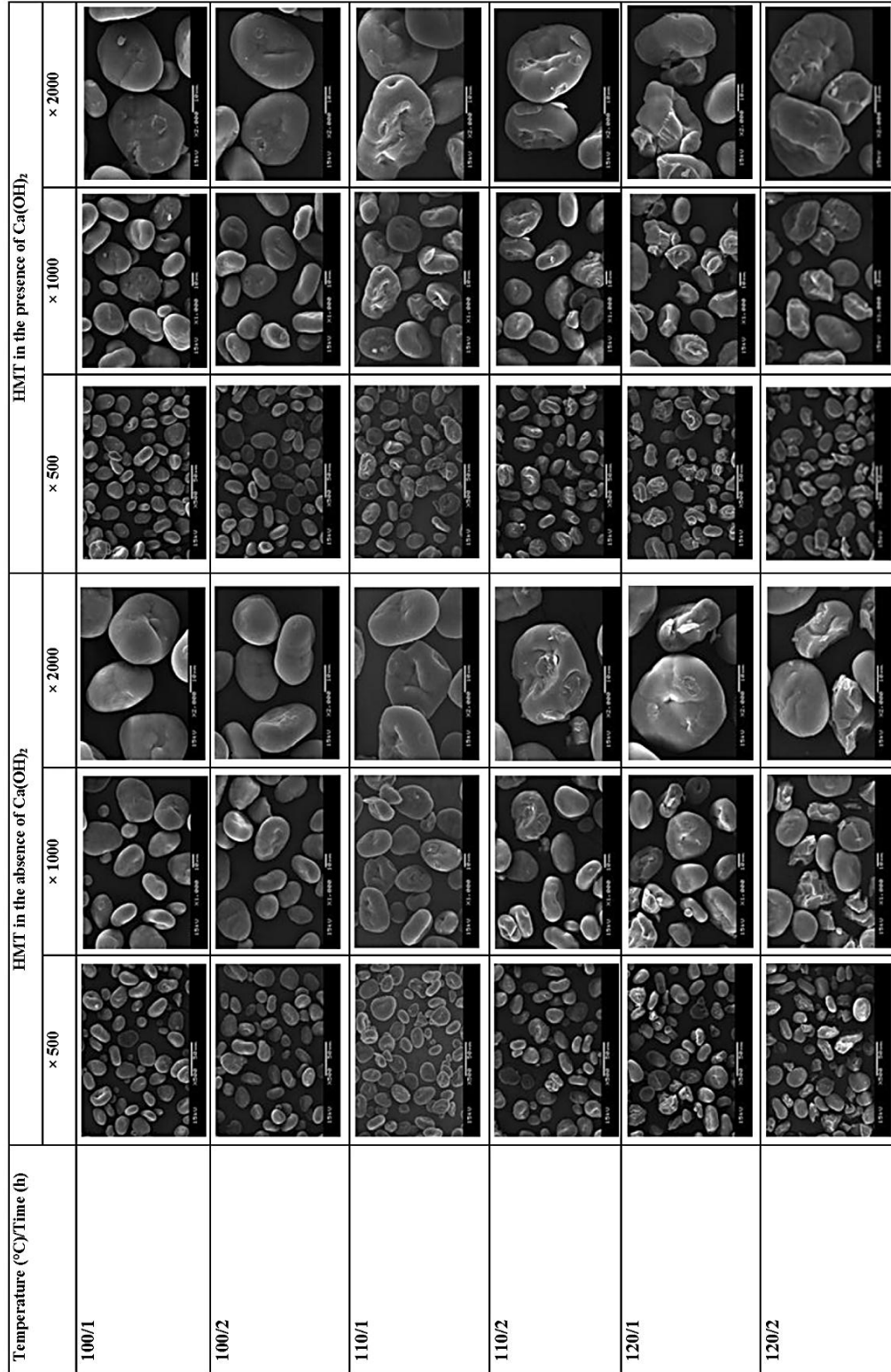
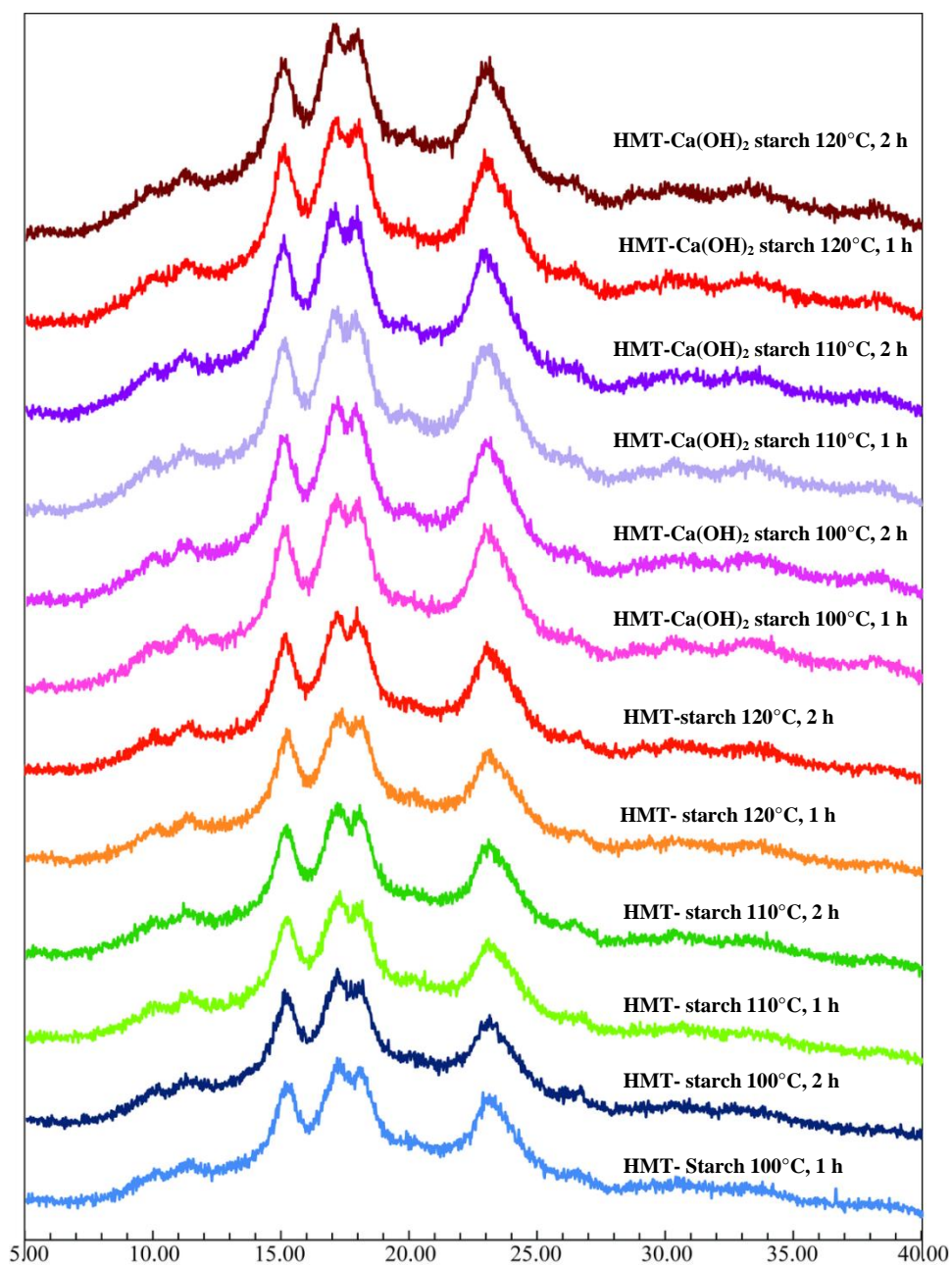


Figure 4.8 Scanning electron micrographs of starch granules

4.3.1.3 X-ray diffraction and relative crystallinity

Figure 4.9 shows the crystalline patterns of the HMT-starch and HMT-Ca(OH)₂ starch treated at different temperatures and times. The XRD pattern for these starches indicates A-type diffraction patterns, with diffraction strong peaks at 15.2°, 17.2° 18.1° and 23.1° 2θ and weak peaks at 11.5°, 20.0°, 26.5° and 30.3° 2θ (Horng, 2007). The intensity of diffraction peak and % RC decreased with an increase in treatment temperature. Generally, comparing heat-moisture treatment at constant temperature and time, the peak intensity at 11.5°, 15.2°, 17.2° 18.1° 20.0° and 23.1° 2θ and % RC of HMT-Ca(OH)₂ starches were higher than those of the HMT-starches (Table 4.12). The % RC of HMT-starch was 29.49–32.95%, while that of HMT-Ca(OH)₂ starches was 31.00–34.50%. It was also found that % RC decreased with an increase in treatment temperature or time. Changes in the intensities of diffraction peaks as heat-moisture treatment temperature and time increased are considered a result of an increase in thermal energy. This could be attributed to the fact that the double helices were disturbed and more mobile (Chung *et al.*, 2009; Li *et al.*, 2011), and then reassociation within the crystalline domain of the starch granules; consequently, the amount of direct hydrogen bonds increased (da Rosa Zavareze and Dias, 2011; Klein *et al.*, 2013; Sui *et al.*, 2015). Therefore, the increase in heat-moisture treatment temperature and time accelerated molecular rearrangement that led to a strengthening of the association of double helices.



20

Figure 4.9 The X-ray pattern Effect of HMT-starch and HMT- Ca(OH)_2 starch at the Ca^{2+} -starch ratio of 0:1 and 0.0007:1

Table 4.12 Peak intensities from X-ray diffractograms and relative crystallinity of HMT-starch and HMT-Ca(OH)₂ starch at the Ca²⁺-starch ratio of 0:1 and 0.0007:1

Treatment	Temperature (°C) and Time (h)	Peak Intensity (CPS)							RC (%)
		11.49	15.18	17.20	18.10	20.00	23.10	26.50	
HMT in the absence of Ca(OH) ₂	100/1	1090 ^e	1930 ^d	2115 ^d	2102 ^d	1331 ^{da}	1833 ^d	1023 ^c	32.95 ^b ± 0.40
	100/2	1087 ^c	1849 ^e	2045 ^e	2003 ^e	1275 ^e	1715 ^e	983 ^d	32.20 ^{bc} ± 0.32
	110/1	1086 ^c	1805 ^f	2014 ^e	1914 ^f	1371 ^d	1600 ^f	905 ^e	31.09 ^c ± 0.10
	110/2	1075 ^c	1808 ^e	2029 ^e	1915 ^f	1293 ^e	1618 ^f	904 ^e	30.59 ^d ± 0.17
	120/1	1046 ^d	1816 ^{ef}	2050 ^e	1907	1294 ^e	1609 ^f	955 ^d	30.22 ^d ± 0.35
	120/2	1018 ^d	1707 ^g	1931 ^f	1872 ^g	1219 ^f	1611 ^f	913 ^e	29.49 ^e ± 0.14
HMT in the presence of Ca(OH) ₂	100/1	1390 ^a	2427 ^a	2750 ^a	2692 ^a	1768 ^a	2361 ^a	1329 ^a	34.45 ^a ± 0.30
	100/2	1384 ^a	2432 ^a	2770 ^a	2648 ^a	1759 ^a	2354 ^a	1321 ^a	34.50 ^a ± 0.14
	110/1	1380 ^a	2379 ^b	2642 ^b	2611 ^b	1719 ^b	2316 ^b	1318 ^a	34.08 ^a ± 0.67
	110/2	1368 ^a	2410 ^{ab}	2699 ^{ab}	2628 ^{ab}	1712 ^b	2350 ^a	1302 ^a	34.01 ^a ± 0.54
	120/1	1311 ^b	2280 ^c	2613 ^b	2562 ^b	1649 ^c	2253 ^c	1254 ^b	32.50 ^b ± 0.33
	120/2	1307 ^b	2233 ^c	2519 ^c	2462 ^c	1618 ^c	2222 ^c	1262 ^b	31.00 ^c ± 0.28

CPS: count per second.

The reported values are means (SD).

Means with different letters (a, b, ...) in each column are significantly different ($P \leq 0.05$).

4.3.2 Swelling power, % solubility and amylose leaching

Table 4.13 shows that swelling power, % solubility and amylose leaching of the HMT-starch and HMT-Ca(OH)₂ starch decreased with an increase in treatment temperature ($p \leq 0.05$). Generally, comparing heat-moisture treatment at constant temperature and time, these three properties of HMT-Ca(OH)₂ starches were lower than those of the HMT-starches. For HMT-starch, swelling power decreased as treatment time increased at a constant temperature of 100°C and 110°C ($p \leq 0.05$). Its % solubility increased with an increase in treatment time at 100°C, and vice versa for 110°C and 120°C ($p \leq 0.05$). Amylose leaching decreased with treatment time at 110°C ($p \leq 0.05$). For HMT-Ca(OH)₂ starch, the swelling power and amylose leaching of HMT-Ca(OH)₂ increased as treatment time increased at 100°C ($p \leq 0.05$). At 120°C, treatment time did cause a decrease in % solubility and an increase in amylose leaching.

The decrease in swelling power, % solubility and amylose leaching as the heat-moisture treatment temperature and time increased could be attributed to the existence of strong binding forces particularly in the existing crystallites (Adebowale *et al.*, 2005). The decrease in swelling power also was assigned to some transformation of amorphous amylose into a helical form, an increase in interactions between starch molecule chains such as amylose-amylose, amylose-amylopectin and amylopectin-amylopectin chains to form the ordered structure (double helical), and alteration in the interaction between the crystalline and the amorphous matrix during HMT (Eerlingen *et al.*, 1997; Gunaratne and Hoover, 2002; Lawal, 2005; Li *et al.*, 2011; Olayinka *et al.*, 2008; Sun *et al.*, 2014; Varatharajan *et al.*, 2010). As previously discussed before, heat-moisture treatment of starch with Ca(OH)₂ can

stabilize starch granules which resulted in less swelling of granules, and less soluble leaching from the granules.



Table 4.13 Swelling power, % solubility and amylose leaching at 95°C of HMT starch and HMT-Ca(OH)₂ starch at the Ca²⁺-starch ratio of 0:1 and 0.0007:1

Treatment	Temperature (°C) and Time (h)	Swelling Power (g/g)	Solubility (%)	Amylose Leaching (%)
HMT in the absence of Ca(OH) ₂	100/1	12.63 ^b ± 0.62	18.20 ^c ± 0.54	42.82 ^c ± 1.36
	100/2	11.14 ^c ± 0.42	19.14 ^b ± 0.39	42.82 ^c ± 0.73
	110/1	10.50 ^{cd} ± 0.22	17.45 ^{cd} ± 0.37	37.26 ^e ± 0.56
	110/2	7.40 ^f ± 0.35	16.11 ^e ± 0.54	33.70 ^f ± 0.37
	120/1	4.91 ^{hi} ± 0.26	12.49 ^f ± 0.56	21.11 ^h ± 0.43
	120/2	4.21 ^j ± 0.70	11.07 ^f ± 0.26	20.33 ^{hi} ± 0.43
HMT in the presence of Ca(OH) ₂	100/1	8.28 ^e ± 0.26	16.03 ^{de} ± 0.61	38.85 ^d ± 0.82
	100/2	10.13 ^d ± 0.28	17.54 ^{de} ± 0.57	44.00 ^b ± 0.93
	110/1	5.80 ^{ef} ± 0.40	10.33 ^{ef} ± 0.34	23.99 ^{ef} ± 0.15
	110/2	5.45 ^{gh} ± 0.42	10.54 ^{ef} ± 0.60	24.04 ^{ef} ± 0.75
	120/1	4.05 ^j ± 0.11	9.26 ^h ± 0.56	19.54 ⁱ ± 0.42
	120/2	3.42 ^j ± 0.75	8.23 ⁱ ± 0.31	20.84 ^h ± 0.42

The reported values are means ± SD.

Means with different letters (a, b, ..) in each column are significantly different ($P \leq 0.05$).

4.3.3 Pasting properties of starches

The pasting properties of HMT-starch and HMT-Ca(OH)₂ starch are presented in Table 4.14. Generally the viscosity at the end of the heating period at 95°C (η_h) and viscosity at the end of the cooling period at 50°C (η_c) of HMT-starch and HMT-Ca(OH)₂ decreased as treatment temperature and time increased ($p \leq 0.05$), except at 100°C both values increased with treatment time. Compared to HMT-starch, the η_h and η_c of HMT-Ca(OH)₂ starches were lower. Moreover, the treatment temperature and time did not significantly affect the pasting temperature of all HMT-starch and HMT-Ca(OH)₂ starch ($p > 0.05$). The effect of temperature and time on η_h and η_c were correlated with their low swelling power, % solubility and amylose leaching (Table 4.13). On account of the restricted swelling of starch granules, which was limiting the leaching of amylose into the medium led to decrease in viscosity. Moreover, decrease in η_h and η_c of HMT-Ca(OH)₂ was a result of a decrease in swelling of starch granules led to a small amount of amylose leaching, therefore viscosity decreased.

It seems common that the heat-moisture treatment with the higher temperature and/or longer heating time resulted in decrease in peak and final viscosities of starches. For examples, these phenomena occurred in maize starch as reported by Sui *et al.* (2015) and also in rice, cassava and pinhao starches as reported by Klein *et al.* (2013). The common explanation for these phenomena given by these researchers was that the higher temperature and/or longer heating time brought about the better packaged (more densely packed structure) and ordered crystalline array (A-type) in starch granules during heat-moisture treatment led to restricted swelling and a small amount of amylose leaching, therefore, these viscosities decreased.

Table 4.14 Viscosity at the end of the heating period (η_h) and viscosity at the end of the cooling period (η_c) of 10% w/w HMT-starch and HMT-Ca(OH)₂ starch at the Ca²⁺-starch ratio of 0:1 and 0.0007:1

Treatment	Temperature (°C) and Time (h)	Viscosity at the end of the heating period (95°C) (mPa.s)	Viscosity at the end of the cooling period (50°C) (mPa.s)	Pasting temperature (°C)
HMT in the absence of Ca(OH) ₂	100/1	989.67 ^e ± 16.44	1360.33 ^e ± 18.15	94.15 ^{bed} ± 0.43
	100/2	1057.64 ^b ± 13.05	1594.33 ^b ± 70.44	94.72 ^{abc} ± 0.06
	110/1	833.33 ^d ± 16.01	1209.67 ^d ± 25.23	95.13 ^{ab} ± 0.12
	110/2	758.33 ^{de} ± 67.95	1150.00 ^d ± 75.50	95.07 ^{abc} ± 0.13
	120/1	528.00 ^e ± 29.82	904.67 ^e ± 50.65	94.97 ^{abc} ± 0.16
	120/2	168.33 ⁱ ± 22.37	334.67 ^e ± 42.22	93.27 ^d ± 0.92
HMT in the presence of Ca(OH) ₂	100/1	796.33 ^{de} ± 46.09	1202.67 ^d ± 30.02	95.47 ^e ± 0.03
	100/2	1301.00 ^e ± 41.97	1694.67 ^a ± 37.50	95.15 ^{ab} ± 0.40
	110/1	653.86 ^f ± 27.79	998.00 ^e ± 28.64	94.93 ^{abc} ± 0.06
	110/2	616.00 ^f ± 53.51	906.67 ^e ± 86.23	94.87 ^{abc} ± 0.03
	120/1	246.33 ^h ± 43.39	469.00 ^f ± 69.20	94.07 ^{bed} ± 1.61
	120/2	108.33 ^j ± 9.07	243.00 ^h ± 11.53	93.83 ^{cd} ± 1.03

The reported values are means ± SD. Means with different letters (a, b, ...) in each column are significantly different ($P < 0.05$).

4.3.4 Rheological properties

The flow behavior of all starch gels studied in this section at 25°C and shear rate ranging between 0.1-1000 s⁻¹ also showed a pseudo-plastic with yield stress following the Herschel-Bukley model with $R^2 \geq 0.97$. Their τ_0 , K and n values are reported in Table 4.15. The τ_0 of HMT-starch decreased with an increase in treatment temperature and time. At constant temperature and time, HMT-Ca(OH)₂ starch had lower τ_0 than HMT-starch. For HMT-starch, the K value decreased as treatment temperature and time increased. Its n value decreased with an increase in treatment time at 100°C, and vice versa for 110°C. At 120°C, treatment time did not affect the n value of HMT-starch. For the HMT-Ca(OH)₂ starch, K value decreased with an increase in treatment temperature, but was not affected by treatment time. Its n value increased with an increase in treatment temperature, but it also did not affected by treatment time. The K value of starch gel depends on the effect of swollen granules and amylose leaching which thicken the viscosity of the continuous phase (Osundahunsi *et al.*, 2011). The lower swelling power and amylose leaching (see section 4.3.2) resulted in a lower K value.

Figures 4.10a and 4.10b show that G' was higher than G'' for every treatment of HMT-starch and HMT-Ca(OH)₂ starch. The G' of HMT-starch gel was higher than that of the HMT-Ca(OH)₂ starch. At constant temperature and time, the G'_1 , G''_1 , $(\tan \delta)_1$ and the obtained exponent constants (a , b and c with R^2 ranging 0.90-0.98) are reported in Table 4.16. An increase in the treatment temperature and time decreased the G'_1 and G''_1 . The $(\tan \delta)_1$ was not affected by treatment temperature and time. For all treatments, both HMT- and HMT-Ca(OH)₂ starch gel gave the “ a ” value of < 0.09 (near zero) and $(\tan \delta)_1$ of < 1 . This indicated that they had a weak to

stable gel structure and behaved as an elastic-like solid (Acevedo *et al.*, 2013; Maache-Rezzoug *et al.*, 2010; Osundahunsi *et al.*, 2011).



Table 4.15 Herschel-bulkley constants [yield stress (τ_0), consistency coefficient (K) and flow behavior index (n)] of 5 % w/w HMT-starch and HMT- $\text{Ca}(\text{OH})_2$ starch at the Ca^{2+} -starch ratio of 0:1 and 0.0007:1 at 25°C and shear rate between 0.1-1000 s^{-1}

Treatment	Temperature (°C) and Time (h)	τ_0 (Pa)	K (Pa·s ⁿ)	n
HMT in the absence of $\text{Ca}(\text{OH})_2$	100/1	6.62 ^a (0.30)	0.28 ^a (0.03)	0.75 ^{bc} (0.01)
	100/2	6.14 ^b (0.13)	0.25 ^{bc} (0.04)	0.69 ^d (0.01)
	110/1	5.45 ^c (0.11)	0.26 ^b (0.01)	0.69 ^d (0.02)
	110/2	5.45 ^c (0.04)	0.25 ^b (0.00)	0.78 ^b (0.03)
	120/1	1.73 ^f (0.19)	0.19 ^g (0.02)	0.83 ^a (0.02)
	120/2	0.96 ^g (0.03)	0.17 ^g (0.00)	0.83 ^a (0.01)
HMT in the presence of $\text{Ca}(\text{OH})_2$	100/1	2.73 ^d (0.24)	0.23 ^c (0.01)	0.73 ^c (0.02)
	100/2	2.30 ^e (0.22)	0.22 ^c (0.01)	0.76 ^b (0.01)
	110/1	2.73 ^d (0.19)	0.11 ^h (0.02)	0.82 ^a (0.02)
	110/2	2.46 ^e (0.10)	0.11 ^h (0.01)	0.81 ^a (0.03)
	120/1	0.84 ^g (0.13)	0.11 ^h (0.00)	0.84 ^a (0.01)
	120/2	0.80 ^g (0.06)	0.11 ^h (0.02)	0.84 ^a (0.02)

The reported values are means (SD).

Means with different letters (a, b, ..) in each column are significantly different ($P \leq 0.05$).

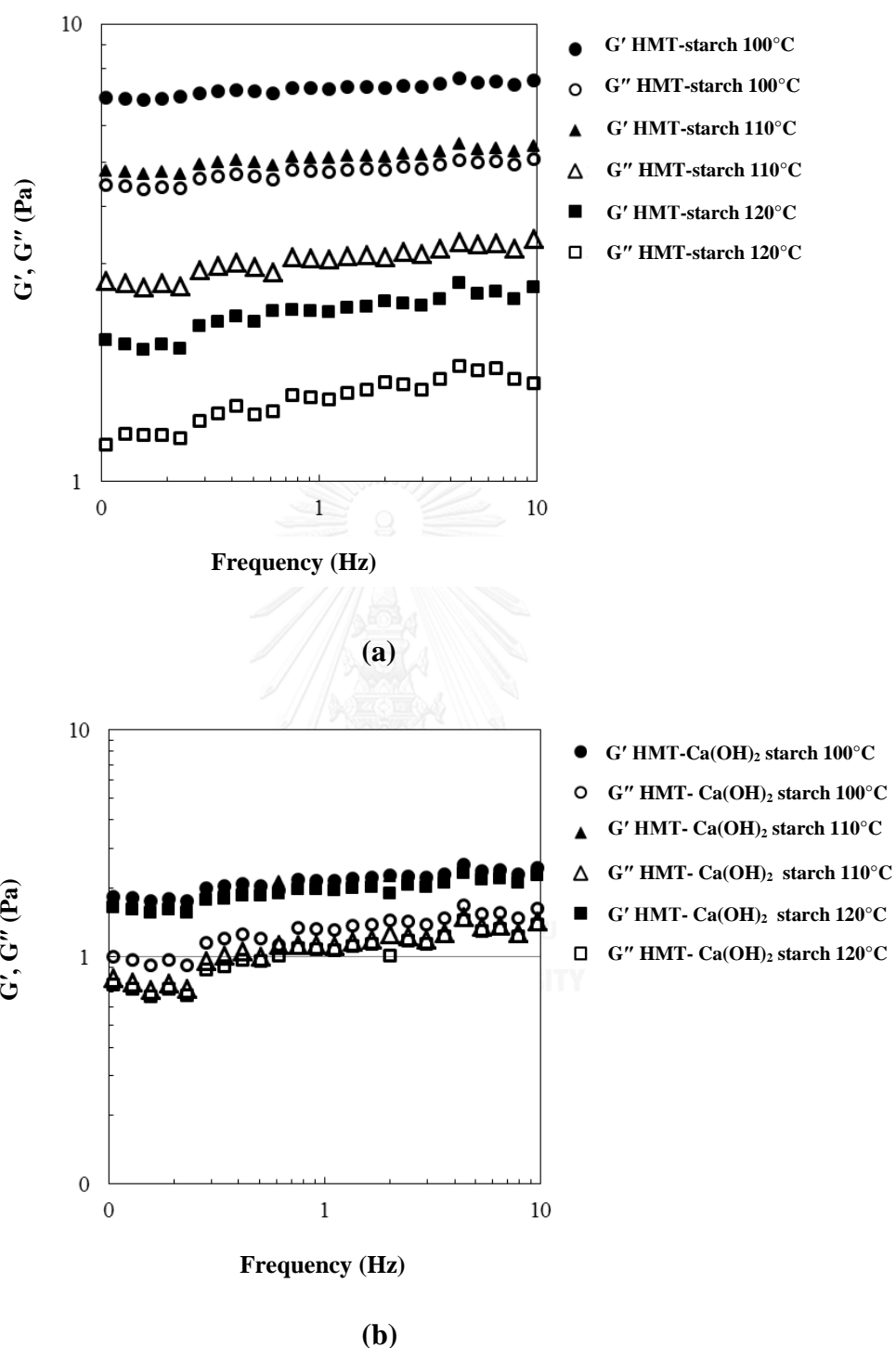


Figure 4.10 Viscoelastic properties of 5% w/w HMT-starch (a) and HMT- $\text{Ca}(\text{OH})_2$ starch (b) at the Ca^{2+} -starch ratio of 0:1 and 0.0007:1 at 25°C, 1% strain and frequency ranging 0.1 to 10 Hz

Table 4.16 Rheological properties of gels. The power law model was fitted to experimental measurements

Treatment	Temperature (°C) and Time (h)	G'_1 (Pa)	a^*	G''_1 (Pa)	b^*	$(\tan \delta)_1$	c^*
HMT in the absence of Ca(OH)_2	100/1	7.02 ^a (0.21)	0.02 ^f (0.00)	4.94 ^a (0.07)	0.03 ^h (0.00)	0.70 ^b (0.03)	0.01 ^b (0.00)
	100/2	6.24 ^b (0.05)	0.03 ^e (0.00)	4.93 ^a (0.06)	0.03 ^h (0.00)	0.79 ^a (0.00)	0.01 ^b (0.00)
Ca(OH)_2	110/1	4.77 ^c (0.02)	0.04 ^d (0.00)	2.94 ^b (0.07)	0.06 ^g (0.00)	0.62 ^d (0.02)	0.02 ^b (0.00)
	110/2	4.36 ^d (0.13)	0.04 ^d (0.00)	2.54 ^c (0.01)	0.06 ^g (0.00)	0.58 ^e (0.02)	0.03 ^b (0.00)
	120/1	2.39 ^e (0.05)	0.07 ^c (0.00)	1.53 ^d (0.02)	0.11 ^f (0.00)	0.64 ^c (0.00)	0.04 ^b (0.00)
	120/2	2.09 ^{fg} (0.07)	0.08 ^b (0.00)	1.25 ^f (0.01)	0.13 ^d (0.00)	0.60 ^{de} (0.02)	0.05 ^b (0.00)
HMT in the presence of Ca(OH)_2	100/1	2.18 ^f (0.03)	0.08 ^b (0.00)	1.35 ^e (0.03)	0.12 ^e (0.00)	0.62 ^d (0.01)	0.04 ^b (0.00)
	100/2	2.23 ^f (0.08)	0.08 ^b (0.00)	1.19 ^g (0.01)	0.14 ^c (0.00)	0.54 ^f (0.02)	0.06 ^b (0.00)
	110/1	2.18 ^f (0.04)	0.08 ^b (0.00)	1.13 ^h (0.02)	0.15 ^b (0.00)	0.53 ^f (0.00)	0.07 ^a (0.00)
	110/2	2.00 ^g (0.06)	0.08 ^b (0.00)	1.06 ⁱ (0.02)	0.16 ^b (0.00)	0.53 ^f (0.01)	0.07 ^a (0.00)
	120/1	1.95 ^g (0.01)	0.09 ^a (0.00)	1.06 ⁱ (0.01)	0.16 ^b (0.00)	0.54 ^f (0.01)	0.07 ^a (0.00)
	120/2	1.82 ^h (0.03)	0.09 ^a (0.00)	0.96 ^j (0.00)	0.18 ^a (0.00)	0.53 ^f (0.01)	0.09 ^a (0.00)

The reported values are means (SD).

Means with different letters (a, b, ..) in each column are significantly different ($P \leq 0.05$).

*The exponents (a , b and c) were obtained from fitting the data using the power law model (Equations 5 to 7).

4.3.5 Thermal properties and retrogradation

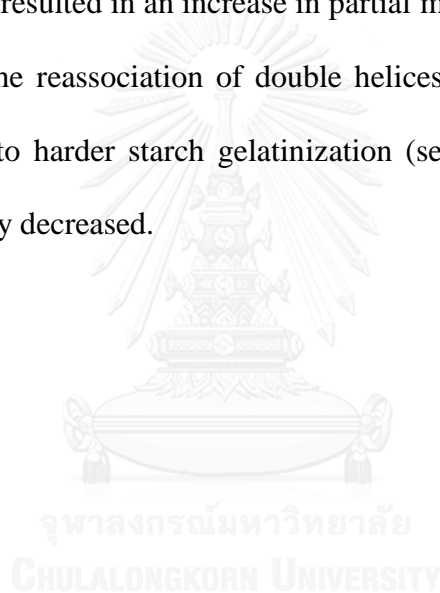
The DSC thermograms and thermal properties of the HMT-starch and HMT-Ca(OH)₂ starch treated at different treatment temperatures and times are shown in Figure 4.11 and Table 4.17, respectively. In general, increases in treatment temperature and time increased the T_o , T_{p1} , T_{p2} and T_c of HMT-starch and HMT-Ca(OH)₂ starch, but decreased ΔH_g . Compared to HMT-starch (without Ca(OH)₂), the T_o , T_p and T_c of HMT-Ca starch were significantly increased ($p \leq 0.05$), and decreased ΔH_g . The $(T_c - T_o)$ of the HMT-starch and HMT-Ca(OH)₂ starch decreased as treatment time increased at constant temperature, except for at 120°C.

After storage the starch pastes at $5 \pm 1^\circ\text{C}$ for 7 and 14 days, all the retrograded starches showed the melting of retrograded starch endotherms at lower temperatures, wider $(T_c - T_o)$ and lower ΔH_r than those at 0 day. However, the longer storage time (14 days) resulted in higher melting temperatures of retrograded starch, narrower $(T_c - T_o)$ and higher ΔH_r (Tables 4.18 and 4.19). The effect of treatment temperature and time on the thermal properties of all retrogradation starches for 7 and 14 days were similar to those of their counterpart starches.

For both HMT-starch and HMT-Ca(OH)₂ starch pastes, the % retrogradation increased with storage time, and an increase in treatment temperature and time decreased % retrogradation (Table 4.20). The % retrogradation of HMT-starch paste was higher than that of the HMT-Ca(OH)₂ starch paste.

An increase in the T_o , T_p and T_c of starches with increase in heat-moisture treatment temperature (100-120°C) and time (1-2 h) caused interactions between amylose molecules with the amylopectin chains present in the branched crystalline regions, consequently reducing the mobility of the amylopectin chains,

which resulted in an increase in the melting temperatures (Arns *et al.*, 2015; Hoover and Manuel, 1996; Hoover and Vasanthan, 1994). A high heat-moisture treatment temperature leads to high T_o , T_p and T_c , and the changes in these thermal properties are also due to some of the weak crystallites being destroyed during heat-moisture treatment and the stronger and stable crystallites in starch granules remaining with melting of retrograded starch at higher temperature (Altay and Gunasekaran, 2006; Lim *et al.*, 2001; Yadav *et al.*, 2013). Increase in the heat-moisture treatment temperature and time resulted in an increase in partial melting (see section 4.3.1.1 and 4.3.1.2), as well as the reassociation of double helices strengthening the crystalline domain and leading to harder starch gelatinization (see section 4.3.1.3). Therefore, gelatinization enthalpy decreased.



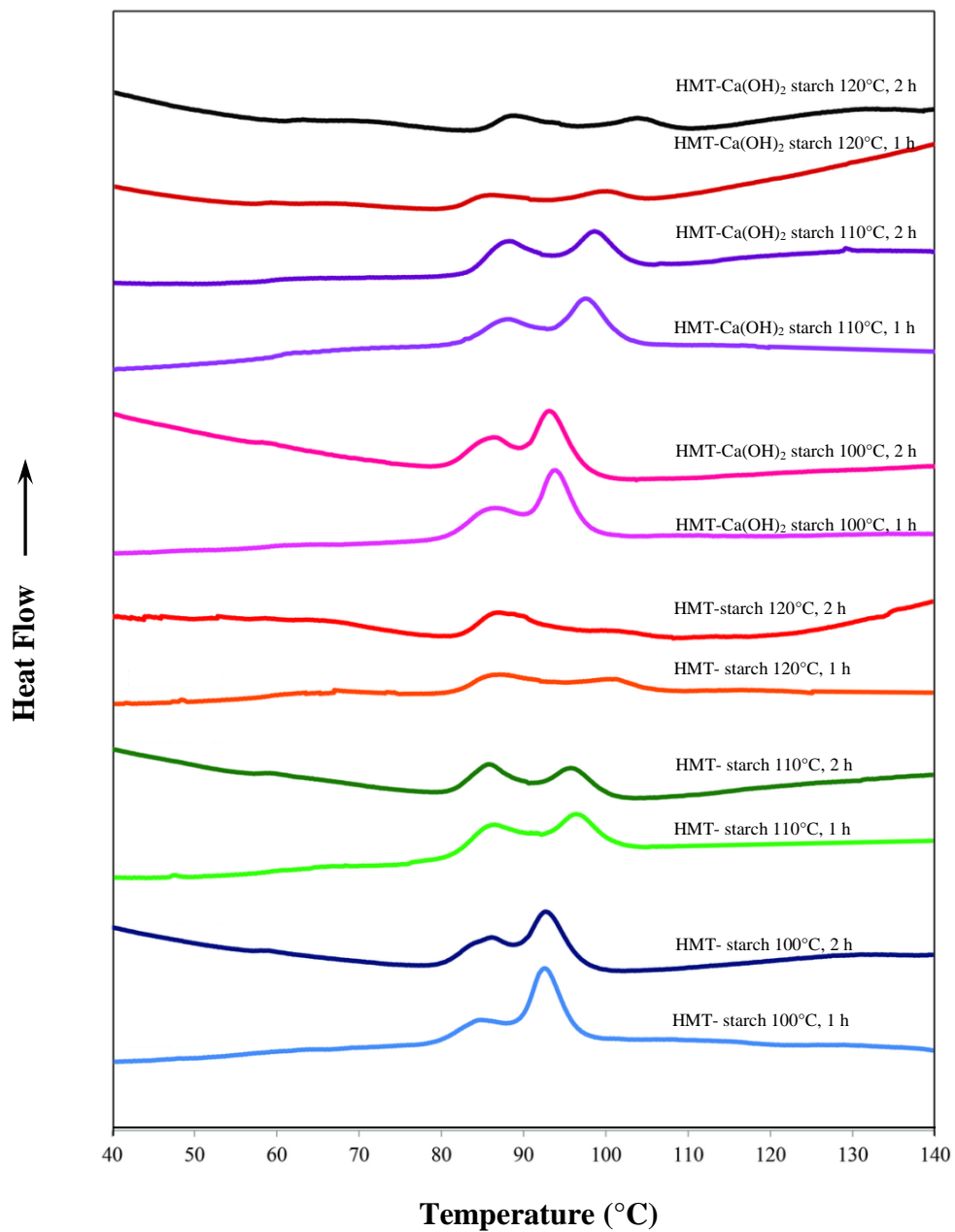


Figure 4.11 Thermogram of HMT-starch and HMT-Ca(OH)₂ starch at the Ca²⁺-starch ratio of 0:1 and 0.0007:1

Table 4.17 Thermal properties of HMT-starch and HMT-Ca(OH)₂ starch at the Ca²⁺-starch ratio of 0:1 and 0.0007:1

Treatment	Temperature (°C) and Time (h)	T _o (°C)	T _{p1} (°C)	T _{p2} (°C)	T _c (°C)	T _c -T _o (°C)	ΔH _g (J/g)
HMT in the absence of Ca(OH) ₂	100/1	76.60 ^j ± 0.07	85.91 ^g ± 0.09	89.62 ^f ± 0.34	97.17 ⁱ ± 0.17	20.57 ^b ± 0.23	13.31 ^a ± 0.17
	100/2	79.97 ^g ± 0.17	89.79 ^d ± 0.15	94.34 ^d ± 0.26	99.24 ^e ± 0.26	19.26 ^{cd} ± 0.12	11.36 ^b ± 0.25
	110/1	80.03 ^g ± 0.19	86.41 ^h ± 0.14	94.38 ^d ± 0.31	99.33 ^e ± 0.34	19.30 ^{cd} ± 0.16	10.39 ^c ± 0.24
	110/2	84.52 ^d ± 0.09	90.40 ^e ± 0.08	95.82 ^e ± 0.25	102.98 ^e ± 0.44	18.46 ^e ± 0.36	8.46 ^d ± 0.28
	120/1	83.50 ^e ± 0.48	86.62 ^f ± 0.37	86.91 ^e ± 0.41	104.94 ^e ± 0.26	21.44 ^a ± 0.30	4.66 ^f ± 0.08
	120/2	86.04 ^b ± 0.39	92.19 ^a ± 0.56	92.52 ^e ± 0.38	107.63 ^a ± 0.36	21.59 ^a ± 0.52	3.65 ^g ± 0.19
HMT in the presence of Ca(OH) ₂	100/1	79.21 ^h ± 0.13	86.77 ^f ± 0.02	94.35 ^d ± 0.31	98.55 ^h ± 0.46	19.34 ^{cd} ± 0.33	8.52 ^d ± 0.39
	100/2	82.07 ^f ± 0.10	90.39 ^e ± 0.59	97.25 ^b ± 0.47	100.62 ^f ± 0.31	18.55 ^e ± 0.41	7.50 ^e ± 0.43
	110/1	82.78 ^f ± 0.22	88.01 ^e ± 0.24	97.10 ^b ± 0.26	104.56 ^{cd} ± 0.40	21.78 ^a ± 0.46	7.78 ^e ± 0.01
	110/2	85.62 ^e ± 0.15	91.51 ^b ± 0.06	99.10 ^a ± 0.40	104.39 ^{cd} ± 0.36	18.77 ^{de} ± 0.35	7.56 ^e ± 0.22
	120/1	84.49 ^d ± 0.13	90.01 ^{cd} ± 0.45	89.87 ^f ± 0.10	104.30 ^d ± 0.53	19.81 ^c ± 0.58	3.54 ^g ± 0.44
	120/2	86.61 ^a ± 0.15	92.41 ^a ± 0.20	92.11 ^e ± 0.35	106.44 ^b ± 0.16	19.84 ^c ± 0.20	3.52 ^g ± 0.43

T_o, T_{p1}, T_{p2}, T_c, T_c-T_o represent the onset, first peak, second peak, conclusion of gelatinization, and the gelatinization temperature range, respectively. ΔH_g represents the enthalpy of gelatinization.

The reported values are means ± SD.

Means with different letters (a, b, ...) in each column are significantly different ($P \leq 0.05$).

Table 4.18 Thermal properties of retrograded HMT-starch and HMT-Ca(OH)₂ starch at the Ca²⁺-starch ratio of 0:1 and 0.0007:1 stored at 5°C for 7 days

Treatment	Temperature (°C) and Time (h)	T _o (°C)	T _p (°C)	T _c (°C)	T _c -T _o (°C)	ΔH _{r7} (J/g)
HMT in the absence of Ca(OH) ₂	100/1	43.48 ^h (0.45)	54.65 ^h (0.41)	74.59 ^f (0.12)	31.11 ^a (0.32)	6.53 ^a (0.01)
	100/2	48.80 ^e (0.45)	58.74 ^g (0.20)	76.41 ^e (0.36)	27.79 ^d (0.36)	5.27 ^b (0.09)
	110/1	45.63 ^g (0.47)	62.65 ^c (0.26)	76.29 ^e (0.16)	30.40 ^a (0.47)	4.99 ^c (0.04)
	110/2	50.44 ^c (0.50)	63.57 ^b (0.46)	77.49 ^d (0.36)	27.05 ^d (0.28)	3.95 ^d (0.08)
	120/1	49.34 ^d (0.32)	61.59 ^e (0.08)	79.61 ^c (0.22)	30.26 ^{ab} (0.50)	2.19 ⁱ (0.09)
	120/2	53.32 ^a (0.13)	63.49 ^b (0.33)	80.37 ^b (0.39)	27.05 ^d (0.51)	1.69 ^j (0.07)
HMT in the presence of Ca(OH) ₂	100/1	47.55 ^f (0.09)	60.46 ^f (0.26)	77.98 ^d (0.24)	30.43 ^a (0.12)	3.51 ^e (0.08)
	100/2	50.83 ^{bc} (0.10)	62.15 ^d (0.10)	80.03 ^{bc} (0.64)	29.20 ^c (0.71)	2.98 ^f (0.08)
	110/1	48.85 ^{de} (0.19)	64.64 ^a (0.00)	77.80 ^{bc} (0.15)	31.03 ^a (0.18)	2.72 ^g (0.07)
	110/2	50.48 ^c (0.34)	63.57 ^b (0.46)	79.95 ^{bc} (0.21)	29.48 ^{bc} (0.55)	2.60 ^h (0.05)
	120/1	50.37 ^c (0.21)	63.87 ^b (0.11)	81.36 ^a (0.46)	30.99 ^a (0.61)	1.25 ^k (0.05)
	120/2	51.38 ^b (0.52)	63.62 ^b (0.51)	81.71 ^a (0.19)	30.33 ^a (0.36)	1.20 ^k (0.12)

T_o, T_p, T_c, T_c-T_o represent the onset, peak, conclusion of gelatinization, and the gelatinization temperature range, respectively.

ΔH_{r7} represent enthalpy of retrogradation at 7 days.

The reported values are means (SD).

Means with different letters (a, b, ..) in each column are significantly different ($P \leq 0.05$).

Table 4.19 Thermal properties of retrograded HMT-starch and HMT-Ca(OH)₂ starch at the Ca²⁺-starch ratio of 0:1 and 0.0007:1 stored at 5°C for 14 days

Treatment	Temperature (°C) and Time (h)	T _o (°C)	T _p (°C)	T _c (°C)	T _c -T _o (°C)	ΔH _{r14} (J/g)
HMT in the absence of Ca(OH) ₂	100/1	48.53 ^h	60.36 ^e	76.48 ⁱ	27.95 ^c	7.37 ^a
		(0.41)	(0.23)	(0.06)	(0.40)	(0.06)
	100/2	52.64 ^e	62.53 ^d	78.96 ^f	26.33 ^e	6.13 ^b
		(0.31)	(0.39)	(0.21)	(0.36)	(0.04)
	110/1	49.69 ^g	63.49 ^c	77.50 ^h	27.81 ^{cd}	5.52 ^c
		(0.35)	(0.56)	(0.42)	(0.76)	(0.10)
110/2	52.23 ^e	63.54 ^c	78.37 ^g	26.09 ^e	4.22 ^d	
	(0.21)	(0.40)	(0.16)	(0.37)	(0.08)	
120/1	53.60 ^d	63.15 ^c	78.66 ^{fg}	25.06 ^f	2.37 ^h	
	(0.15)	(0.02)	(0.26)	(0.46)	(0.05)	
120/2	54.31 ^c	63.50 ^c	80.19 ^e	25.88 ^e	1.76 ⁱ	
	(0.16)	(0.12)	(0.24)	(0.41)	(0.07)	
HMT in the presence of Ca(OH) ₂	100/1	51.34 ^f	62.63 ^d	80.15 ^e	28.79 ^b	4.03 ^e
		(0.29)	(0.19)	(0.09)	(0.29)	(0.05)
	100/2	52.63 ^e	65.13 ^c	81.43 ^d	28.79 ^b	3.43 ^f
		(0.17)	(0.20)	(0.28)	(0.36)	(0.05)
	110/1	53.64 ^d	65.26 ^a	82.55 ^c	28.91 ^b	3.22 ^g
		(0.17)	(0.06)	(0.10)	(0.08)	(0.07)
110/2	53.63 ^d	65.26 ^a	83.27 ^b	29.64 ^a	3.12 ^g	
	(0.20)	(0.28)	(0.21)	(0.29)	(0.17)	
120/1	55.33 ^b	64.40 ^b	82.52 ^c	27.19 ^d	1.38 ⁱ	
	(0.18)	(0.37)	(0.35)	(0.22)	(0.13)	
120/2	55.81 ^a	65.22 ^a	83.74 ^a	27.93 ^c	1.24 ^k	
	(0.10)	(0.17)	(0.13)	(0.21)	(0.08)	

T_o, T_p, T_c, T_c-T_o represent the onset, peak, conclusion of gelatinization, and the gelatinization temperature range, respectively.

ΔH_{r14} represent enthalpy of retrogradation at 14 days.

The reported values are means (SD).

Means with different letters (a, b, ..) in each column are significantly different ($P \leq 0.05$).

Table 4.20 Gelatinization and melting of retrograded starch enthalpy of HMT-starch and HMT-Ca(OH)₂ starch at the Ca²⁺-starch ratio of 0:1 and 0.0007:1

Treatment	Temperature (°C) and Time (h)	ΔH_g (J/g)	ΔH_{r7} (J/g)	ΔH_{r14} (J/g)	%Retrogradation ₇	%Retrogradation ₁₄
HMT in the absence of Ca(OH) ₂	100/1	13.31 ^{aA} (0.17)	6.53 ^{aC} (0.01)	7.37 ^{aB} (0.06)	48.66 ^{aB} (0.62)	54.92 ^{aA} (0.37)
	100/2	11.36 ^{bA} (0.25)	5.27 ^{bC} (0.09)	6.13 ^{bB} (0.04)	46.38 ^{bB} (0.45)	53.97 ^{bA} (0.58)
	110/1	10.39 ^{cA} (0.24)	4.99 ^{cC} (0.04)	5.52 ^{cB} (0.10)	48.06 ^{abB} (0.84)	53.19 ^{abA} (0.47)
	110/2	8.46 ^{dA} (0.28)	3.95 ^{dC} (0.08)	4.22 ^{dB} (0.08)	46.68 ^{bB} (1.01)	49.97 ^{dA} (0.10)
	120/1	4.66 ^{fA} (0.08)	2.19 ^{iB} (0.09)	2.37 ^{hB} (0.05)	46.93 ^{bcB} (0.70)	50.77 ^{cA} (0.48)
	120/2	3.65 ^{gA} (0.19)	1.69 ^{iB} (0.07)	1.76 ^{iB} (0.07)	46.24 ^{bB} (0.80)	48.30 ^{dA} (0.86)
HMT in the presence of Ca(OH) ₂	100/1	8.52 ^{dA} (0.39)	3.51 ^{eC} (0.08)	4.03 ^{eB} (0.05)	41.22 ^{dB} (1.04)	47.10 ^{eA} (0.80)
	100/2	7.50 ^{eA} (0.43)	2.98 ^{fC} (0.08)	3.43 ^{fB} (0.05)	39.79 ^{eB} (0.27)	45.82 ^{fA} (1.17)
	110/1	7.78 ^{eA} (0.19)	2.72 ^{gC} (0.07)	3.22 ^{gB} (0.07)	34.97 ^{fB} (0.85)	41.42 ^{gA} (0.19)
	110/2	7.56 ^{eA} (0.22)	2.60 ^{hC} (0.05)	3.12 ^{gB} (0.17)	34.42 ^{fB} (0.60)	41.25 ^{gA} (0.60)
	120/1	3.54 ^{gA} (0.44)	1.25 ^{kB} (0.05)	1.38 ^{iB} (0.13)	35.64 ^{fB} (0.98)	39.01 ^{hA} (0.98)
	120/2	3.52 ^{gA} (0.43)	1.20 ^{kB} (0.12)	1.24 ^{kB} (0.08)	34.29 ^{fB} (0.76)	35.38 ^{iA} (0.76)

The reported values are means (SD).

Means with different letters (a, b, ...) in each column are significantly different ($P \leq 0.05$).

Means with different letters (A, B, ...) in each column are significantly different ($P \leq 0.05$).

4.3.6 Freeze-thaw stability

The results in Table 4.21 shows that the HMT-Ca(OH)₂ starch pastes gave lower % syneresis than the HMT-starch pastes (without Ca(OH)₂). As freeze-thaw cycles increased, % syneresis increased. However, after five freeze-thaw cycles, the HMT- Ca(OH)₂ starch at 120°C and 2 h gave the minimum % syneresis of 35.14 ($p \leq 0.05$), while the HMT starch at 100°C and 1 h gave the maximum % syneresis of 56.55 ($p \leq 0.05$). Therefore, this result suggests that the HMT-Ca(OH)₂ starch at the Ca²⁺-starch ratio of 0.0007:1 treated at 120°C and 2 h gave the best freeze-thaw stability. Compared to the HMT-starch, heat-moisture treatment of starch with Ca(OH)₂ can stabilize starch granules, lower % syneresis due to the fact that it had lower swelling power and % amylose leaching.

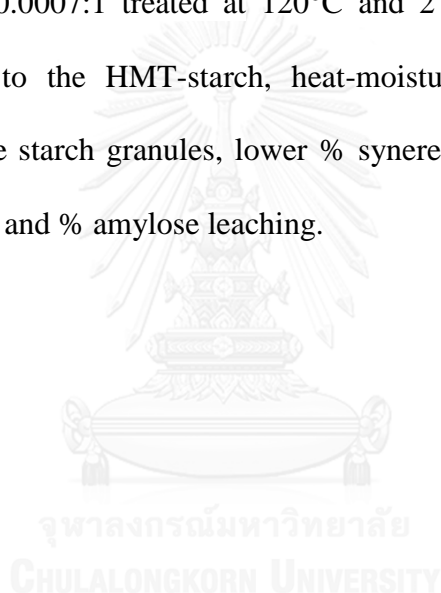


Table 4.21 The % syneresis of 5% w/w HMT-starch and HMT-Ca(OH)₂ starch at the Ca²⁺-starch ratio of 0:1 and 0.0007:1

Treatment	Temperature (°C) and Time (h)	Syneresis (%) for Cycle				
		1	2	3	4	5
HMT in the absence of of Ca(OH) ₂	100/1	26.87 ^{ab} ± 0.39	31.11 ^b ± 0.74	41.63 ^a ± 0.75	47.50 ^a ± 0.92	56.55 ^a ± 0.34
	100/2	26.93 ^{ab} ± 0.96	33.54 ^b ± 0.63	39.09 ^b ± 1.39	41.18 ^b ± 0.26	50.64 ^c ± 1.12
	110/1	27.56 ^a ± 1.32	35.87 ^a ± 0.69	41.65 ^a ± 0.94	46.75 ^a ± 0.64	54.71 ^b ± 0.94
	110/2	26.83 ^{ab} ± 0.80	27.04 ^a ± 0.56	34.78 ^d ± 0.67	41.39 ^b ± 1.07	44.50 ^{ef} ± 0.25
	120/1	26.93 ^{ab} ± 0.61	31.42 ^c ± 0.54	33.71 ^{de} ± 0.45	40.59 ^b ± 0.76	52.02 ^e ± 1.00
	120/2	25.61 ^{bc} ± 0.40	27.70 ^e ± 0.43	32.01 ^f ± 0.83	38.91 ^e ± 0.84	45.54 ^e ± 1.02
HMT in the presence of of Ca(OH) ₂	100/1	24.51 ^c ± 0.29	30.21 ^{cd} ± 0.71	37.30 ^e ± 1.14	40.42 ^b ± 0.14	43.50 ^{fg} ± 0.75
	100/2	25.15 ^c ± 0.68	29.35 ^d ± 0.18	35.15 ^d ± 0.91	38.71 ^c ± 0.53	40.95 ^h ± 1.17
	110/1	28.07 ^a ± 0.46	32.92 ^b ± 0.98	37.81 ^{bc} ± 0.46	38.54 ^c ± 0.84	42.36 ^g ± 0.72
	110/2	26.92 ^{ab} ± 1.04	23.33 ^h ± 1.01	28.14 ^g ± 0.99	34.82 ^d ± 0.47	37.73 ^j ± 0.42
	120/1	24.56 ^c ± 0.21	26.39 ^f ± 0.14	32.25 ^{ef} ± 0.42	37.86 ^c ± 0.85	39.50 ⁱ ± 0.76
	120/2	20.99 ^d ± 0.67	23.77 ^{gh} ± 1.21	28.29 ^g ± 1.20	31.65 ^e ± 0.99	35.14 ^k ± 0.74

The reported values are means ± SD.
Means with different letters (a, b, ...) in each column are significantly different ($P \leq 0.05$).

4.4 The links between XRD study and physical properties (swelling power, amylose leaching, % retrogradation, K , G' and % syneresis)

All obtained data from native, HMT-starch and HMT-Ca starches showed that there were the links between XRD study and physical properties (swelling power, amylose leaching, % retrogradation, consistency coefficient (K), storage modulus (G') and % syneresis). The results of XRD study, swelling power and amylose leaching suggested that the heat-moisture treatment, especially in the presence of calcium compounds, gave more rigid starch granules (lower swelling power and amylose leaching) with less number (lower % RC) but stronger crystallites (A-type instead of C-type found in the native starch). The lower amylose leaching gave the lower % retrogradation. The results showed that % retrogradation decreased as % RC decreased. This indicated that crystallites in those starch granules, which had lower number of crystallites, were stronger. Consequently, those starch granules, which had lower % RC and % retrogradation, had lower K , G' and % syneresis.

4.5 Suggested concentration of starch used for applications

Concentration of starch is very important for their applications as it controls viscosity of starch suspension/product. Most applications required the close packing concentration, which can be calculated from the swelling power using Equation 10 derived by Willett (2001). This concentration for starches in this research was calculated and showed in Table 4.22 and 4.23.

$$\text{Close packing concentration} = \frac{\text{maximum packing fraction (\%)} \times \text{density (g/ml)}}{\text{swelling power (g/g)}} \quad [10]$$

Table 4.22 The close packing concentration of starches studied in this research

Type of pigeonpea starch	Type of Calcium Compound	Ca ²⁺ :Starch	Close Packing Concentration (%)
Native starch	-	-	2.89 ± 0.70
Heat-moisture treated at 110°C, 1 h	-	0:1	5.71 ± 0.22
	Ca(OH) ₂	0.0001:1	7.18 ± 0.36
		0.0004:1	8.94 ± 0.25
		0.0007:1	10.34 ± 0.40
	CaCl ₂	0.0001:1	6.65 ± 0.34
		0.0004:1	6.55 ± 0.13
		0.0007:1	5.49 ± 0.45
	C ₆ H ₁₀ CaO ₆	0.0001:1	7.04 ± 0.40
		0.0004:1	8.21 ± 0.36
0.0007:1		11.32 ± 0.24	

Table 4.23 The close packing concentration of starches studied in this research

Treatment	Temperature (°C) and Time (h)	Close Packing Concentration (%)
HMT in the absence of Ca(OH) ₂	100/1	4.75 ± 0.62
	100/2	5.39 ± 0.42
	110/1	5.71 ± 0.22
	110/2	8.11 ± 0.35
	120/1	12.22 ± 0.26
	120/2	14.25 ± 0.70
HMT in the presence of Ca(OH) ₂	100/1	7.25 ± 0.26
	100/2	5.92 ± 0.28
	110/1	10.34 ± 0.40
	110/2	11.01 ± 0.42
	120/1	14.81 ± 0.11
	120/2	17.54 ± 0.75



CHAPTER V

CONCLUSIONS

The results of this research proved the proposed hypothesis that HMT in the presence of a calcium compound strengthened the rigidity of starch granules as compared to common HMT (in the absence of any calcium compound). The effects of heat-moisture treatment on the properties of starch are as follows:

- The X-ray diffraction shows that the native starch has the characteristic “C” pattern, while the HMT-starch and HMT-Ca starch have an “A” pattern with higher peak intensities and lower relative crystallinity. The heat-moisture treatment causes partial loss of birefringence of starch granules. The heat-moisture treatment reduces the swelling power and amylose leaching of native starch. The heat-moisture treatment increased the gelatinization temperatures of native starch. Retrogradation increased as the duration of the storage of gelatinized starch increased. However, retrogradation reduced after HMT.
- All starch gel showed pseudo-plastic with yield stress and the storage modulus (G') was higher than the loss modulus (G'').
- Using calcium compounds increased the loss of birefringence, freeze-thaw stability, flow behavior index (n) and gelatinization temperatures but decreased relative crystallinity, swelling power amylose leaching, η_h , η_c , consistency coefficient (K) and % retrogradation.

- Using Ca(OH)_2 and $\text{C}_6\text{H}_{10}\text{CaO}_6$ decreased swelling power, amylose leaching, η_h and η_c more intensely than using CaCl_2 .
- An increase in the Ca^{2+} -starch ratio decreased the swelling power and amylose leaching of HMT-Ca starches, while the gelatinization temperatures and % relative crystallinity of HMT-Ca starches increased. The HMT- Ca(OH)_2 gave the highest freeze-thaw stability starches was observed at the Ca^{2+} -starch ratios of 0.0007:1.
- The higher HMT temperature and longer HMT time resulted in lower swelling power, amylose leaching, yield stress (τ_0), consistency coefficient (K) and % retrogradation, but in higher gelatinization temperatures and freeze-thaw stability.
- By using different types of calcium compounds and varying Ca^{2+} -starch ratio, diverse functional properties of HMT-Ca starches could be obtained for assorted applications both food and non-food.
- From physicochemical properties of HMT-Ca starches, they may be used in foods that require lower swelling, lower viscosity, higher thermal stability and higher freeze-thaw stability.
- The starch with the best freeze-thaw stability could be obtained by HMT at 120°C for 2 h in the presence of Ca(OH)_2 at the Ca^{2+} -starch ratio of 0.0007:1.

Recommendations for future research

Further studies could:

1. The effects of salt concentration on physicochemical properties of HMT- CaCl_2 were different from those of HMT- $\text{Ca}(\text{OH})_2$ and HMT- $\text{C}_6\text{H}_{10}\text{CaO}_6$ starches. These may be due to the fact that the concentration of CaCl_2 used in this research is considered low (0.014-0.063 mol/L) as compared to that commonly used in other researches (~ 4M). Therefore, further research using higher concentration of CaCl_2 should be investigated.
2. According to experimental results, freeze-thaw stability of HMT-Ca starch was better than HMT-starch. Therefore, application of HMT-Ca starch in frozen food should be tested.

REFERENCES

- Acevedo, B. A., Avanza, M. V., Cháves, M. G., and Ronda, F. (2013). Gelation, thermal and pasting properties of pigeon pea (*Cajanus cajan* L.), dolichos bean (*Dolichos lablab* L.) and jack bean (*Canavalia ensiformis*) flours. *Journal of Food Engineering* **119**, 65-71.
- Adebowale, K., Afolabi, T., and Olu-Owolabi, B. (2005). Hydrothermal treatments of Finger millet (*Eleusine coracana*) starch. *Food Hydrocolloids* **19**, 974-983.
- Adebowale, K., Henle, T., Schwarzenbolz, U., and Doert, T. (2009). Modification and properties of African yam bean (*Sphenostylis stenocarpa* Hochst. Ex A. Rich.) Harms starch I: Heat moisture treatments and annealing. *Food Hydrocolloids* **23**, 1947-1957.
- Adebowale, K. O., and Lawal, O. S. (2003). Microstructure, physicochemical properties and retrogradation behaviour of *Mucuna* bean (*Mucuna pruriens*) starch on heat moisture treatments. *Food Hydrocolloids* **17**, 265-272.
- Altay, F., and Gunasekaran, S. (2006). Influence of drying temperature, water content, and heating rate on gelatinization of corn starches. *Journal of Agricultural and Food Chemistry* **54**, 4235-4245.
- AOAC (2012). "Official Methods of Analysis," 19th/Ed. The Association of the Official Analytical Chemists, Maryland.
- Arns, B., Bartz, J., Radunz, M., do Evangelho, J. A., Pinto, V. Z., da Rosa Zavareze, E., and Dias, A. R. G. (2015). Impact of heat-moisture treatment on rice starch, applied directly in grain paddy rice or in isolated starch. *LWT-Food Science and Technology* **60**, 708-713.
- Bao, J., and Bergman, C. J. (2004). The functionality of rice starch. In "Starch in Food: Structure, function, and application" (A. C. Eliasson, ed.). CRC Press, Cambridge.
- Barrera, G. N., Bustos, M. C., Iturriaga, L., Flores, S. K., León, A. E., and Ribotta, P. D. (2013). Effect of damaged starch on the rheological properties of wheat starch suspensions. *Journal of Food Engineering* **116**, 233-239.
- Belitz, H.-D., Grosch, W., and Schieberle, P. (2009). "Food Chemistry," Springer-Verlag, New York.
- BeMiller, J. N., and Whistler, R. L. (1996). Carbohydrates. In "Food Chemistry" (O. R. Fennema, ed.), pp. 157-223. Marcel Dekker, Inc., New York.
- Biliaderis, C. G., Page, C. M., Maurice, T. J., and Juliano, B. O. (1986). Thermal characterization of rice starches: A polymeric approach to phase transitions of granular starch. *Journal of Agricultural and Food Chemistry* **34**, 6-14.
- Bogacheva, T. Y., Cairns, P., Noel, T., Hulleman, S., Wang, T., Morris, V., Ring, S., and Hedley, C. (1999). The effect of mutant genes at the *r*, *rb*, *rug3*, *rug4*, *rug5* and *lam* loci on the granular structure and physico-chemical properties of pea seed starch. *Carbohydrate Polymers* **39**, 303-314.
- Boltz, K. W., and Thompson, D. B. (1999). Initial heating temperature and native lipid affects ordering of amylose during cooling of high-amylose starches. *Cereal Chemistry* **76**, 204-212.
- Bryant, C. M., and Hamaker, B. R. (1997). Effect of lime on gelatinization of corn flour and starch 1. *Cereal Chemistry* **74**, 171-175.

- Buléon, A., Colonna, P., Planchot, V., and Ball, S. (1998). Starch granules: structure and biosynthesis. *International Journal of Biological Macromolecules* **23**, 85-112.
- Ceballos, H., Sánchez, T., Morante, N., Fregene, M., Dufour, D., Smith, A. M., Denyer, K., Pérez, J. C., Calle, F., and Mestres, C. (2007). Discovery of an amylose-free starch mutant in cassava (*Manihot esculenta* Crantz). *Journal of Agricultural and Food Chemistry* **55**, 7469-7476.
- Chang, S.-M., and Liu, L.-C. (1991). Retrogradation of rice starches studied by differential scanning calorimetry and influence of sugars, NaCl and lipids. *Journal of Food Science* **56**, 564-566.
- Chen, L., Tong, Q., Ren, F., and Zhu, G. (2014). Pasting and rheological properties of rice starch as affected by pullulan. *International Journal of Biological Macromolecules* **66**, 325-331.
- Chrastil, J. (1987). Improved colorimetric determination of amylose in starches or flours. *Carbohydrate Research* **159**, 154-158.
- Chung, H.-J., Liu, Q., and Hoover, R. (2009). Impact of annealing and heat-moisture treatment on rapidly digestible, slowly digestible and resistant starch levels in native and gelatinized corn, pea and lentil starches. *Carbohydrate Polymers* **75**, 436-447.
- Cooke, D., and Gidley, M. J. (1992). Loss of crystalline and molecular order during starch gelatinisation: origin of the enthalpic transition. *Carbohydrate Research* **227**, 103-112.
- da Rosa Zavareze, E., and Dias, A. R. G. (2011). Impact of heat-moisture treatment and annealing in starches: A review. *Carbohydrate Polymers* **83**, 317-328.
- da Rosa Zavareze, E., Storck, C. R., de Castro, L. A. S., Schirmer, M. A., and Dias, A. R. G. (2010). Effect of heat-moisture treatment on rice starch of varying amylose content. *Food Chemistry* **121**, 358-365.
- Day, L., Fayet, C., and Homer, S. (2013). Effect of NaCl on the thermal behaviour of wheat starch in excess and limited water. *Carbohydrate Polymers* **94**, 31-37.
- Dias, A. R. G., da Rosa Zavareze, E., Spier, F., de Castro, L. A. S., and Gutkoski, L. C. (2010). Effects of annealing on the physicochemical properties and enzymatic susceptibility of rice starches with different amylose contents. *Food Chemistry* **123**, 711-719.
- Donovan, J., Lorenz, K., and Kulp, K. (1983). Differential scanning calorimetry of heat-moisture treated wheat and potato starches. *Cereal Chemistry* **60**, 381-387.
- Duke, J. A. (1981). "Handbook of Legumes of World Economic Importance," Plenum Press, New York.
- Eerlingen, R. C., Jacobs, H., Block, K., and Delcour, J. A. (1997). Effects of hydrothermal treatments on the rheological properties of potato starch. *Carbohydrate Research* **297**, 347-356.
- Eliasson, A. (1985). Retrogradation of starch as measured by differential scanning calorimetry. In "New Approaches to Research on Cereal Carbohydrates" (R. D. Hill and L. Munck, eds.), pp. 93-98. Elsevier Science, Amsterdam.
- Eliasson, A. C. (1980). Effect of water content on the gelatinization of wheat starch. *Starch-Stärke* **32**, 270-272.

- Eliasson, A. C., and Gudmundsson, M. (1996). Starch: physicochemical and functional aspects. *In* "Carbohydrates in Food" (A. C. Eliasson, ed.), pp. 431-504. Marcel Dekker, Inc., New York.
- FDA (2008). Food and Drugs Administration [Online]. Available from: <http://www.fda.gov/Food/default.htm> [2016, January 14].
- Fitt, L. E., and Snyder, E. M. (1984). Photomicrographs of starches. *In* "Starch Chemistry and Technology" (R. Whistler, J. N. BeMiller and E. F. Paschall, eds.), pp. 675. Academic Press, Orlando.
- Gough, B., and Pybus, J. (1973). Effect of metal cations on the swelling and gelatinization behaviour of large wheat starch granules. *Starch-Stärke* **25**, 123-130.
- Gunaratne, A., and Hoover, R. (2002). Effect of heat–moisture treatment on the structure and physicochemical properties of tuber and root starches. *Carbohydrate Polymers* **49**, 425-437.
- Hizukuri, S. (1985). Relationship between the distribution of the chain length of amylopectin and the crystalline structure of starch granules. *Carbohydrate Research* **141**, 295-306.
- Hizukuri, S. (1986). Polymodal distribution of the chain lengths of amylopectins, and its significance. *Carbohydrate Research* **147**, 342-347.
- Hizukuri, S. (1996). Starch: analytical aspects. *In* "Carbohydrates in Food" (A. C. Eliasson, ed.), pp. 347-411. Maecel Dekker, Inc., New York.
- Hoover, R., Li, Y., Hynes, G., and Senanayake, N. (1997). Physicochemical characterization of mung bean starch. *Food Hydrocolloids* **11**, 401-408.
- Hoover, R., and Manuel, H. (1996). The effect of heat–moisture treatment on the structure and physicochemical properties of normal maize, waxy maize, dull waxy maize and amylo maize V starches. *Journal of Cereal Science* **23**, 153-162.
- Hoover, R., and Sosulski, F. (1985). Studies on the functional characteristics and digestibility of starches from *Phaseolus vulgaris* biotypes. *Starch-Stärke* **37**, 181-191.
- Hoover, R., Swamidas, G., and Vasanthan, T. (1993). Studies on the physicochemical properties of native, defatted, and heat-moisture treated pigeon pea (*Cajanus cajan* L) starch. *Carbohydrate Research* **246**, 185-203.
- Hoover, R., and Vasanthan, T. (1994). Effect of heat-moisture treatment on the structure and physicochemical properties of cereal, legume, and tuber starches. *Carbohydrate Research* **252**, 33-53.
- Horndok, R., and Noomhorm, A. (2007). Hydrothermal treatments of rice starch for improvement of rice noodle quality. *LWT-Food Science and Technology* **40**, 1723-1731.
- Horng, J. L. (2007). The isolation and characterisation of starches from legume grains and their application in food formulations, RMIT University.
- Huang, J., Schols, H. A., van Soest, J. J., Jin, Z., Sulmann, E., and Voragen, A. G. (2007). Physicochemical properties and amylopectin chain profiles of cowpea, chickpea and yellow pea starches. *Food Chemistry* **101**, 1338-1345.
- Imberty, A., Buléon, A., Tran, V., and Pérez, S. (1991). Recent advances in knowledge of starch structure. *Starch-Stärke* **43**, 375-384.

- Jacobs, H., and Delcour, J. A. (1998). Hydrothermal modifications of granular starch, with retention of the granular structure: A review. *Journal of Agricultural and Food Chemistry* **46**, 2895-2905.
- Jane, J.-L., and Robyt, J. F. (1984). Structure studies of amylose-V complexes and retro-graded amylose by action of alpha amylases, and a new method for preparing amyloextrins. *Carbohydrate Research* **132**, 105-118.
- Jane, J. L. (1993). Mechanism of starch gelatinization in neutral salt solutions. *Starch-Stärke* **45**, 161-166.
- Jayakody, L., and Hoover, R. (2008). Effect of annealing on the molecular structure and physicochemical properties of starches from different botanical origins—A review. *Carbohydrate Polymers* **74**, 691-703.
- Jayakody, L., Hoover, R., Liu, Q., and Donner, E. (2009). Studies on tuber starches III. Impact of annealing on the molecular structure, composition and physicochemical properties of yam (*Dioscorea* sp.) starches grown in Sri Lanka. *Carbohydrate Polymers* **76**, 145-153.
- Jiang, X., Jiang, T., Gan, L., Zhang, X., Dai, H., and Zhang, X. (2012). The plasticizing mechanism and effect of calcium chloride on starch/poly (vinyl alcohol) films. *Carbohydrate Polymers* **90**, 1677-1684.
- Jiranuntakul, W., Puttanlek, C., Rungsardthong, V., Pancha-Arnon, S., and Uttapap, D. (2011). Microstructural and physicochemical properties of heat-moisture treated waxy and normal starches. *Journal of Food Engineering* **104**, 246-258.
- Jouppila, K. (1996). Mono- and disaccharides: physicochemical and functional aspects. In "Carbohydrates in Food" (A. C. Eliasson, ed.), pp. 41-82. Marcel Dekker Inc., New York.
- Karim, A. A., Norziah, M., and Seow, C. (2000). Methods for the study of starch retrogradation. *Food Chemistry* **71**, 9-36.
- Kaur, M., and Sandhu, K. S. (2010). In vitro digestibility, structural and functional properties of starch from pigeon pea (*Cajanus cajan*) cultivars grown in India. *Food Research International* **43**, 263-268.
- Kaushal, P., Kumar, V., and Sharma, H. (2012). Comparative study of physicochemical, functional, antinutritional and pasting properties of taro (*Colocasia esculenta*), rice (*Oryza sativa*) flour, pigeonpea (*Cajanus cajan*) flour and their blends. *LWT-Food Science and Technology* **48**, 59-68.
- Khunae, P., Tran, T., and Sirivongpaisal, P. (2007). Effect of Heat-Moisture Treatment on Structural and Thermal Properties of Rice Starches Differing in Amylose Content. *Starch-Stärke* **59**, 593-599.
- Kim, J.-Y., and Huber, K. C. (2013). Heat-moisture treatment under mildly acidic conditions alters potato starch physicochemical properties and digestibility. *Carbohydrate Polymers* **98**, 1245-1255.
- Klein, B., Pinto, V. Z., Vanier, N. L., da Rosa Zavareze, E., Colussi, R., do Evangelho, J. A., Gutkoski, L. C., and Dias, A. R. G. (2013). Effect of single and dual heat-moisture treatments on properties of rice, cassava, and pinhao starches. *Carbohydrate Polymers* **98**, 1578-1584.
- Lai, V. M.-F., Lu, S., and Lii, C.-y. (2000). Molecular characteristics influencing retrogradation kinetics of rice amylopectins. *Cereal Chemistry* **77**, 272-278.
- Lan, H., Hoover, R., Jayakody, L., Liu, Q., Donner, E., Baga, M., Asare, E., Hucl, P., and Chibbar, R. (2008). Impact of annealing on the molecular structure and

- physicochemical properties of normal, waxy and high amylose bread wheat starches. *Food Chemistry* **111**, 663-675.
- Laria, J., Meza, E., and Peña, J. (2007). Water and calcium uptake by corn kernel during alkaline treatment with different temperature profiles. *Journal of Food Engineering* **78**, 288-295.
- Lawal, O. S. (2005). Studies on the hydrothermal modifications of new cocoyam (*Xanthosoma sagittifolium*) starch. *International Journal of Biological Macromolecules* **37**, 268-277.
- Li, S., Ward, R., and Gao, Q. (2011). Effect of heat-moisture treatment on the formation and physicochemical properties of resistant starch from mung bean (*Phaseolus radiatus*) starch. *Food Hydrocolloids* **25**, 1702-1709.
- Lim, S.-T., Chang, E.-H., and Chung, H.-J. (2001). Thermal transition characteristics of heat-moisture treated corn and potato starches. *Carbohydrate Polymers* **46**, 107-115.
- Liu, H., Yu, L., Chen, L., and Li, L. (2007). Retrogradation of corn starch after thermal treatment at different temperatures. *Carbohydrate Polymers* **69**, 756-762.
- Liu, H., Yu, L., Xie, F., and Chen, L. (2006). Gelatinization of cornstarch with different amylose/amylopectin content. *Carbohydrate Polymers* **65**, 357-363.
- Liu, Q. (2005). Understanding starches and their role in food. In "Food Carbohydrates" (S. W. Cui, ed.), pp. 309-355. Taylor & Francis Group, New York.
- Lu, S., Chen, C.-Y., and Lii, C. (1996). Gel-chromatography fractionation and thermal characterization of rice starch affected by hydrothermal treatment. *Cereal Chemistry* **73**, 5-11.
- Lu, Z.-H., Sasaki, T., Li, Y.-Y., Yoshihashi, T., Li, L.-T., and Kohyama, K. (2009). Effect of amylose content and rice type on dynamic viscoelasticity of a composite rice starch gel. *Food Hydrocolloids* **23**, 1712-1719.
- Maache-Rezzoug, Z., Zarguili, I., Loisel, C., and Doublier, J.-L. (2010). Study of DIC hydrothermal treatment effect on rheological properties of standard maize (SMS), waxy maize (WMS), wheat (WTS) and potato (PTS) starches. *Journal of Food Engineering* **99**, 452-458.
- Maache-Rezzoug, Z., Zarguili, I., Loisel, C., Queveau, D., and Buleon, A. (2008). Structural modifications and thermal transitions of standard maize starch after DIC hydrothermal treatment. *Carbohydrate Polymers* **74**, 802-812.
- Matsuki, J., Park, J. y., Shiroma, R., Ike, M., Yamamoto, K., and Tokuyasu, K. (2012). Effect of lime treatment and subsequent carbonation on gelatinization and saccharification of starch granules. *Starch-Stärke* **64**, 452-460.
- Mendez-Montecalvo, G., Sánchez-Rivera, M., Paredes-López, O., and Bello-Perez, L. A. (2006). Thermal and rheological properties of nixtamalized maize starch. *International Journal of Biological Macromolecules* **40**, 59-63.
- Miao, M., Zhang, T., and Jiang, B. (2009). Characterisations of kabuli and desi chickpea starches cultivated in China. *Food Chemistry* **113**, 1025-1032.
- Miles, M. J., Morris, V. J., Orford, P. D., and Ring, S. G. (1985). The roles of amylose and amylopectin in the gelation and retrogradation of starch. *Carbohydrate Research* **135**, 271-281.

- Mita, T. (1992). Structure of potato starch pastes in the ageing process by the measurement of their dynamic moduli. *Carbohydrate Polymers* **17**, 269-276.
- Mondragón, M., Bello-Perez, L. A., Agama, E., Melo, A., Betancur-Ancona, D., and Peña, J. (2004a). Effect of nixtamalization on the modification of the crystalline structure of maize starch. *Carbohydrate Polymers* **55**, 411-418.
- Mondragón, M., Bello-Pérez, L. A., Agama-Acevedo, E., Betancur-Ancona, D., and Peña, J. L. (2004b). Effect of cooking time, steeping and lime concentration on starch gelatinization of corn during nixtamalization. *Starch-Stärke* **56**, 248-253.
- Mondragón, M., Mendoza-Martínez, A., Bello-Perez, L. A., and Peña, J. (2006). Viscoelastic behavior of nixtamalized maize starch gels. *Carbohydrate Polymers* **65**, 314-320.
- Morrison, W. R., and Karkalas, J. (1990). Starch. In "Methods in Plant Biochemistry" (P. M. Dey, ed.), Vol. 2, pp. 323-352. Academic Press, London.
- Nara, S., and Komiya, T. (1983). Studies on the relationship between water-saturated state and crystallinity by the diffraction method for moistened potato starch. *Starch-Stärke* **35**, 407-410.
- Nayouf, M., Loisel, C., and Doublier, J. (2003). Effect of thermomechanical treatment on the rheological properties of crosslinked waxy corn starch. *Journal of Food Engineering* **59**, 209-219.
- Noda, T., Takahata, Y., Sato, T., Ikoma, H., and Mochida, H. (1996). Physicochemical properties of starches from purple and orange fleshed sweet potato roots at two levels of fertilizer. *Starch-Stärke* **48**, 395-399.
- Nwokolo, E. (1987). Nutritional evaluation of pigeon pea meal. *Plant Foods for Human Nutrition* **37**, 283-290.
- Odeny, D. A. (2007). The potential of pigeonpea (*Cajanus cajan* (L.) Millsp.) in Africa. In "Natural Resources Forum", Vol. 31, pp. 297-305. Wiley Online Library.
- Olayinka, O. O., Adebawale, K. O., and Olu-Owolabi, B. I. (2008). Effect of heat-moisture treatment on physicochemical properties of white sorghum starch. *Food Hydrocolloids* **22**, 225-230.
- Oosten, B. (1990). Interactions between starch and electrolytes. *Starch-Stärke* **42**, 327-330.
- Osundahunsi, O. F., Seidu, K. T., and Mueller, R. (2011). Dynamic rheological and physicochemical properties of annealed starches from two cultivars of cassava. *Carbohydrate Polymers* **83**, 1916-1921.
- Perera, C., Hoover, R., and Martin, A. (1997). The effect of hydroxypropylation on the structure and physicochemical properties of native, defatted and heat-moisture treated potato starches. *Food Research International* **30**, 235-247.
- Phaikaew, C., Pholsen, P., Chuenpreecha, T., and Suksaran, W. (1996). "Effect of cutting height and cutting frequency of pigeon pea on total herbage yield and quality of grass-legume mixed pasture." Forage Research Group, Division of Animal Nutrition, Bangkok, Thailand.
- Pongsawatmanit, R., and Srijunthongsiri, S. (2008). Influence of xanthan gum on rheological properties and freeze-thaw stability of tapioca starch. *Journal of Food Engineering* **88**, 137-143.

- Pukkahuta, C., Suwannawat, B., Shobsngob, S., and Varavinit, S. (2008). Comparative study of pasting and thermal transition characteristics of osmotic pressure and heat–moisture treated corn starch. *Carbohydrate Polymers* **72**, 527-536.
- Puncha-arnon, S., and Uttapap, D. (2013). Rice starch vs. rice flour: Differences in their properties when modified by heat–moisture treatment. *Carbohydrate Polymers* **91**, 85-91.
- Ratnayake, W., Hoover, R., Shahidi, F., Perera, C., and Jane, J. (2001). Composition, molecular structure, and physicochemical properties of starches from four field pea (*Pisum sativum* L.) cultivars. *Food Chemistry* **74**, 189-202.
- Ring, S. G., Colonna, P., I'Anson, K. J., Kalichevsky, M. T., Miles, M. J., Morris, V. J., and Orford, P. D. (1987). The gelation and crystallisation of amylopectin. *Carbohydrate Research* **162**, 277-293.
- Robles, R., Murray, E., and Paredes-López, O. (1988). Physicochemical changes of maize starch during the lime-heat treatment for tortilla making. *International Journal of Food Science and Technology* **23**, 91-98.
- Rodríguez, M. E., Yáñez-Limón, M., Alvarado-Gil, J. J., Vagas, H., Sánchez-Sinencioi, F., Figueroa, J. D. C., Martínez-Bustos, F., -Montes, J. L. M., González-Hernández, J., Silva, M. D., and Miranda, L. C. M. (1996). Influence of the structural changes during alkaline cooking on the thermal, rheological, and dielectric properties of corn tortillas. *Cereal Chemistry* **73**, 593-600.
- Roskhrua, P., Tran, T., Chaiwanichsiri, S., Kupongsak, S., and Pradipasena, P. (2014). Physicochemical properties of thermal alkaline treated pigeonpea (*Cajanus cajan* L.) flour. *Food Science and Biotechnology* **23**, 381-388.
- Ruiz-Guérrez, M. G., Quintero-Ramos, A., Meléndez-Pizarro, C. O., Talamás-Abbud, R., Barnard, J., Márquez-Meléndez, R., and Lardizábal-Gutiérrez, D. (2012). Nixtamalization in two steps with different calcium salts and the relationship with chemical, texture and thermal properties in masa and tortilla. *Journal of Food Process Engineering* **35**, 772-783.
- Sahagian, M. E., and Goff, H. D. (1996). Fundamental aspects of the freezing process. In "Freezing Effects on Food Quality" (L. E. Jeremiah, ed.), pp. 1-50. Marcel Dekker, Inc., New York.
- Sandhu, K. S., and Lim, S.-T. (2008). Digestibility of legume starches as influenced by their physical and structural properties. *Carbohydrate Polymers* **71**, 245-252.
- Sandhu, K. S., and Singh, N. (2007). Some properties of corn starches II: Physicochemical, gelatinization, retrogradation, pasting and gel textural properties. *Food Chemistry* **101**, 1499-1507.
- Sasaki, T., Yasui, T., and Matsuki, J. (2000). Effect of amylose content on gelatinization, retrogradation, and pasting properties of starches from waxy and nonwaxy wheat and their F1 seeds. *Cereal Chemistry* **77**, 58-63.
- Sefa-Dedeh, S., Cornelius, B., Sakyi-Dawson, E., and Afoakwa, E. O. (2004). Effect of nixtamalization on the chemical and functional properties of maize. *Food Chemistry* **86**, 317-324.
- Singh, J., Kaur, L., and McCarthy, O. (2007). Factors influencing the physico-chemical, morphological, thermal and rheological properties of some

- chemically modified starches for food applications—A review. *Food Hydrocolloids* **21**, 1-22.
- Singh, N., Kaur, L., Sandhu, K. S., Kaur, J., and Nishinari, K. (2006). Relationships between physicochemical, morphological, thermal, rheological properties of rice starches. *Food Hydrocolloids* **20**, 532-542.
- Smith, P. S. (1982). Starch derivatives and their use in foods. In "Food Carbohydrates" (D. R. Lineback and G. E. Inglett, eds.), pp. 237-249. AVI Publishing Company, Inc., Westport, Connecticut.
- Sui, Z., Yao, T., Zhao, Y., Ye, X., Kong, X., and Ai, L. (2015). Effects of heat-moisture treatment reaction conditions on the physicochemical and structural properties of maize starch: Moisture and length of heating. *Food Chemistry* **173**, 1125-1132.
- Sun, Q., Han, Z., Wang, L., and Xiong, L. (2014). Physicochemical differences between sorghum starch and sorghum flour modified by heat-moisture treatment. *Food Chemistry* **145**, 756-764.
- Swinkels, J. (1985). Sources of starch: its chemistry and physics. In "Starch Conversion Technology" (G. V. Belyum and J. A. Roels, eds.). Marcel Dekker, Inc., New York.
- Tester, R. F., and Morrison, W. R. (1990). Swelling and gelatinization of cereal starches. I. Effects of amylopectin, amylose, and lipids. *Cereal Chemistry* **67**, 551-557.
- Tropical Forages (2016). *Cajanus cajan* [Online]. Available from: http://www.tropicalforages.info/key/Forages/Media/Html/Cajanus_cajan.htm [2016, April 16].
- Vandeputte, G., Derycke, V., Geeroms, J., and Delcour, J. (2003). Rice starches. II. Structural aspects provide insight into swelling and pasting properties. *Journal of Cereal Science* **38**, 53-59.
- Varatharajan, V., Hoover, R., Liu, Q., and Seetharaman, K. (2010). The impact of heat-moisture treatment on the molecular structure and physicochemical properties of normal and waxy potato starches. *Carbohydrate Polymers* **81**, 466-475.
- Varavinit, S., Shobsngob, S., Varayanond, W., Chinachoti, P., and Naivikul, O. (2002). Freezing and thawing conditions affect the gel stability of different varieties of rice flour. *Starch-Stärke* **54**, 31-36.
- Varavinit, S., Shobsngob, S., Varayanond, W., Chinachoti, P., and Naivikul, O. (2003). Effect of amylose content on gelatinization, retrogradation and pasting properties of flours from different cultivars of Thai rice. *Starch-Stärke* **55**, 410-415.
- Waduge, R., Hoover, R., Vasanthan, T., Gao, J., and Li, J. (2006). Effect of annealing on the structure and physicochemical properties of barley starches of varying amylose content. *Food Research International* **39**, 59-77.
- Wallis, E. S., Woolcock, R. F., and Byth, D. E. (1988). "Potential for pigeonpea in Thailand, Indonesia and Burma," The CGPRT Center.
- Walstra, P. (2003). Studying food colloids: past, present and future. In "Food Colloids, Biopolymers and Materials" (E. Dickinson and T. V. Vliet, eds.), pp. 391-399. The Royal Society of Chemistry, Cambridge.

- Ward, K., Hosney, R., and Seib, P. (1994). Retrogradations of amylopectin from maize and wheat starches. *Cereal Chemistry* **71**, 150-155.
- Watcharatewinkul, Y., Puttanlek, C., Rungsardthong, V., and Uttapap, D. (2009). Pasting properties of a heat-moisture treated canna starch in relation to its structural characteristics. *Carbohydrate Polymers* **75**, 505-511.
- Whistler, R. L., and BeMiller, J. N. (1999). "Carbohydrate Chemistry for Food Scientists," Eagan Press, St. Paul, Minnesota.
- Willett, J. (2001). Packing characteristics of starch granules. *Cereal Chemistry* **78**, 64-68.
- Yadav, B. S., Guleria, P., and Yadav, R. B. (2013). Hydrothermal modification of Indian water chestnut starch: Influence of heat-moisture treatment and annealing on the physicochemical, gelatinization and pasting characteristics. *LWT-Food Science and Technology* **53**, 211-217.
- Yoshimura, M., Takaya, T., and Nishinari, K. (1996). Effects of konjac-glucomannan on the gelatinization and retrogradation of corn starch as determined by rheology and differential scanning calorimetry. *Journal of Agricultural and Food Chemistry* **44**, 2970-2976.
- Yoshimura, M., Takaya, T., and Nishinari, K. (1999). Effects of xyloglucan on the gelatinization and retrogradation of corn starch as studied by rheology and differential scanning calorimetry. *Food Hydrocolloids* **13**, 101-111.
- Yu, L., and Christie, G. (2005). Microstructure and mechanical properties of orientated thermoplastic starches. *Journal of Materials Science* **40**, 111-116.
- Zobel, H. F. (1964). X-ray analysis of starch granules. In "Methods in Carbohydrate Chemistry" (R. L. Whistler, ed.), Vol. 4, pp. 109-113. FL Academic Press, Orlando.
- Zobel, H. F., and Stephen, A. M. (1995). Starch: structure, analysis, and application. In "Food Polysaccharides and Their Applications" (A. M. Stephen, ed.), pp. 19-50. Marcel Dekker, Inc., New York.
- Zobel, H. F., Young, S. N., and Rocca, L. A. (1988). Starch gelatinization: An X-ray diffraction study. *Cereal Chemistry* **65**, 443-446.
- สังเวียน โพธิศรี ดุสิต มานะจติ และ วีรพล ธรรมคุณ (2521). "ถั่วมะแฮะพืชเพิ่มอาหารโปรตีนบนที่สูง," คณะเกษตรศาสตร์ มหาวิทยาลัยเชียงใหม่, เชียงใหม่.

APPENDIX



จุฬาลงกรณ์มหาวิทยาลัย
CHULALONGKORN UNIVERSITY

APPENDIX A

Figure of results

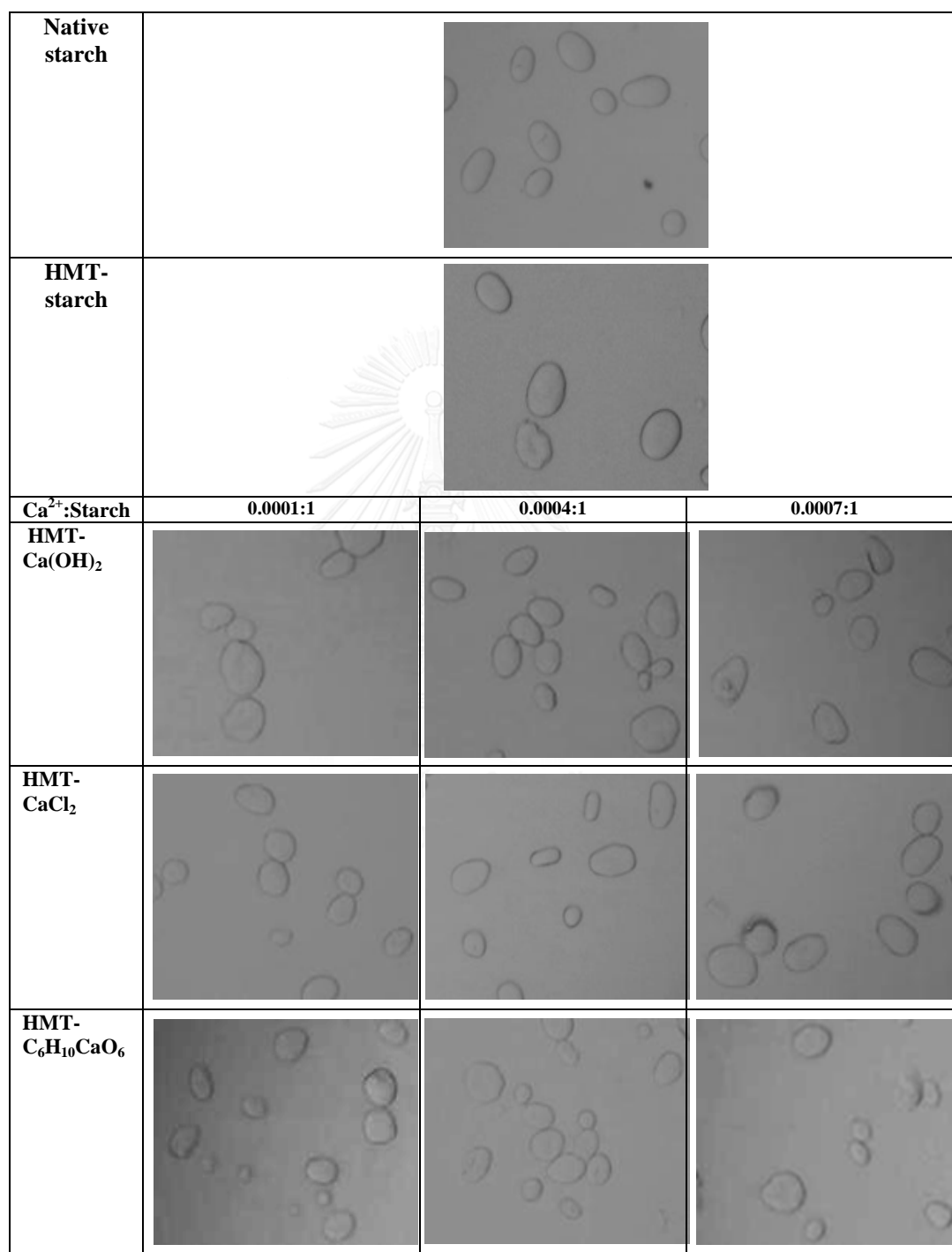


Figure A.1 Light microscope images of starch granules.

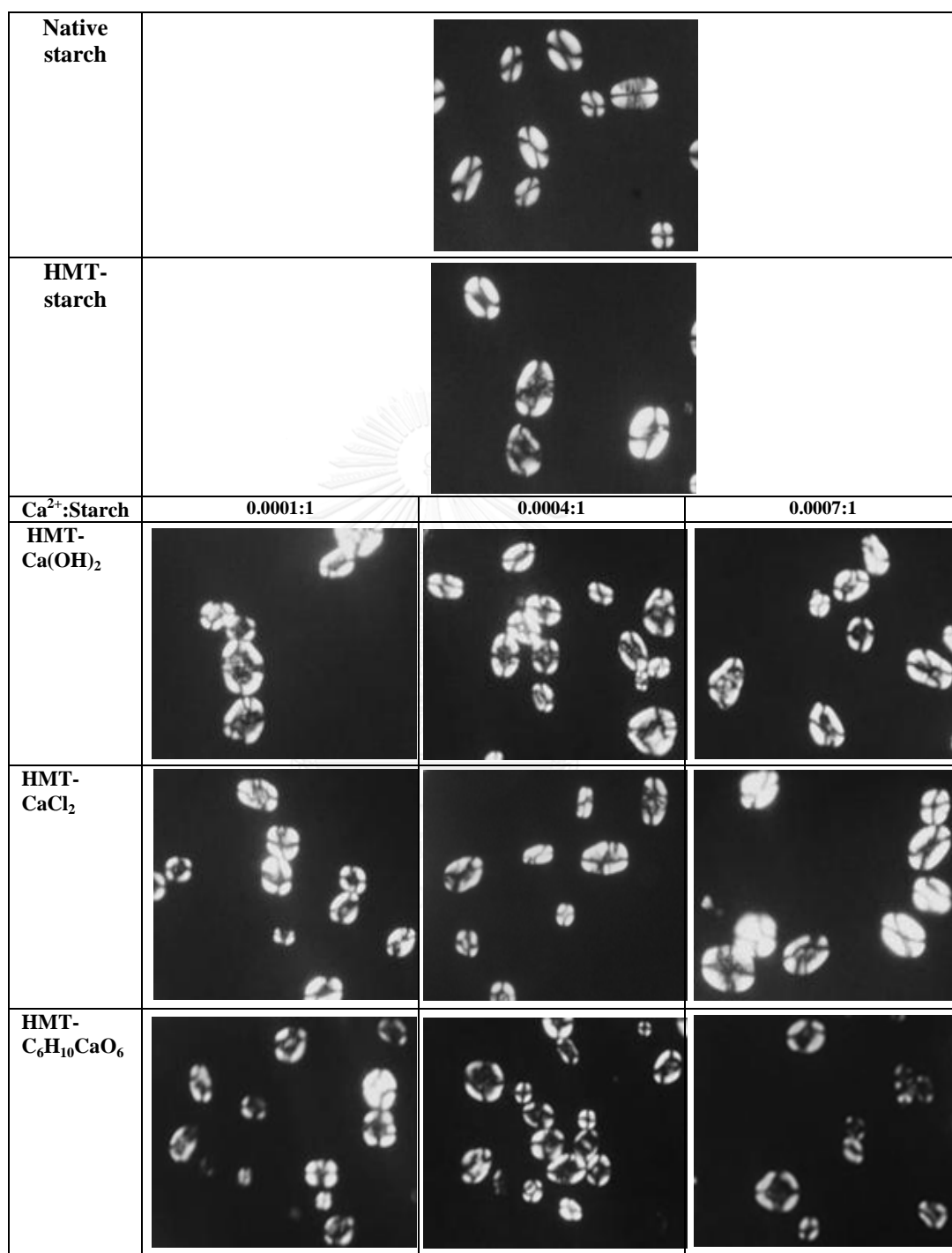


Figure A.2 Polarized light microscope images of starch granules

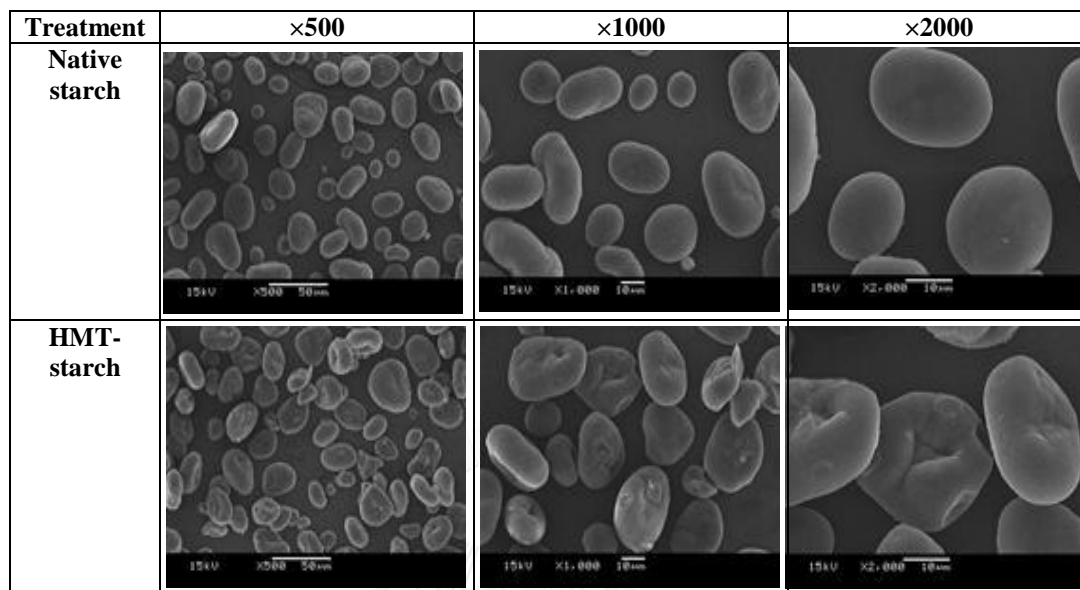
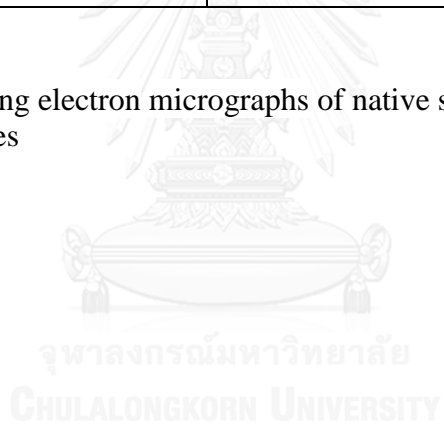


Figure A.3 Scanning electron micrographs of native starch and HMT-starch granules



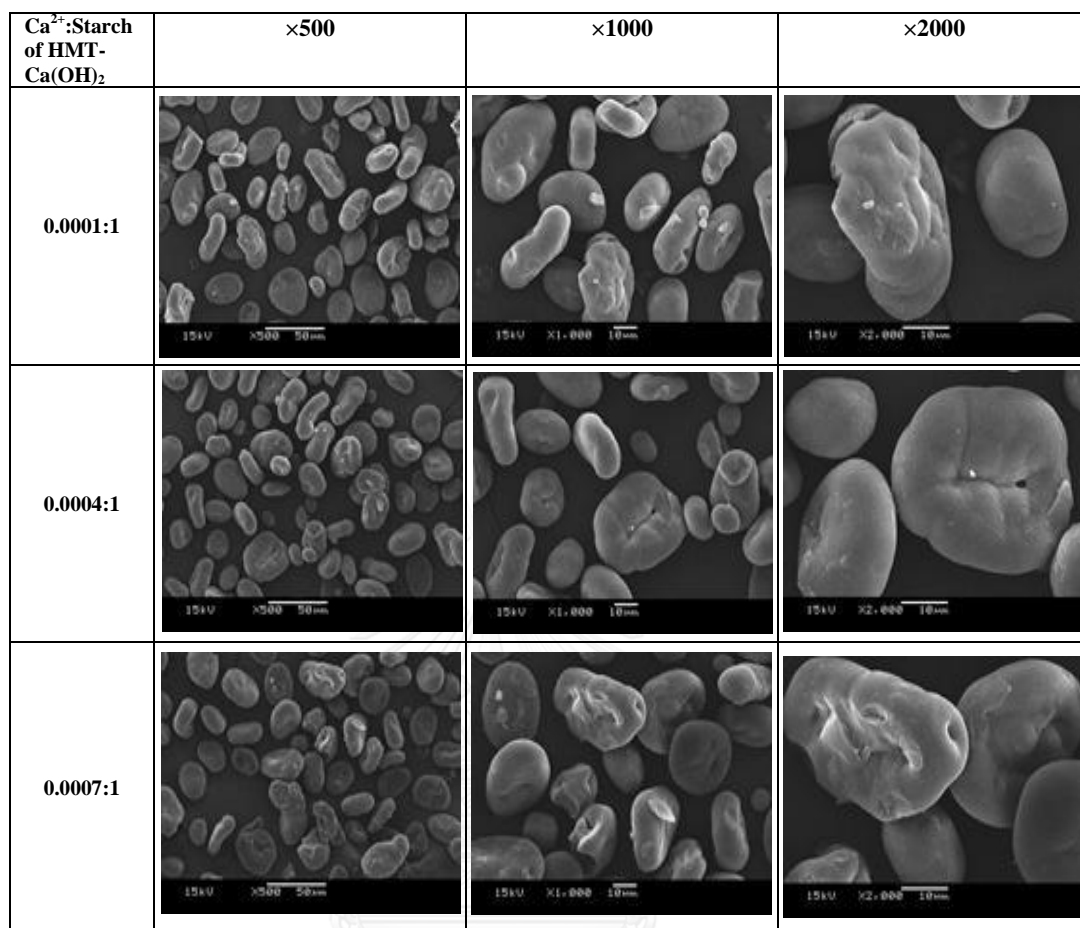
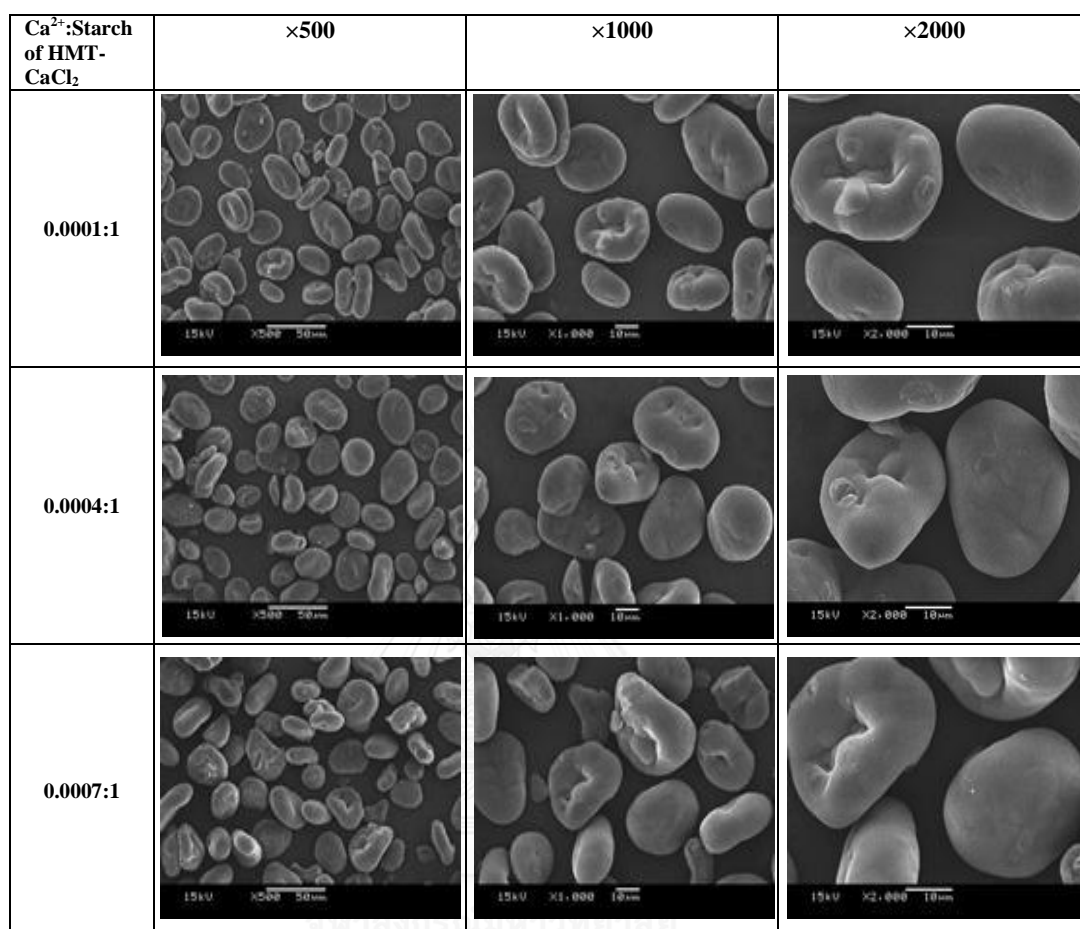


Figure A.4 Scanning electron micrographs of HMT-Ca(OH)₂ starch granules



CHULALONGKORN UNIVERSITY

Figure A.5 Scanning electron micrographs of HMT- CaCl_2 starch granules

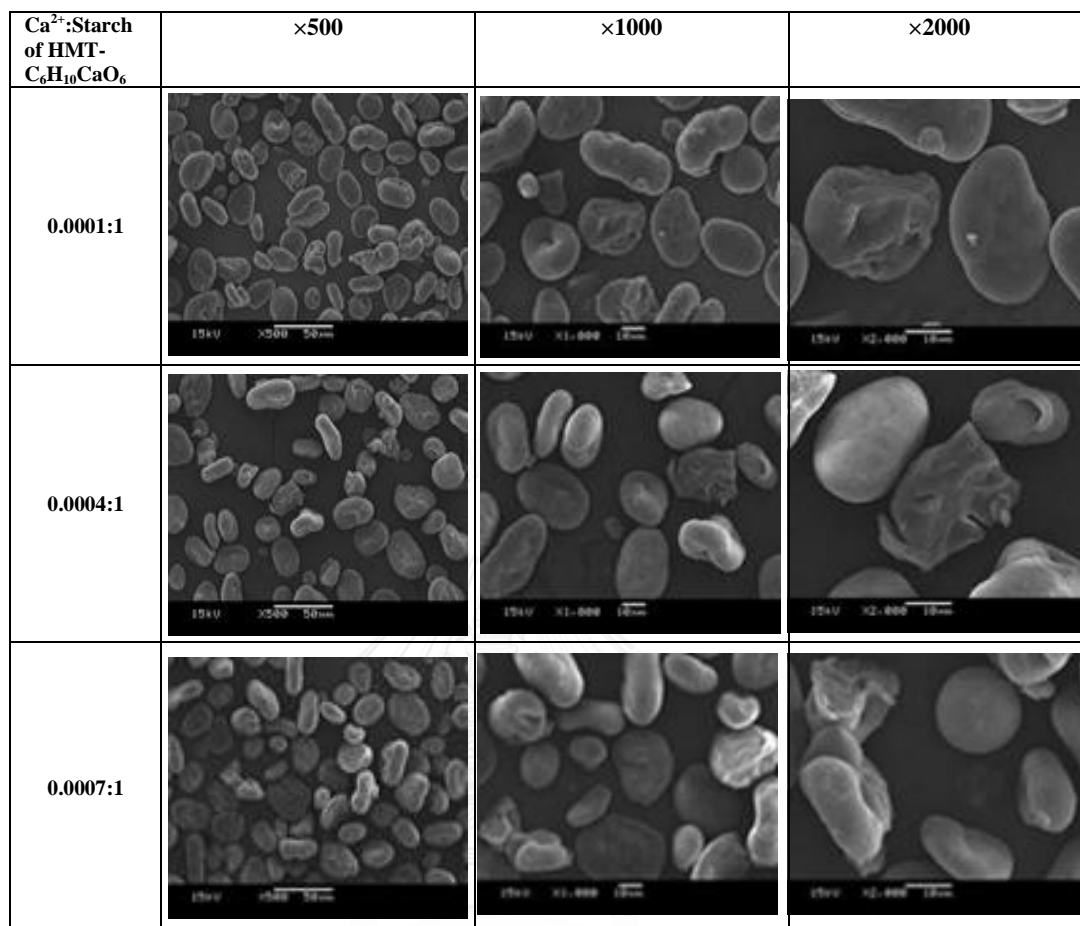


Figure A.6 Scanning electron micrographs of HMT- $\text{C}_6\text{H}_{10}\text{CaO}_6$ starch granules

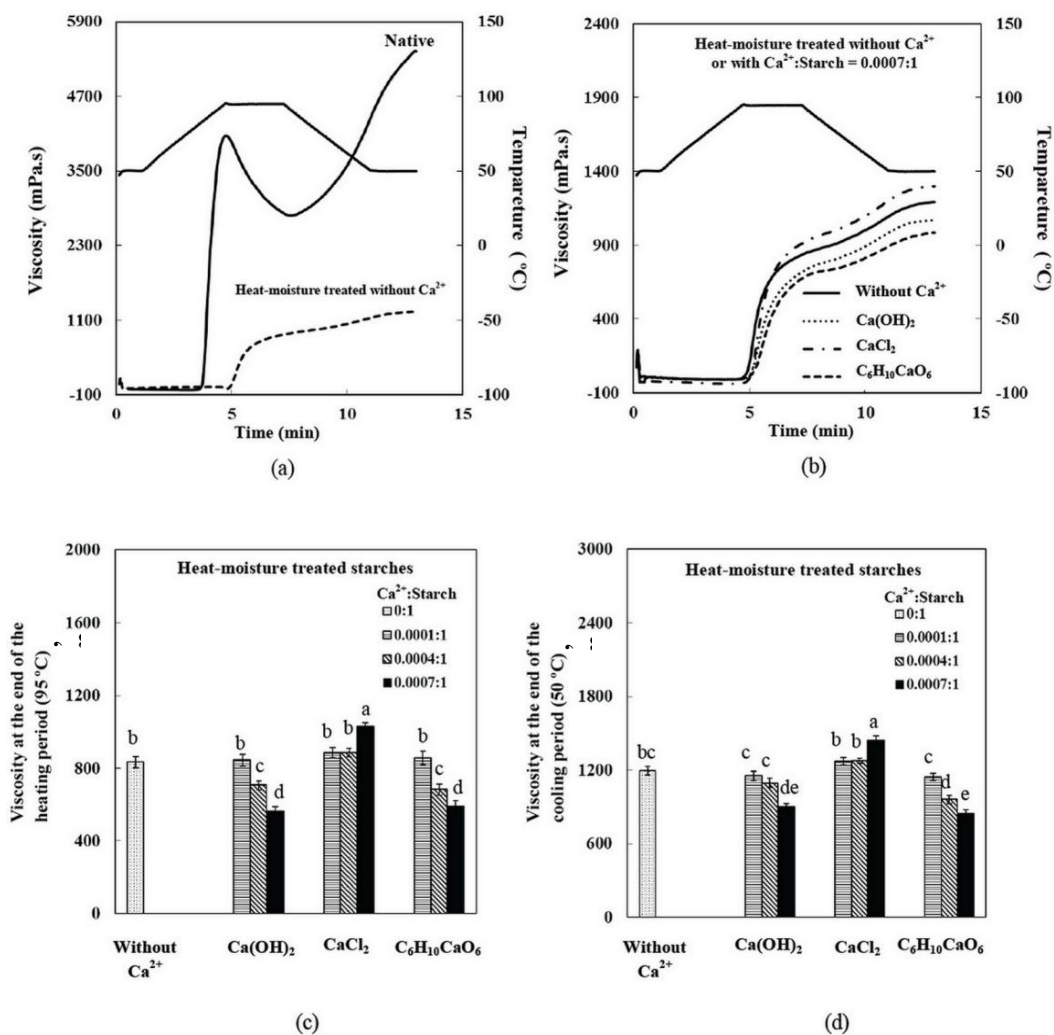


Figure A.7 Pasting profile and viscosity of 10% w/w native starch and HMT-starches that treated at 110°C for 1 h

Means with different letters (a, b, ..) in each graph are significantly different ($P \leq 0.05$).

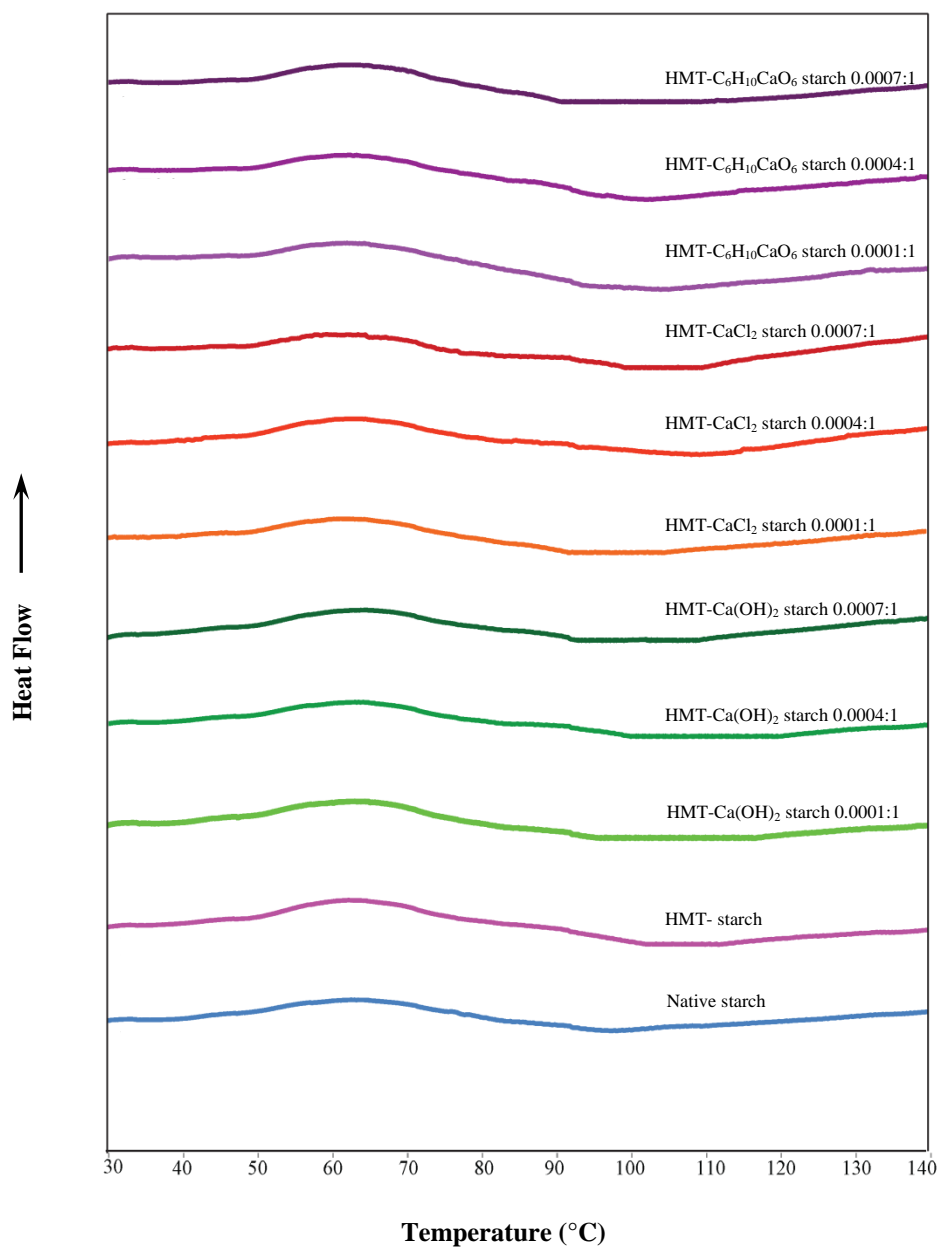


Figure A.8 Thermogram of retrograded native starch and HMT-starches that treated at 110°C for 1 h stored at 5°C for 7 days

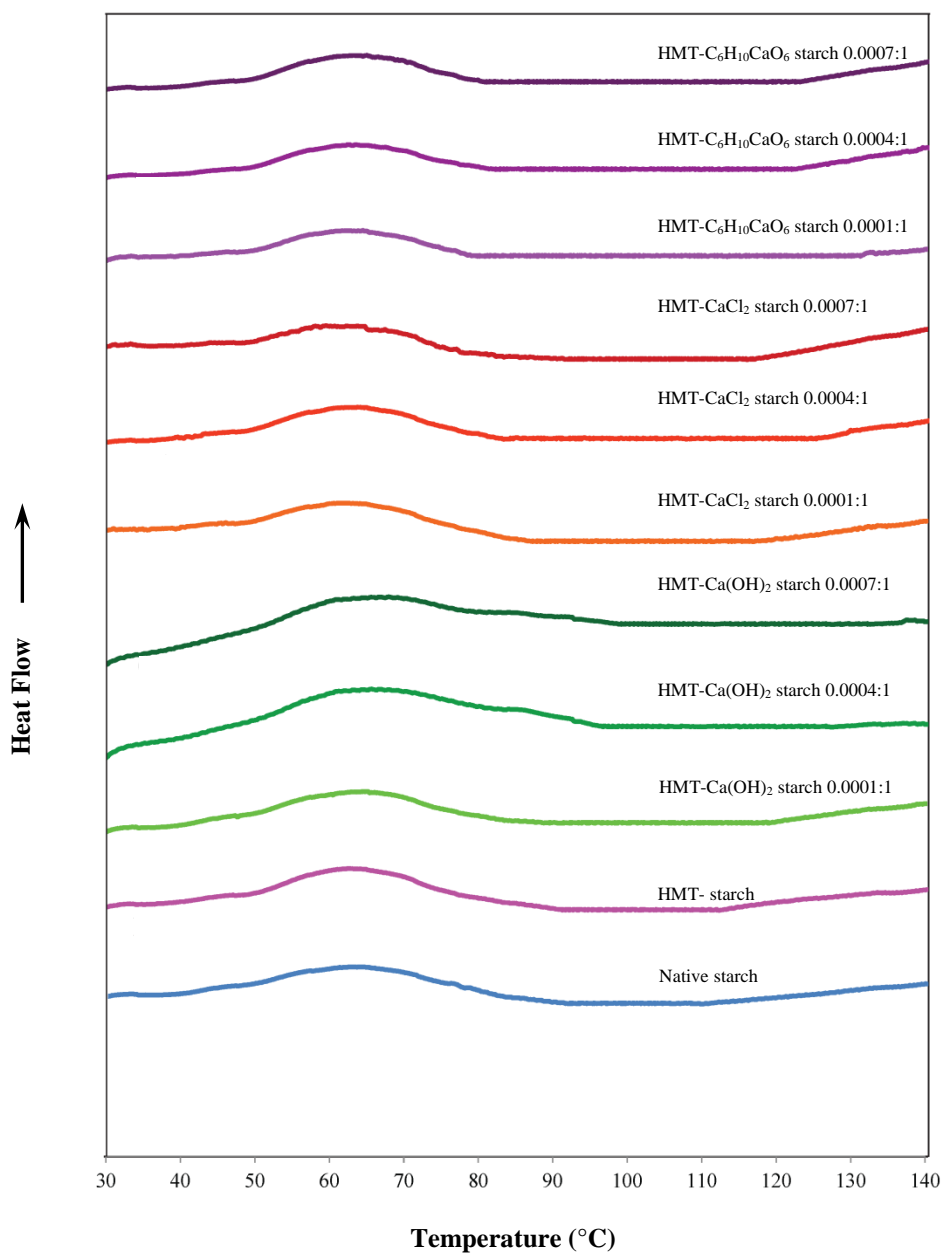


Figure A.9 Thermogram of retrograded native starch and HMT-starches that treated at 110°C for 1 h stored at 5°C for 14 days

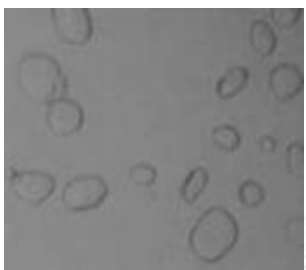
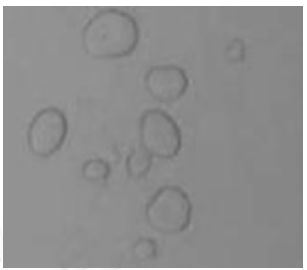

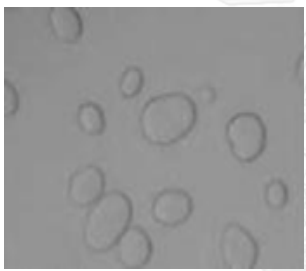

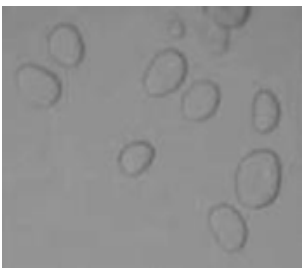


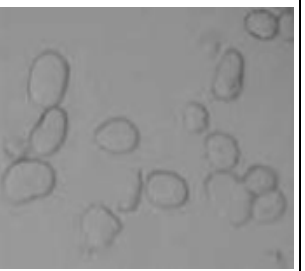
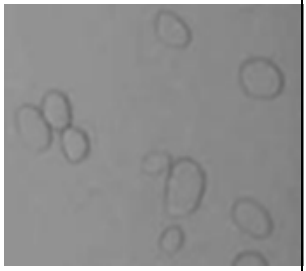


	HMT in the absence of $\text{Ca}(\text{OH})_2$		
Temperature (°C) / Time (h)	100°C	110°C	120°C
1 h			
2 h			
	HMT in the presence of $\text{Ca}(\text{OH})_2$		
1 h			
2 h			

Figure A.10 Light microscope images of starch granules

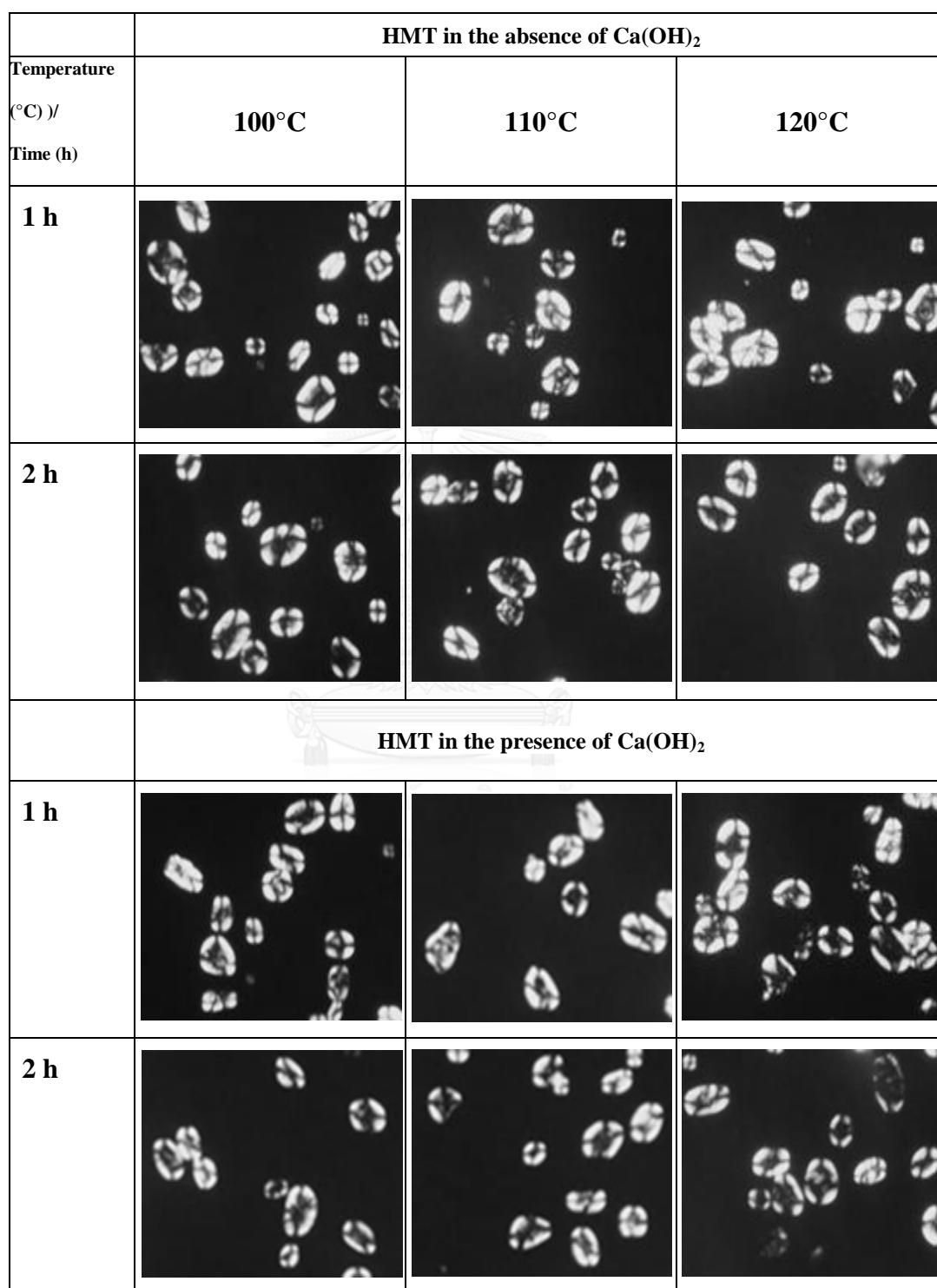


Figure A.11 Polarized light microscope images of starch granules

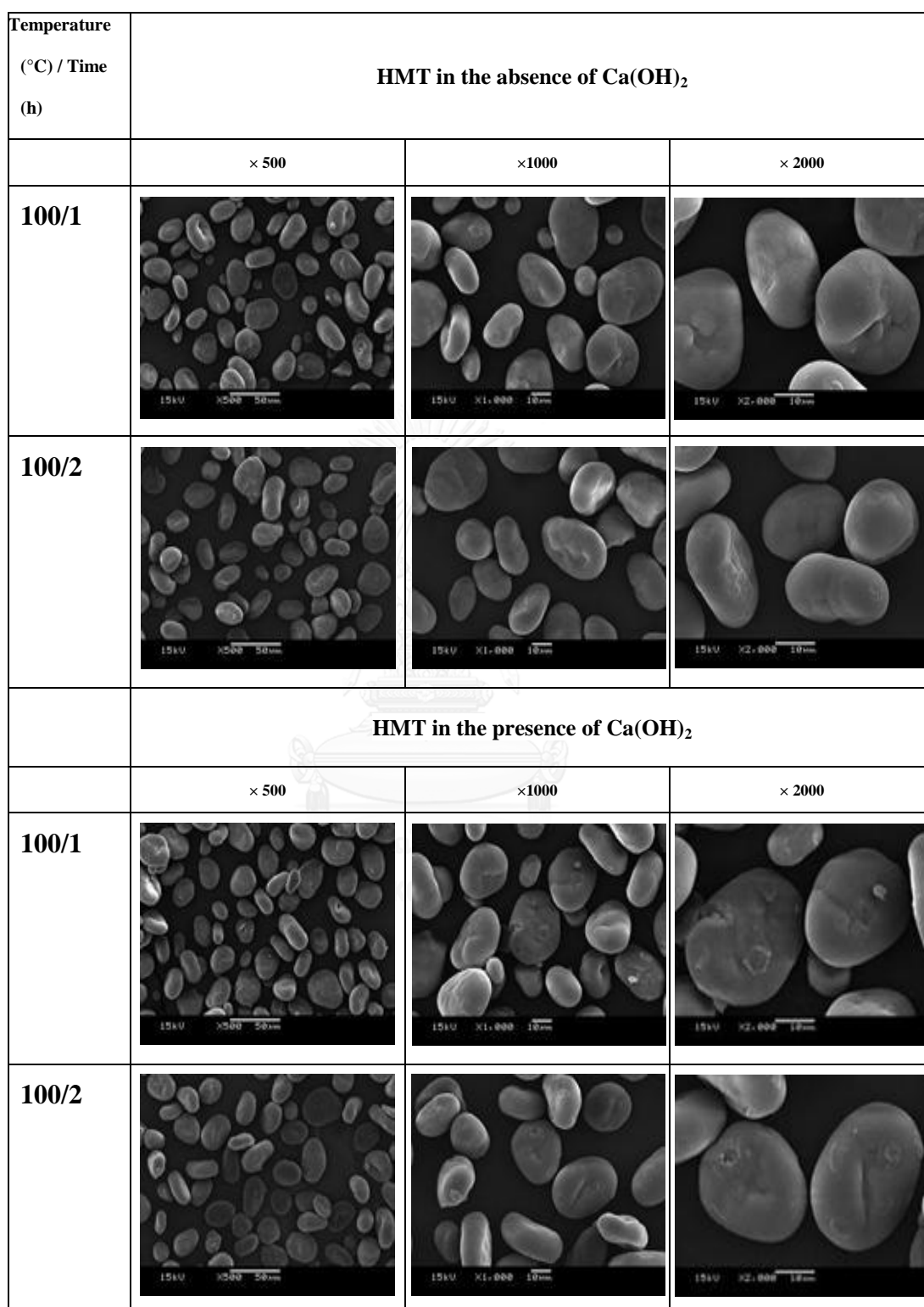


Figure A.12 Scanning electron micrographs of HMT-starch granules that treated at 100°C

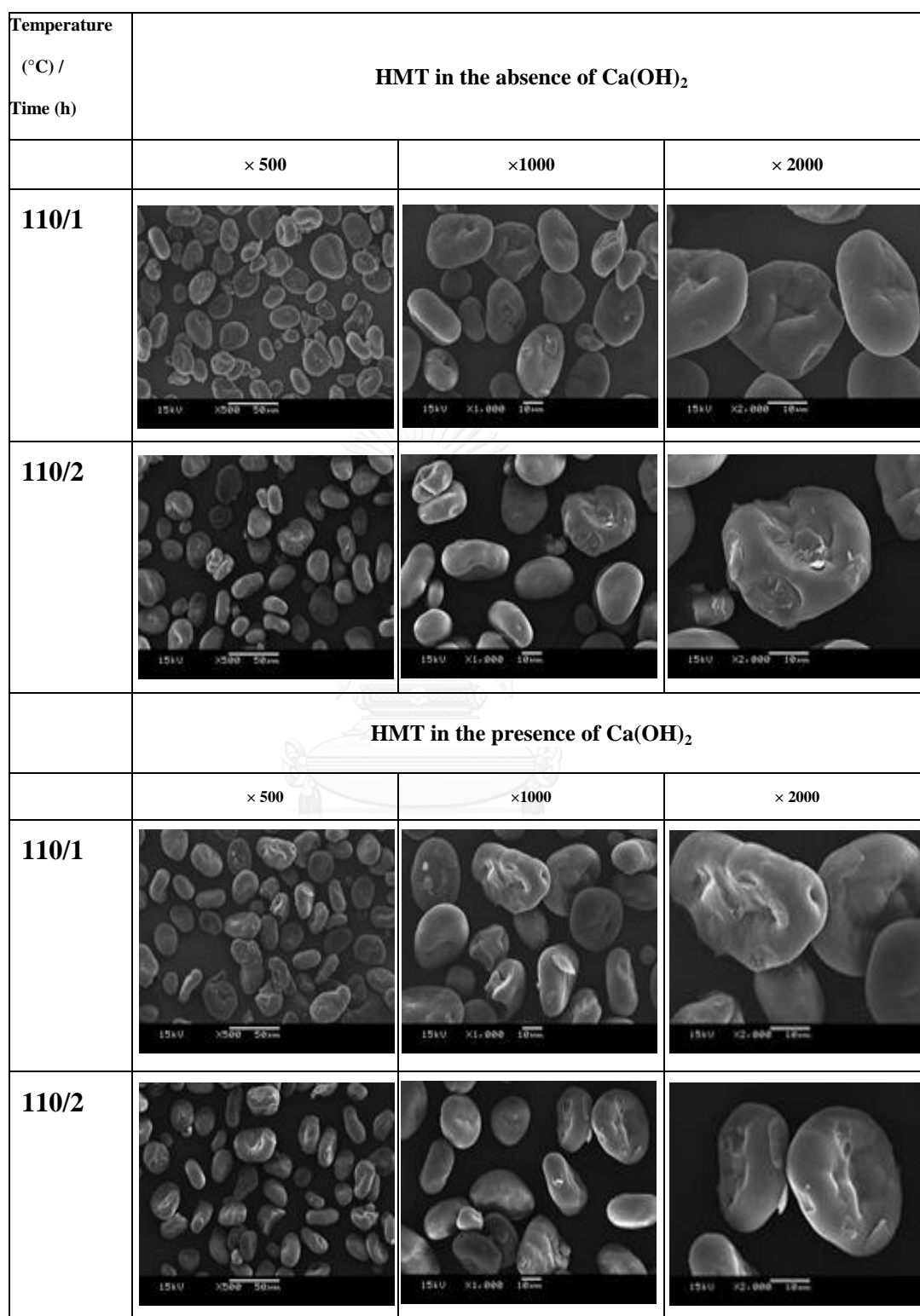


Figure A.13 Scanning electron micrographs of HMT-starch granules that treated at 110°C

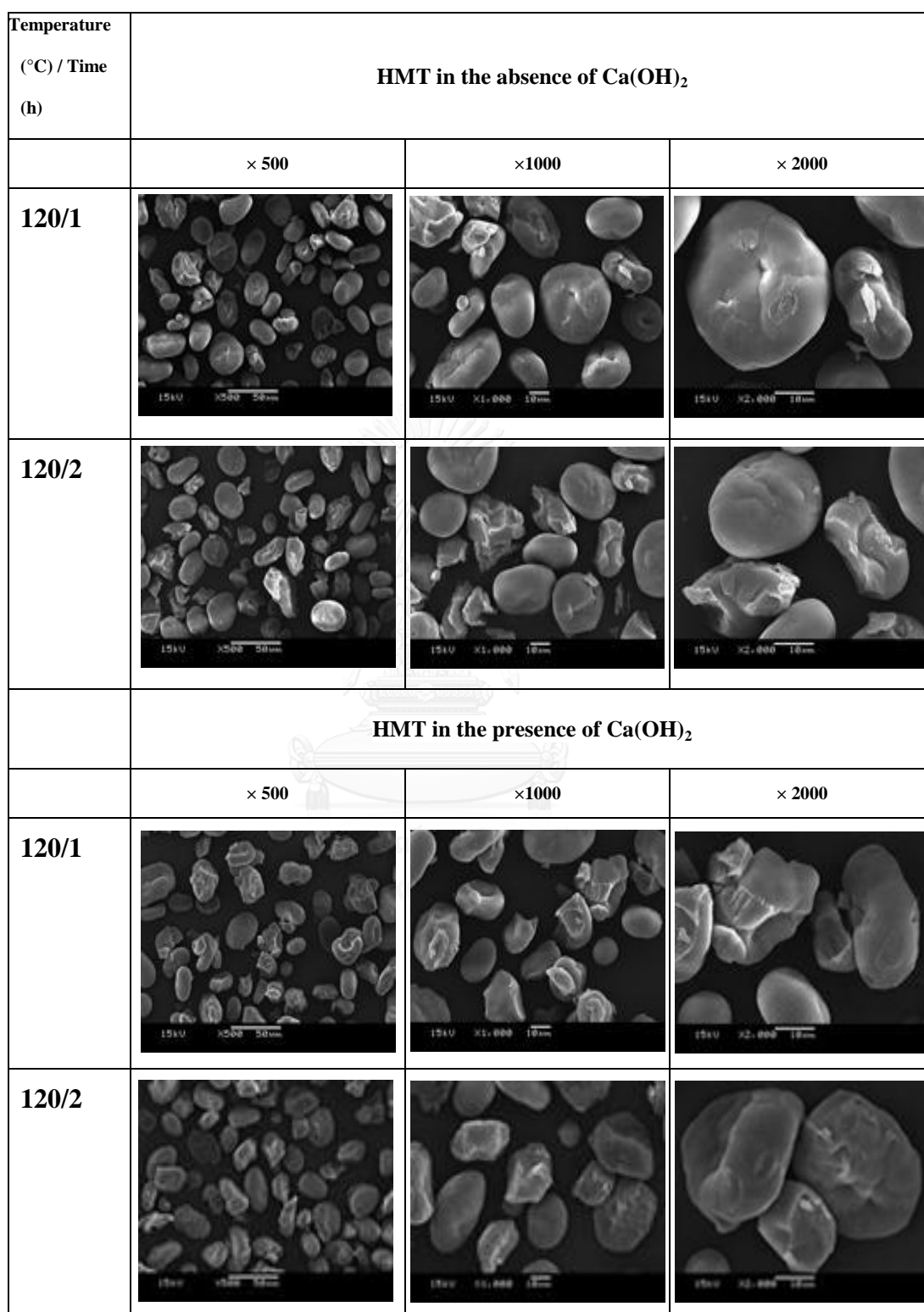


Figure A.14 Scanning electron micrographs of HMT-starch granules that treated at 120°C

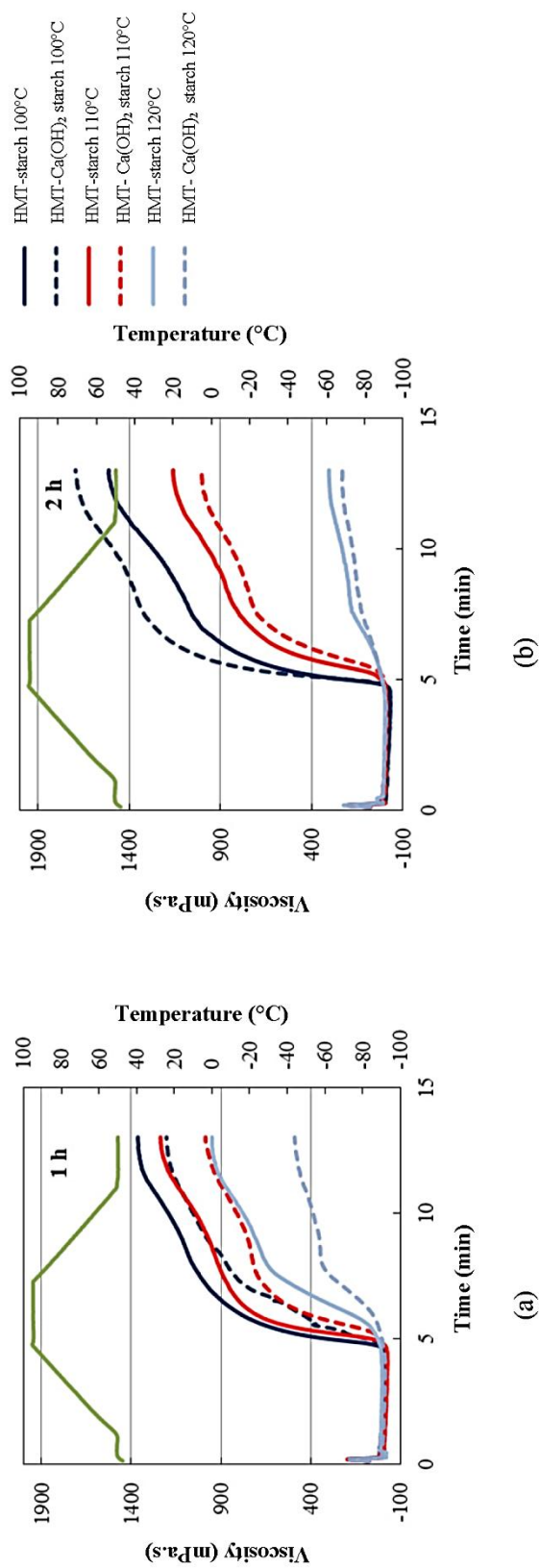


Figure A.15 Pasting profile of 10% w/w HMT-starch and HMT-Ca(OH)₂ starch at the Ca²⁺-starch ratio of 0:1 and 0.0007:1

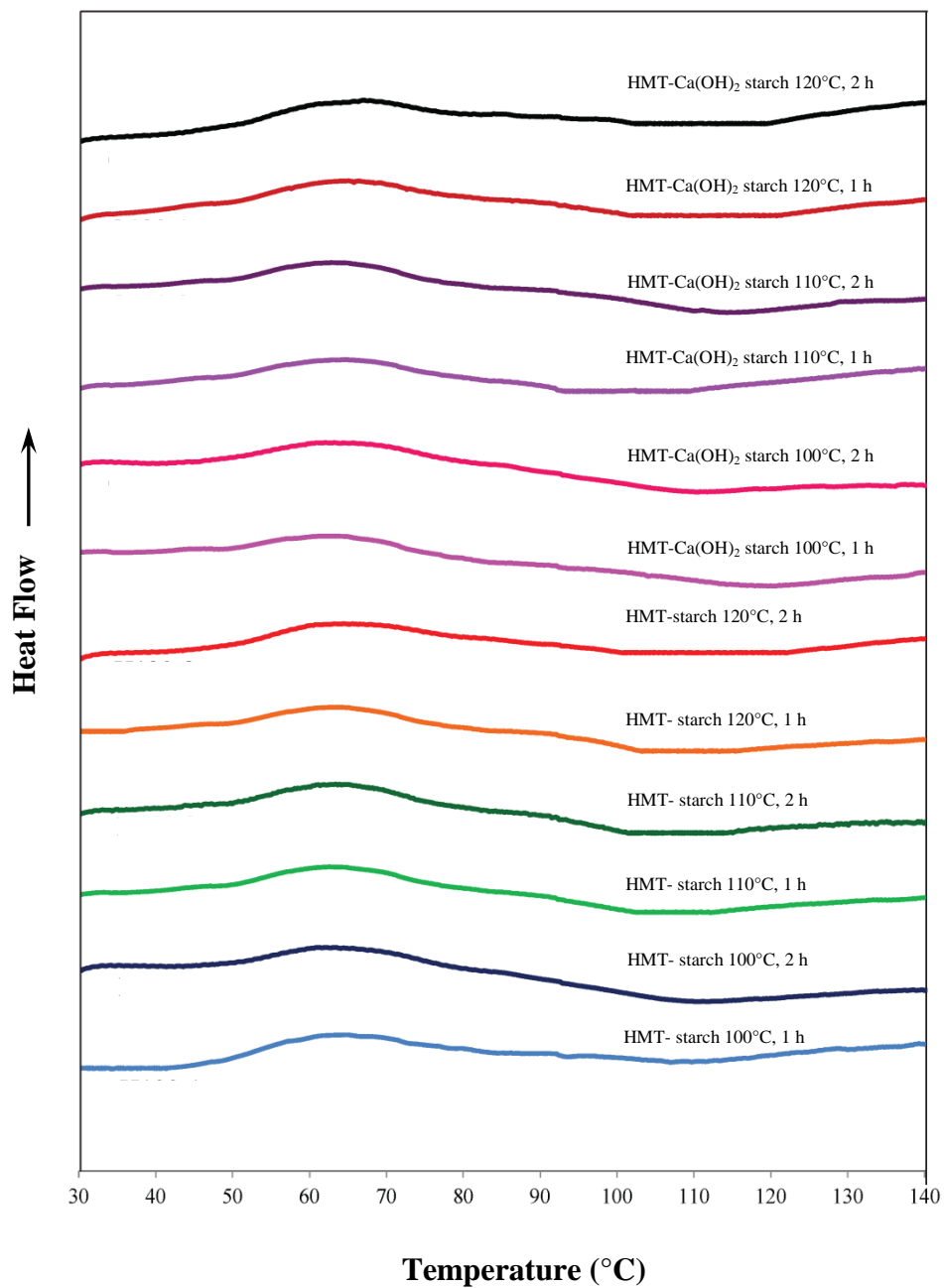


Figure A.16 Thermogram of retrograded HMT-starch and HMT-Ca(OH)₂ starch at the Ca²⁺-starch ratio of 0:1 and 0.0007:1 stored at 5°C for 7 days

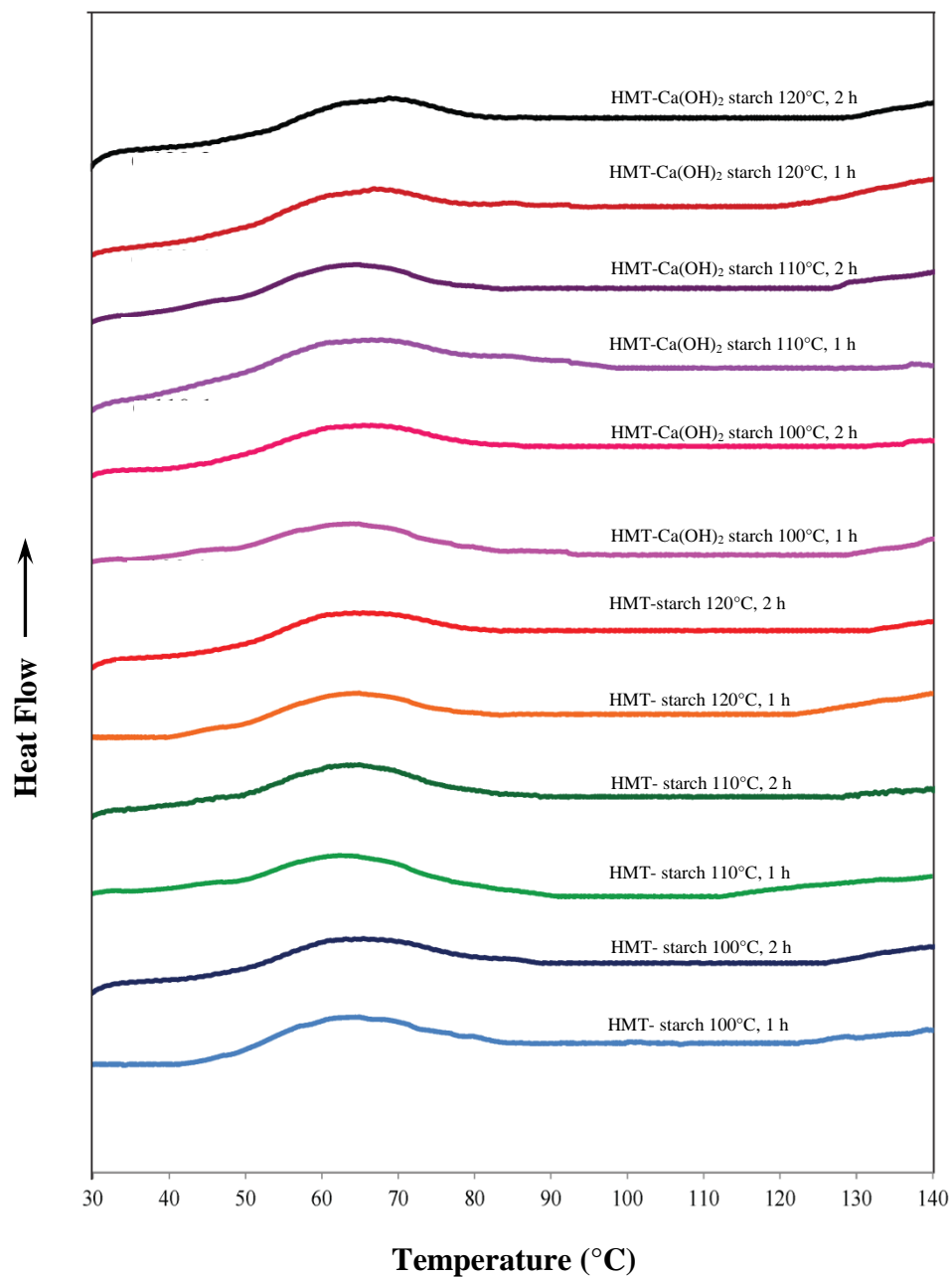


Figure A.17 Thermogram of retrograded HMT-starch and HMT-Ca(OH)₂ starch at the Ca²⁺-starch ratio of 0:1 and 0.0007:1 stored at 5°C for 14 days

APPENDIX B

Procedure for amylose standard curve for amylose leaching

Accurate weights of all compounds were obtained at ± 0.002 g (BSA224S, Sartorius, Mettler Toledo, Switzerland)

0.01 N I₂-KI preparation

- Prepare 0.01 N I₂-KI solution
 - Weigh 0.13 g iodine (QRecTM, NZ) and 0.30 g potassium iodide (Ajax Finechem, NZ) in a 100 ml volumetric flask
 - Adjust volume to 100 ml with distilled water

Standard amylose solution preparation

- Prepare 1 mg/ml amylose stock solution
 - Weigh 200 mg pure amylose standard from potato (Sigma, UK) in a 50 ml volumetric flask
 - Adjust volume to 50 ml with 0.3 M NaOH
 - Heat at 95 °C for 30 min in a controlled shaking water bath.
 - Cool the amylose standard solution in an ice bath
- Prepare 2.00, 4.03, 6.04, 8.05, 10.07, 12.08, 16.10, 20.13 and 24.16 mg/ml amylose standard solutions
 - Pipette 0.5, 1.0, 1.5, 2.0, 2.5, 3, 4, 5 or 6 ml of 1 mg/ml amylose stock solution into a 50 ml volumetric flask to obtain 2.00, 4.03, 6.04, 8.05, 10.07, 12.08, 16.10, 20.13 and 24.16 mg/ml amylose standard solutions, respectively
 - Adjust volume to 50 ml with 0.3 M NaOH

- Pipette 0.1 ml of amylose solution into 5 ml of 0.5% Trichloroacetic acid (AppliChem Panreac, Germany) and 0.05 ml of 0.01N I₂-KI solution
- Keep the solution in a dark room for 30 min
- Measure the OD of each amylose solution with spectrophotometer at 630 nm.

Amylose standard curve construction

- Plot amylose concentration (mg/l) versus OD

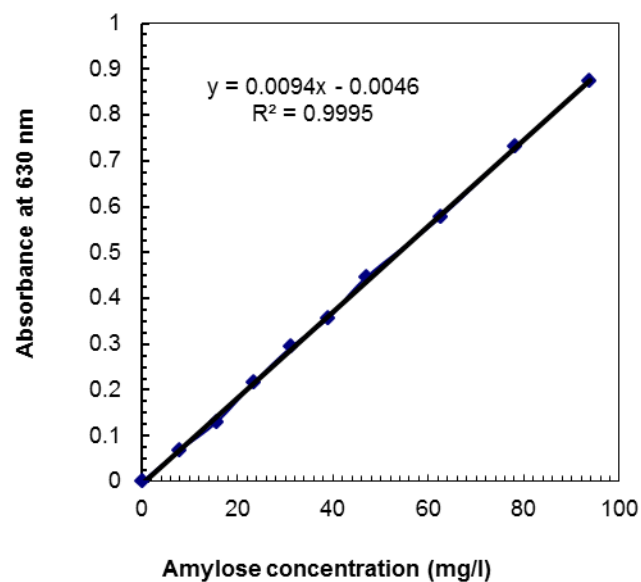


Figure A.18 Amylose standard curve for determination of amylose concentration in the supernatant obtained in section 3.4.3

APPENDIX C
AOAC Official Method 943.02

pH of flour

Weigh 10.0 g test portions into clean, dry Erlenmeyer and add 100 ml recently boiled water at 25°C. Shake until particles are evenly suspended and mixture is free of lumps. Digest 30 min, shaking frequently. Let stand 10 min more, decant supernate into 250 ml beaker, and immediately determine pH, using electrode and potentiometer standardized by buffer solutions of pH 4.01, and of pH 9.18, both at 25°C.



APPENDIX D
AOAC Official Method 975.03

Metals in Plants and Pet Foods

Atomic Absorption Spectrophotometric Method

(Applicable to calcium, copper, iron, magnesium, manganese, potassium, and zinc.)

A. Apparatus and Reagents

Deionized water may be used, and following:

- (a) Potassium stock solution.-1000 $\mu\text{g K/ml}$. Dissolve 1.9066 g dried (2 h at 105°C) KCl in H_2O and dilute to 1 L.
- (b) Calcium stock solutions.-Prepare Ca stock solution and working standards.
- (c) Cu, Fe, Mg, Mn, and Zn stock solutions.
- (d) Working standard solutions.-Dilute aliquots of solutions, (c), with 10% HCl to make ≥ 4 standard solutions of each element within range of determination.

B. Preparation of Test Solutions

- (a) Dry ashing.-Accurately weigh 1 g test portion, dried and ground, in to glazed, high-form porcelain crucible. Ash 2 h at 500°C, and let cool. Wet ash with 10 drops H_2O , and carefully add 3-4 ml HNO_3 (1 + 1). Evaporate excess HNO_3 on hot plate set at 100-120°C. Return crucible to furnace and ash additional 1 h at 500°C. Cool crucible, dissolve ash in 10 ml HCl (1 + 1), and transfer quantitatively to 50 ml volumetric flask.
- (b) Wet ashing.-Accurately weigh 1 g test portion, dried and ground, into 150 ml beaker. Add 10 ml HNO_3 and let soak thoroughly. Add 3 ml 60% HClO_4 and heat on hot plate, slowly at first, until frothing ceases. Heat until HNO_3 is almost evaporated. If charring occurs, cool, add 10 ml HNO_3 , and continue

heating. Heat to white fumes of HClO_4 . Cool, add 10 ml HCl (1 + 1), and transfer quantitatively to 50 ml volumetric flask.

C. Determination

To solution in 50 ml volumetric flask, add 10 ml 5% La solution, and dilute to volume. Let silica settle, decant supernate.

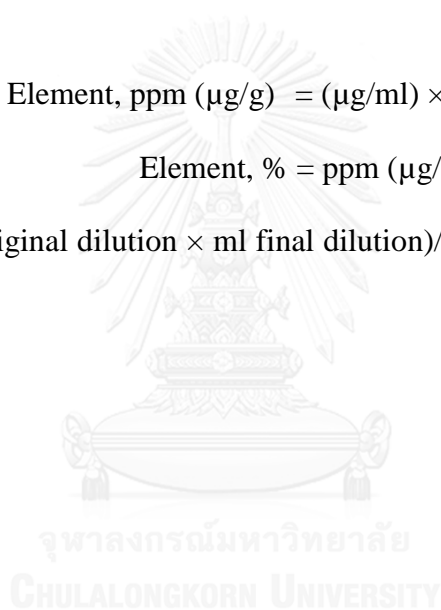
Make necessary dilution with 10% HCl to obtain solutions within range of instrument.

D. Calculations

$$\text{Element, ppm } (\mu\text{g/g}) = (\mu\text{g/ml}) \times F/\text{g test portion}$$

$$\text{Element, \%} = \text{ppm } (\mu\text{g/g}) \times 10^{-4}$$

Where $F = (\text{ml original dilution} \times \text{ml final dilution})/\text{ml aliquot}$ if original 50 ml is diluted.



APPENDIX E
AOAC Official Method 984.27

**Calcium, Copper, Iron, Magnesium, Manganese, Phosphorus, Potassium,
Sodium, and Zinc in Infant Formula**

A. Principle

Test portion is digested in $\text{HNO}_3/\text{HClO}_4$ and elements are determined by ICP emission spectroscopy.

B. Reagents

- (a) *Water*.-Distilled, deionized. Use throughout.
- (b) *Perchloric acid*.-Double-distilled. Dilute 10 ml to 50 ml with H_2O .
- (c) *Standards*.-All preparations yield 1000 $\mu\text{g}/\text{ml}$.

(1) *Calcium*.-Place 2.4973 g CaCO_3 in 1 L volumetric flask with 300 ml H_2O , add 10 ml HCl, and after CO_2 has been released, dilute to 1 L.

(2) *Copper*.-Dissolve 1.000g Cu in 10 ml HCl plus 5 ml H_2O to which HNO_3 is added dropwise until dissolution is complete. Boil to expel fumes, cool, and dilute to 1 L with H_2O .

(3) *Iron*.-Dissolve 1.000 g Fe wire in 20 ml 5M HCl; dilute to 1 L with H_2O .

(4) *Potassium*.-Dissolve 1.9067 g KCl in H_2O and dilute to 1 L with H_2O .

(5) *Magnesium*.-Dissolve 1.000 g Mg in 50 ml 1M HCl and dilute to 1 L with H_2O .

(6) *Manganese*.-Dissolve 1.000 g Mn in 10 ml HCl plus 1 ml HNO_3 and dilute to 1 L with H_2O .

(7) *Sodium*.-Dissolve 2.5421 g NaCl in H_2O and dilute to 1 L with H_2O .

(8) *Phosphorus*.-Dissolve 4.263 g $(\text{NH}_4)\text{HPO}_4$ in H_2O and dilute to 1 L with H_2O .

(9) *Zinc*.-Dissolve 1.000 g Zn in 10 ml HCl and dilute to 1 L with H_2O .

Commercially available certified standards may be substituted for any of the above element solutions.

(d) *Calibration standards*.-Prepare to concentration indicated in Table E.1, using standards above. All calibration standards should be prepared to contain 20% HClO_4 to approximate HClO_4 concentration in diluted digest.

C. Apparatus

(a) *ICP emission spectrometer*.-Model 975 Plasma Atom Comp, or equivalent, capable of simultaneous or sequential determination of Ca, Cu, Fe, K, Mg, Mn, Na^+ , P^- , and Zn. Miniplus 2 peristaltic pump, or equivalent, used to feed glass crossflow nebulizer. Suggested operating parameters: warm-up time (plasma on), 30 min; exposure time, 5s; integration cycles, 1 cycle (2 on line exposures, 1 off line exposure); forward power, 1.1 KW; reflected power, <5 watts; analyte uptake rate (w/pump), 0.8 ml/min; observation height: 16 mm above load coil (optimized for Mn).

(b) *Controllable heating mantle and acid scrubber*.-Lanconco 60301, or equivalent.

(c) *Glassware*.-Soak overnight in 10% HNO_3 and thoroughly rinse with H_2O .

D. Procedure

Vigorously shake container of infant formula ensure complete mixing. Measure 15.0 ml of ready to feed (10.0 ml if concentrated, 1.5 g if powdered) infant formula into 100 ml Kjeldahl flask. Add 30 ml $\text{HNO}_3\cdot\text{HClO}_4$ (2 + 1) to flask along with 3 or 4 glass boiling beads. Let test portions sit overnight in acid. Carry 2 reagent blanks through entire procedure along with test portions.

Before starting digestion, have ice bath available for cooling Kjeldahl flasks. HNO_3 should also be readily available. To start digestion, place each Kjeldahl flask on heating mantle set at low temperature. Once boiling is initiated, red-orange fume of NO_2 will be driven off. Continue gentle heating until HNO_3 and H_2O have been driven off. At this point effervescent reaction occurs between organic material and HClO_4 . Place flask on cool heating mantle and let digestion proceed with occasional heating from mantle. It is important that reaction between organic material and HClO_4 not go too fast, because charring will occur. If charring occurs, immediately place flask in ice bath to stop digestion. Add 1 ml HNO_3 and resume gentle heating.

After reaction of test portion with HClO_4 is complete (identified by cessation of effervescent reaction between organic material and HClO_4) apply high heat for ca 2 min; *do not heat to dryness* because this can cause explosion. Remove flask from heating mantle and let cool.

Transfer each digest to 50 ml volumetric flask and dilute to volume with H_2O . Some precipitation is likely to occur (especially with high salt content products) after dilution. Precipitate will dissolve if shaken and allowed to sit overnight. Final acid content of digests is a 20% HClO_4 .

Elemental determination is accomplished by inductively coupled plasma (ICP) emission spectroscopy (see Table E.1 For parameters). Calibration standards may be used as single standards (i.e., one element per standard) or as mixed standard containing 2 or more elements. Whether single or mixed standards should be used for calibration will depend on computer software requirements of particular ICP system in use.

Table E.1 Suggested operating parameters for ICP emission spectroscopy

Element	Wavelength, nm	Background correction	Standard, µg/ml	
			Low	High
Ca	317.9	N	0	200
Cu	324.7	H	0	5
Fe	259.9	N	0	10
K	766.5	N	0	200
Mg	383.2	N	0	5
Mn	257.6	N	0	5
Na	589.0	N	0	200
P	214.9	N	0	100
Zn	213.8	H	0	5

^a H = High side; N = no correction.

After calibration is complete, analyze test solutions. Check calibration of instrument after every 10 tests by analyzing calibration standards. If reanalysis of calibration standards indicates that instrument has drifted out of calibration (>3% of original values), recalibrate instrument.

Computer will calculate concentration for each element of each diluted test solution as $\mu\text{g/ml}$. Use following equation to convert this value to $\mu\text{g/ml}$ if original test portion was ready-to-feed or concentrated formula or $\mu\text{g/g}$ if test portion was powder.

$$C = A \times (50 \text{ ml}/B)$$

where A = concentration ($\mu\text{g/ml}$) of element as determined by ICP;
 B = volume or weight of test portion as ml or g;
 C = elemental concentration in



VITA

Miss Suwapat Srijunthongsiri was born on September 7, 1982 in Singburi, Thailand. She obtained the B.Sc. degree (Second Class Honors) in Agro-Industrial Product Development from Faculty of Agro-Industrial, Kasetsart University in 2005 and the M.Sc. in Agro-Industrial Product Development from Faculty of Graduate School, Kasetsart University in 2007. In 2009, she has worked in a position of supervisor in research and development department at Nuboon Co., Ltd., Bangkok, Thailand. In 2010, she desired to study in the Ph.D. program at the Department of Food Technology, Chulalongkorn University.

